

CARMENES input catalogue of M dwarfs

II. High-resolution imaging with FastCam

M. Cortés-Contreras¹, V. J. S. Béjar², J. A. Caballero^{3,4}, B. Gauza², D. Montes¹,
F. J. Alonso-Floriano¹, S. V. Jeffers⁵, J. C. Morales⁶, A. Reiners⁵, I. Ribas⁶, P. Schöfer⁵, A. Quirrenbach⁴,
P. J. Amado⁷, R. Mundt⁸, and W. Seifert⁴

¹ Departamento de Astrofísica y Ciencias de la Atmósfera, Facultad de Ciencias Físicas, Universidad Complutense de Madrid, 28040 Madrid, Spain, e-mail: mcortes@ucm.es

² Instituto de Astrofísica de Canarias, Vía Láctea s/n, 38205 La Laguna, Tenerife, Spain, and Departamento de Astrofísica, Universidad de La Laguna, 38206 La Laguna, Tenerife, Spain

³ Centro de Astrobiología (CSIC-INTA), PO Box 78, 28691 Villanueva de la Cañada, Madrid, Spain

⁴ Landessternwarte, Zentrum für Astronomie der Universität Heidelberg, Königstuhl 12, 69117 Heidelberg, Germany

⁵ Institut für Astrophysik, Friedrich-Hund-Platz 1, 37077 Göttingen, Germany

⁶ Institut de Ciències de l'Espai (CSIC-IEEC), Campus UAB, c/de Can Magrans s/n, 08193 Bellaterra, Spain

⁷ Instituto de Astrofísica de Andalucía (CSIC), Glorieta de la Astronomía s/n, 18008 Granada, Spain

⁸ Max-Planck-Institut für Astronomie, Königstuhl 17, 69117 Heidelberg, Germany

Received 06 Jul 2016; accepted dd Aug 2016

ABSTRACT

Aims. We search for low-mass companions of M dwarfs and characterize their multiplicity fraction with the purpose of helping in the selection of the most appropriate targets for the CARMENES exoplanet survey.

Methods. We obtained high-resolution images in the I band with the lucky imaging instrument FastCam at the 1.5 m Telescopio Carlos Sánchez for 490 mid- to late-M dwarfs. For all the detected binaries, we measured angular separations, position angles, and magnitude differences in the I band. We also calculated the masses of each individual component and estimated orbital periods, using the available magnitude and colour relations for M dwarfs and our own M_I -spectral type and mass- M_I relations. To avoid biases in our sample selection, we built a volume-limited sample of M0.0–M5.0 dwarfs that is complete up to 86 % within 14 pc.

Results. From the 490 observed stars, we detected 80 companions in 76 systems, of which 30 are new discoveries. Another six companion candidates require additional astrometry to confirm physical binding. The multiplicity fraction in our observed sample is $16.7 \pm 2.0\%$. The bias-corrected multiplicity fraction in our volume-limited sample is $19.5 \pm 2.3\%$ for angular separations of 0.2 to 5.0 arcsec (1.4–65.6 au), with a peak in the distribution of the projected physical separations at 2.5–7.5 au. For M0.0–M3.5 V primaries, our search is sensitive to mass ratios higher than 0.3 and there is a higher density of pairs with mass ratios over 0.8 compared to those at lower mass ratios. Binaries with projected physical separations shorter than 50 au also tend to be of equal mass. For 26 of our systems, we estimated orbital periods shorter than 50 a, 10 of which are presented here for the first time. We measured variations in angular separation and position angle that are due to orbital motions in 17 of these systems. The contribution of binaries and multiples with angular separations shorter than 0.2 arcsec, longer than 5.0 arcsec, and of spectroscopic binaries identified from previous searches, although not complete, may increase the multiplicity fraction of M dwarfs in our volume-limited sample to at least 36%.

Key words. stars: binaries: close – stars: late-type – stars: low mass

1. Introduction

The multiplicity of low-mass stars provides constraints to models of stellar and planet formation and evolution (Goodwin et al. 2007; Burgasser et al. 2007; Duchêne & Kraus 2013). M dwarfs, which have approximate masses of between 0.1 and $0.6 M_{\odot}$, account for two thirds of the stars in the solar neighbourhood and probably the Galaxy. However, in spite of their abundance and the increasing number of M-dwarf high-resolution imaging surveys in the past decade (Beuzit et al. 2004; Law et al. 2008; Bergfors et al. 2010; Janson et al. 2012, 2014a; Jódar et al. 2013; Bowler et al. 2015; Ward-Duong et al. 2015), the multiplicity of M dwarfs is not yet well constrained, at least by comparison with the better determination for Sun-like stars (Duquennoy & Mayor 1991; Raghavan et al. 2010; Tokovinin 2011). Published values range between 13.6 % and 42 %. Thus, the binary fraction of M dwarfs seems intermediate between the one of Sun-like stars and

very low mass binaries. In Table 1 we summarise the multiplicity fractions and semi-major axis coverage of some of the main multiplicity surveys carried out from F6 to T dwarfs.

The typical separation of low-mass stars in a binary system tends to decrease with the mass of the primary, which makes the detection of faint companions at resolvable separations more difficult (Jeffries & Maxted 2005; Burgasser et al. 2007; Caballero 2007; Bate 2012; Luhman 2012). In addition, the presence of a stellar companion influences planet formation (Wang et al. 2014a, 2014b, 2015a, 2015b). The limited number of exoplanet hosts in binary and multiple systems (Mugrauer et al. 2007; Mugrauer & Neuhauser 2009; Ginski et al. 2015) and the relatively small number of M dwarfs with known exoplanets detected with radial-velocity and transit methods (Rivera et al. 2005; Charbonneau et al. 2009; Bonfils et al. 2013) prevents a significant statistical analysis of how stellar multiplicity at such low masses affects planet formation.

Table 1. Stellar multiplicity fractions.

Reference	Investigated spectral type	d_{lim} [pc]	Multiplicity fraction [%]	Projected physical separation, s [au]	Survey method ^a
Duquennoy & Mayor 1991	F7–G9	22	~ 65	~ 0.01–225	RV, WI
Raghavan et al. 2010	~ F6–K3	25	44 ± 3	~ 0.005–100 000	RV, AO, S, WI
Reid & Gizis 1997	K2–M6	8	32	~ 0.1–1800	RV, S, WI
Leinert et al. 1997	M0–M6	5	26 ± 9	~ 1–100	S
Fischer & Marcy 1992	M	20	42 ± 9	0–10 000	RV, WI
Jódar et al. 2013	K5–M4	25	20.3 ^{+6.9} _{-5.2}	~ 0–80	LI
Ward-Duong et al. 2015	K7–M6	15	23.5 ± 3.2	~ 3–10 000	AO, WI
Bergfors et al. 2010	M0.0–M6.0	52	32 ± 6	3–180	LI
Janson et al. 2012	M0.0–M5.0	52	27 ± 3	3–227	LI
Law et al. 2008	M4.5–M6.0	15.4 ₆	13.6 ^{+6.5} _{-4.0}	~ 0–80	LI
Siegler et al. 2005	M6.0–M7.5	30	9 ⁺⁴ ₋₃	≥ 3	AO
Janson et al. 2014a	M5.0–M8.0	36	21–27	~ 0.5–100	LI
Close et al. 2003	M8.0–L0.5	33	15 ± 7	15	AO
Bouy et al. 2003	M7.0–L8.0	20	10–15	1–8	HST
Reid et al. 2008	L	20	12.5 ^{+5.3} _{-3.0}	3	HST
Burgasser et al. 2003	T	10 ₆	9 ⁺¹⁵ ₋₄	1–5	HST

Notes. ^(a) AO: Adaptive optics; HST: *Hubble Space Telescope*; LI: Lucky imaging; RV: Radial velocity; S: Speckle; WI: Wide-field imaging.

Because of their low effective temperatures, M dwarfs emit the bulk of their energy in the near-infrared. It makes them difficult to observe with the required radial-velocity precision with the current spectrographs for exoplanet hunting (e.g. HARPS at the 3.6 m ESO La Silla Telescope, HARPS-N at the 3.6 m TNG, and UVES at the 8.2 m ESO VLT), which operate in the optical. The prompt development of stable near-infrared spectrographs with wide wavelength coverage and high spectral resolution for radial-velocity surveys of M dwarfs has therefore been identified as critical by numerous decadal panels, funding agencies, and international consortia. Some noteworthy high-resolution near-infrared spectrographs currently under development are IRD at 8.2 m Subaru (Tamura et al. 2012), HPF at 9.2 m HET (Mahadevan et al. 2014), and SPIRou at 3.6 m CFHT (Donati et al. 2014). The high-resolution spectrograph CARMENES (Amado et al. 2013; Quirrenbach et al. 2014¹) at 3.5 m Calar Alto covers from 520 nm to 1710 nm and has started its science survey in January 2016.

CARMENES is the name of the double-channel spectrograph (near-infrared and optical) of the Spanish-German consortium that built it, and of the science project that is being carried out during guaranteed-time observations (GTO). For at least 600 GTO clear nights in the time frame between 2016 and 2018, CARMENES will spectroscopically monitor about 300 carefully selected M dwarfs with the goal of detecting low-mass planets in their habitable zones. With a long-term 1 m s^{-1} radial-velocity precision, the consortium aims at being able to detect 2 M_\oplus planets orbiting in the habitable zone of M5 V stars and super-Earths around earlier stars (García-Piquer et al. 2016). In addition to the detection of the individual planets themselves, the ensemble of objects will provide sufficient statistics to assess the overall distribution of planets around M dwarfs: frequency, masses, and orbital parameters.

To optimise the observational strategy of the instrument and its scientific return, the consortium has built Carmencita, the CARMENES input catalogue (Caballero et al. 2013; Quirrenbach et al. 2015; Alonso-Floriano et al. 2015a). It consists of almost 2200 of the brightest M dwarfs of each spectral subtype observable from Calar Alto, from which we will select the approximately 300 single GTO stars. By single we mean stars without close visual (physically bound) or optical (unbound) stellar or substellar companions that may induce real or artificial radial-velocity variations and, therefore, contaminate the precise CARMENES measurements (Guenther & Wuchterl 2003; Ehrenreich et al. 2010; Guenther & Tal-Or 2010; Bonfils et al. 2013).

As part of our efforts to determine the multiplicity of M dwarfs and to select the best targets for radial-velocity surveys for exoplanets, we performed a high-resolution imaging search of close companions with the lucky imaging instrument FastCam at the Telescopio Carlos Sánchez, as described in this paper. Preliminary results of this work were presented as conference proceedings by Béjar et al. (2012) and Cortés-Contreras et al. (2015a, 2015b). This paper is the second item of the series called the CARMENES input catalogue of M dwarfs. In the first paper, Alonso-Floriano et al. (2015a) carried out a low-resolution optical spectroscopic analysis of a number of poorly known dwarfs to constrain their spectral types. Furthermore, this work will soon be complemented with on-going searches of unresolved spectroscopic binaries and triples identified in a large collection of high-resolution optical spectra (Montes et al. 2015; Jeffers et al. in prep.) and of wide companions to M dwarfs supported by virtual observatory tools (cf., Cortés-Contreras et al. 2013, 2014; Alonso-Floriano et al. 2015b).

2. Observations

Of the almost 2200 M dwarfs currently in Carmencita, we selected 490 Carmencita targets for being observed with the

¹ <http://carmenes.caha.es>

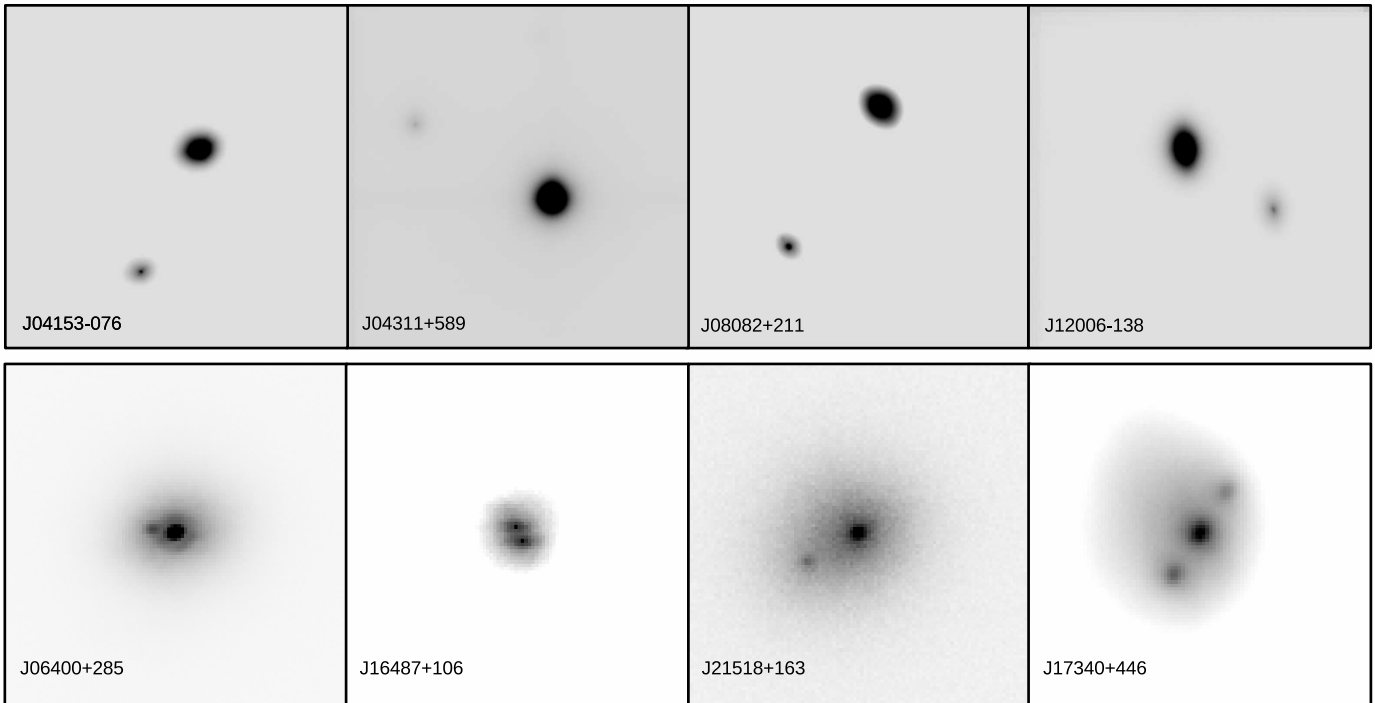


Fig. 1. Selection of images of multiple systems identified by us with FastCam. North is up and east is left. The upper row scale is $20 \times 20 \text{ arcsec}^2$, that of the lower row $4 \times 4 \text{ arcsec}^2$. Images at the top were obtained with the shift & add mode, while the bottom images were obtained with the “lucky image” mode.

The bottom right image (J17340+446) is an example of the so-called false triple effect.

FastCam lucky imager (Oscosz et al. 2008) at the 1.5 m Telescopio Carlos Sánchez at the Observatorio del Teide (Tenerife, Spain). The high-resolution imager FastCam is equipped with an L3CCD Andor 512×512 detector with very low electron noise and high readout speed. It has a field of view of $21.2 \times 21.2 \text{ arcsec}^2$ and an approximate pixel size and orientation of the detector of 0.0425 arcsec and 91.9 deg , respectively. FastCam delivers nearly diffraction-limited images, which at the Telescopio Carlos Sánchez and in the I band have full-width at half maxima of approximately 0.15 arcsec .

We carried out the observations during 26 nights in 15 runs from October 2011 to January 2016. For each target, we obtained typically ten blocks of 1000 frames each in the Johnson-Cousins I band using the electron multiplication mode. Typical frame exposure times were in the 35–50 ms range. On average, each star was imaged during 500 s in total. The typical Strehl ratio in our observations varies with the percentage of the best-quality frames chosen in the reduction process: from 0.2 for the 100% to 0.4 for the 1%. For astrometric calibration purposes, we also observed the globular cluster M3 and 18 astrometric standard binary stars from the Aitken Double Star catalogue (ADS – Aitken 1932; Scardia et al. 1995) with the same method and on several occasions.

Each frame was bias subtracted and then processed with the FastCam dedicated software developed at the Universidad Politécnica de Cartagena (see Labadie et al. 2010; Jódar et al. 2013). We ran the lucky image (on five blocks) and shift & add processing modes separately. The first allows selecting the fraction of the best-quality frames (we chose 1%, 10%, and 50%), aligns the selected frames using the brightest speckle, and combines them, producing six final lucky images per target. The second mode aligns all the block frames and then combines them, resulting in one unique image per target. Shift & add produces

deeper images than the lucky image mode, but with slightly poorer resolution. The M3 standard field was reduced only with the shift & add mode. In Fig. 1 we show a selection of the processed images at two different spatial scales.

In Table A.1, we provide the list of 490 observed M-dwarf targets with the following column information: identification number, our Carmencita identifier (Quirrenbach et al. 2015; Alonso-Floriano et al. 2015a), J2000 coordinates and J -band magnitude from the Two-Micron All-Sky Survey (Skrutskie et al. 2006), spectral type and its reference, distance and its reference, and the FastCam observation date and exposure time. Figure 2 shows the histograms of spectral types, J -band magnitudes, heliocentric distances, and total proper motions of the observed sample. Spectral types range from M0.0 V to M7.0 V, J from 4.2 mag to 10.4 mag, distances from 1.8 pc to 39.1 pc, and proper motions from $0.03 \text{ arcsec } a^{-1}$ to $10.6 \text{ arcsec } a^{-1}$. Because of their closeness, 97% of our targets have total proper motions larger than $100 \text{ mas } a^{-1}$.

Our sample of 490 observed Carmencita targets consisted mainly of the brightest stars in the J band for each spectral subtype (see Sect. 2 in Alonso-Floriano et al. 2015a) that were (*i*) not known spectroscopic binaries, (*ii*) not resolved systems with visual or optical companions at angular separations smaller than 5 arcsec, and (*iii*) not studied with high-resolution imaging devices before the start of our observations by speckle, adaptive optics, or lucky imaging (Beuzit et al. 2004; Law et al. 2008; Bergfors et al. 2010; Jódar et al. 2013; Janson et al. 2012). Some high-resolution imaging (Janson et al. 2014a; Ansdel et al. 2015; Bowler et al. 2015; Ward-Duong et al. 2015) and spectroscopic (Bonfils et al. 2013; Llamas 2014; Schöfer 2015) surveys have been performed afterwards and have tabulated several objects in common with our target list. In addition, we also observed (*a*) some dubious or poorly investigated close multi-

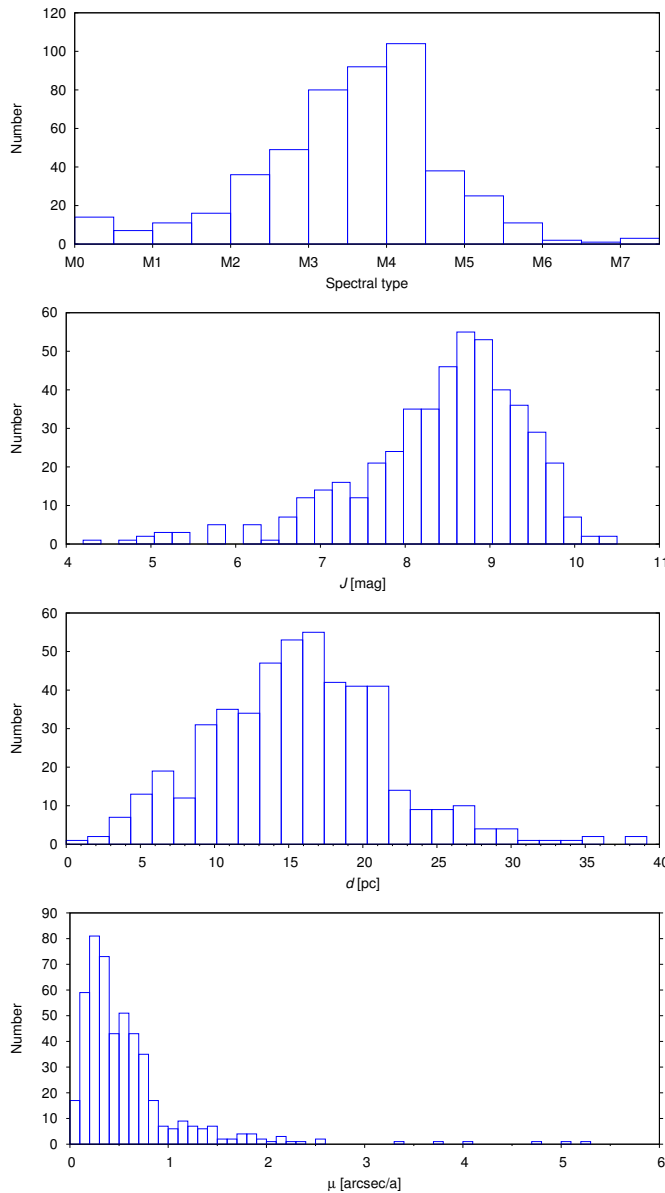


Fig. 2. Distributions of spectral type, J -band magnitude, distance, and proper motion of the 490 observed M-dwarf targets. The sizes of the bins follow the definitions given by Freedman & Diaconis (1981). The lowest panel does not display Barnard's star, with $\mu = 10.4 \text{ arcsec a}^{-1}$.

ple systems (including spectroscopic binary candidates), (b) a few stars with possible visual companions at angular separations smaller than 5 arcsec that needed confirmation or better characterisation, and (c) four known binaries with estimated orbital periods shorter than five years that were previously proposed for follow-up by Cortés-Contreras et al. (2013): J05085–181 (GJ 190), J13317+292 (DG CVn), J23174+196 (G 067–053), and J23455–161 (LP 823–004).

To confirm the physical binding of pairs (i.e. that the components share a common proper motion), we observed 54 targets more than once, and up to eight times. Accounting for the 490 M dwarfs, 18 ADS pairs and M3 calibration field, and the different epochs, we acquired 7670 images in total with FastCam.

Table 2. FastCam adopted plate scale and orientation for each run night.

Observation date ^a	Pixel scale [mas/pix]		Orientation [deg]	
	x	y	x	y
23 Oct 2011*	42.25	42.56	92.08	91.60
24 Oct 2011	42.25	42.56	92.08	91.60
25 Oct 2011	42.25	42.56	92.08	91.60
30 Jan 2012	42.25	42.56	92.08	91.60
31 Jan 2012	42.25	42.56	92.08	91.60
25 Mar 2012*	42.31	42.61	91.79	91.64
26 Mar 2012*	42.30	42.62	91.82	91.65
27 Mar 2012	42.30	42.62	91.82	91.65
10 Jul 2012*	42.48	42.61	92.11	91.91
11 Jul 2012*	42.49	42.64	92.03	91.77
12 Jul 2012*	42.32	42.54	91.96	91.99
16 Sep 2012	42.32	42.54	91.96	91.99
17 Sep 2012	42.32	42.54	91.96	91.99
13 Jan 2013*	42.26	42.69	91.94	91.63
14 Jan 2013*	42.21	42.59	91.85	91.63
28 Feb 2014*	42.26	42.69	91.99	91.70
01 Mar 2014	42.26	42.69	91.99	91.70
02 Mar 2014	42.26	42.69	91.99	91.70
22 May 2014	42.26	42.69	91.99	91.70
09 Dec 2014*	42.26	42.99	91.97	91.96
14 Apr 2015*	42.28	42.37	92.18	91.65
15 Apr 2015	42.28	42.37	92.18	91.65
09 Jun 2015	42.28	42.37	92.18	91.65
29 Jul 2015	42.28	42.37	92.18	91.65
17 Nov 2015	42.28	42.37	92.18	91.65
07 Jan 2016	42.28	42.37	92.18	91.65

calibration field was observed on nights marked with an asterisk.

3. Analysis

3.1. Astrometry

The first step of the analysis was computing the pixel size and detector orientation with common IRAF tasks (Tody 1986). To do this, we determined the centroids of the brightest stars in the M3 standard field with `imcentroid`. Using the celestial coordinates in the ACS Survey of Galactic Globular Clusters (Sarajedini et al. 2007) and the pixel coordinates in our images, we then determined the transformation equations with `cemap` by fitting to a general transformation of order two. Table 2 lists the pixel scales and orientations of the detector for each night. For nights without M3 images, we used the calibration of the closest night with computed plate solution. Pixel scale and rotation angle in the centre of the detector in the x and y axes are similar within the different campaigns with almost negligible variations from night to night. Their mean values are $42.31 \pm 0.09 \text{ mas/pixel}$ and $42.63 \pm 0.15 \text{ mas/pixel}$ in pixel scale and $91.98 \pm 0.12 \text{ deg}$ and $91.74 \pm 0.15 \text{ deg}$ in orientations of the detector in the x and y axes, respectively. The uncertainties are the standard deviations of the measurements.

To double-check that our astrometric solutions were correct, we calculated angular separations (ρ) and position angles (θ) for each ADS binary. To do that, we measured the x and y positions of each star with `imcentroid`, and transformed them into equatorial coordinates using the astrometric solution of the corresponding night with `cctrans`. Table A.2 shows the previously

published values of ρ , θ , the epochs of observation and references, and our measured values in different epochs. Our errors in ρ and θ were derived from the standard deviation of the measurements in all images within the same night and the determined astrometric solutions on different nights. In general, the measured values of ρ and θ of the same pair on different nights were consistent within 3σ between them and with tabulated values from recent works. In some cases, the quality of our measurements surpassed previous publications.

We carried out a visual inspection for companions to our 490 Carmencita targets and found 137 additional sources in 116 systems, for which we measured the relative positions and position angles following the same procedure as described above for the ADS binaries. In some epochs of nine stars with companions very close to the resolution limit of our images, we were unable to measure the photocentroid of both components with `imcentroid` and, hence, we used the brightest pixel to measure their positions. In these cases, the uncertainties in the determination of ρ and θ were larger and we adopted a typical error bar of one pixel.

We classified the 137 sources into three groups: (i) 51 optical companions (i.e. unbound, Table A.3), (ii) 80 physical companions (i.e. bound, Table A.4), and (iii) six unconfirmed companions (bottom of Table A.4). For the classification, we used old photographic plate digitisations and all-sky surveys provided by the Aladin sky atlas (Bonnarel et al. 2000), previous astrometry tabulated by the Washington Double Star Catalogue (WDS, Mason et al. 2001) and/or our own multi-epoch astrometric measurements together with the target proper motions (mostly from van Leeuwen 2007 and Roeser et al. 2010).

Most of the 51 optical companions are null-proper-motion point-like sources in photographic plates of the first National Geographic Society – Palomar Observatory Sky Survey in the mid-1950s. For the rest of the companions, we performed a multi-epoch analysis of their relative positions. We considered as optical (unbound) companions those that show ρ and θ values in different epochs consistent within 3σ with null proper motion and inconsistent by more than 3σ with the proper motion of the M dwarfs. Otherwise, we considered them as physically bound. For five of the six unconfirmed binaries, we only had one epoch, and for the other (J07349+147), the ρ and θ values at different epochs did not allow us to distinguish between null or common proper motion.

Figure 3 displays the measured ρ and θ values of all the detected pairs. It shows a homogeneous distribution of the position angle of the companions, which discards possible false detections associated with, for example, optical ghosts.

3.2. Photometry

In Table A.4 we list magnitude differences in the I band for the 80 physical and six likely physical pairs. To measure the magnitude difference of the binaries, we performed aperture and point spread function (PSF) photometry using the `phot`, `psf`, and `allstar` routines in the `daophot` package of IRAF.

For wide enough pairs, we used the primary star PSF as a reference for the secondary. In these cases, magnitude differences from aperture photometry and PSF fitting did not differ significantly. Since the PSF varies depending on the focus and sky position, for close pairs we chose the most appropriate single star observed during the same night as a reference to compute the PSF. For five pairs, we were unable to measure the ΔI between components using PSF photometry, and we estimated it from the peak flux ratio of the PSF subtracted image, and for J23455–161,

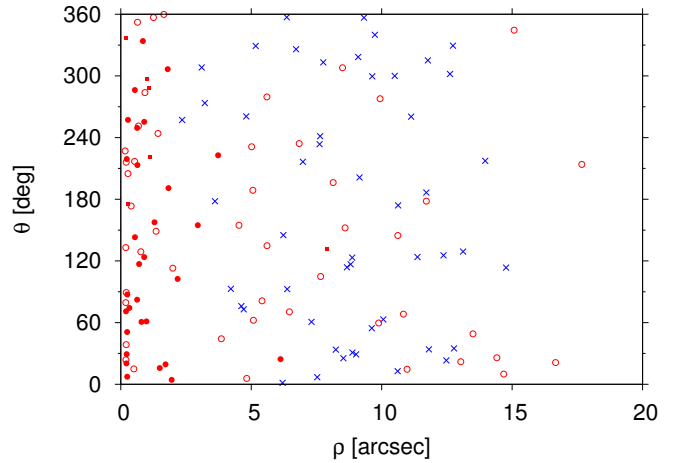


Fig. 3. Diagram of θ vs. ρ for all the 137 measured pairs. Filled red circles are new physically bound pairs, small filled red squares are unconfirmed related pairs, open red circles are known physically bound pairs, and blue crosses are optically unrelated pairs.

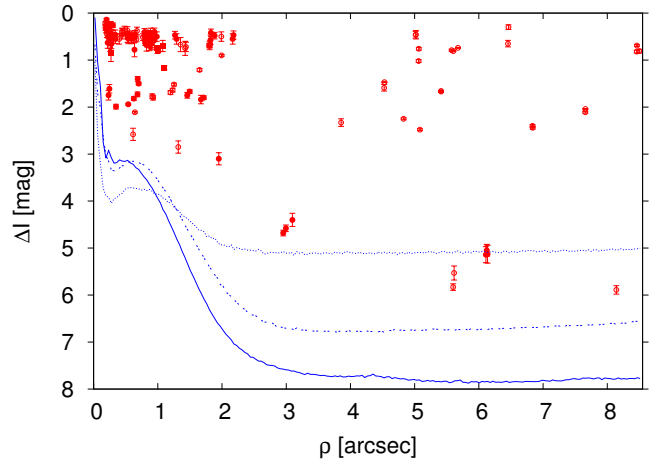


Fig. 4. Diagram of ΔI vs. ρ up to 8.5 arcsec for the physical pairs. Colour and symbol code is as in Fig. 3. Solid, dashed, and dotted lines indicate the 3σ detection limits for primaries in the magnitude ranges $I < 10$ mag, $10 \text{ mag} \leq I < 11$ mag, and $I \geq 11$ mag, respectively.

we perceived the companion and could not measure the magnitude difference.

A few close pairs showed a so-called false triple effect associated with the reduction process by the FastCam software, based on the selection of the brightest pixel. When both components are of similar brightness, this software may not distinguish between the primary and secondary and, in the process of aligning, selects the brightest pixel in one or another star, resulting in an apparent triple system. For equal brightness binaries, this may lead to a degeneracy in the determination of the position angle of 180 deg. The option `2stars` in the FastCam reduction software, which takes this ambiguity into account, solved this effect in most cases. For the rest, we determined the real flux ratio of the pair by following the procedure described by Law (2006):

$$F_R = \frac{2I_{13}}{I_{12}I_{13} + \sqrt{I_{12}^2I_{13}^2 - 4I_{12}I_{13}}}, \quad (1)$$

where $I_{12} = F_1/F_2$ and $I_{13} = F_1/F_3$, and F_1 , F_2 and F_3 are the fluxes of the images in the positions of the true primary, true secondary, and spurious tertiary, respectively.

In Fig. 4 we plot the measured magnitude differences in the I band and angular separations of the companions. Most of them are of similar brightness ($\Delta I \approx 0.0\text{--}1.0$ mag) and are located at angular separations smaller than 2.5 arcsec. Figure 4 also shows the contrast curves of our survey as a function of angular separation. The maximum magnitude difference in each stacked image depends on the brightness of the primary star. For this reason, we considered three different groups in our sample according to their I magnitude, from which we selected four single stars covering different spectral types to obtain a representative mean contrast curve. For each star, we estimated the detection limit as a function of the angular separation as three times the standard deviation of the number of counts in ten-pixel-wide annuli centred on the target. This detection limit was converted into ΔI using the peak flux value of the star. The maximum magnitude difference in the detection of possible companions at angular separations between 0.2 and 1.0 arcsec varies from 3 to 4 mag and from 5 to 7 mag at separations larger than 2 arcsec, depending on the brightness of the primary star. The limiting magnitude of our survey is about $I \approx 17$ mag, and we were able to detect all sources brighter than this limit at angular separations greater than 3 arcsec. This implies that at separations larger than 3 arcsec, the detection of companions earlier than M8 dwarfs is complete up to 40 pc, which corresponds to the entire sample, and the detection of companions earlier than M9 dwarfs is complete up to 25 pc, which is in most of our sample.

4. Results and discussion

4.1. Detected binaries

Of the 490 observed stars, we confirmed with our data 80 companions in 76 systems, of which 30 are presented here for the first time. In addition, there are also six unconfirmed binaries that need additional epochs to confirm the physical binding. The majority of the optical components of the survey were easily identified using previous available data, and most of the remaining ones were confirmed as physically bound companions using our own measurements at different epochs. Therefore, we considered the six unconfirmed binaries as very probably physically bound rather than unbound pairs. We took into account the six binaries for the determination of the multiplicity fraction.

The 86 pairs are listed in Table A.4. In the last column of the table, we include the multiplicity flag from version 1.2 of the Guide Star Catalog (Morrison et al. 2001), which is “False” for 18 of the 30 new confirmed binaries, “True” for 10 of them and has no entry for the close companions of J08082+211 and J15191–127. For the 30 new binaries, and to our knowledge, there are no other references to binarity.

Of the 80 physical companions, 48 are tabulated by WDS (second column in Table A.4), of which two were previously suggested by Behall & Harrington (1976; J05333+448) and Bowler et al. (2015; J15496+348) and confirmed here. Another two were recently presented by Ward-Duong et al. (2015; J05034+531) and Ansdel et al. (2015; J06212+442), and one of the new companions resolved here is most likely associated with a spectroscopic binary identified by Bonfils et al. (2013; J15191–127). The remaining 29 are pairs with no previous binarity references to our knowledge.

Some of the measured companions were not detected in all epochs because of the relative motion of the components and the

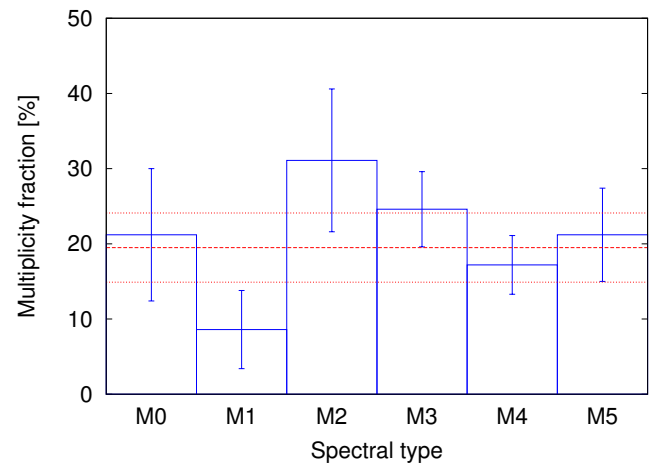


Fig. 5. Multiplicity fraction as a function of spectral type from M0.0 V to M5.0 V in the volume-limited sample with separations from 0.2 to 5.0 arcsec. Error bars are Poissonian. Horizontal dashed and dotted lines are the global multiplicity fraction and the $\pm 2\sigma$ values.

crossing of the companion behind or in front of the primary star (J05078+179 and J05333+448), presence of the companion near the diffraction limit (J13317+292, J15496+348, J16487+106, and J21012+332), and a focus problem (J06400+285).

4.2. Multiplicity fraction

Of the 490 observed M dwarfs, 408 are single and 82 (76+6) are in binary or multiple systems within the FastCam field of view. This gives a close multiplicity fraction of $16.7 \pm 2.0\%$, by assuming a Poissonian distribution of the errors. Nevertheless, it must not be taken as a real M-dwarf multiplicity fraction because of the selection bias of the observed sample: we did not include many stars that were previously observed in similar studies or that had known visual companions at less than 5 arcsec.

For statistical purposes, we grouped all our Carmencita (Sect. 1) and FastCam targets in a combined sample. Of the 2176 Carmencita stars, 1141 M dwarfs have been surveyed with FastCam or with high-resolution imagers with similar capabilities (Beuzit et al. 2004; Lafrenière et al. 2007; Law et al. 2008; Bergfors et al. 2010; Janson et al. 2012, 2014a; Jódar et al. 2013; Bowler et al. 2015; Ward-Duong et al. 2015). For completeness, we considered a range of angular separations from 0.2 to 5 arcsec to our targets. The lower limit was given by the FastCam spatial resolution and the upper limit by the maximum separation at which we could detect companions to at least 90 % of the observed stars. Of the 1141 surveyed M dwarfs, 219 have physical companions in this interval of angular separations (55 from this work and 164 from other publications), which gives a close multiplicity fraction of $19.2 \pm 1.4\%$.

To avoid any selection bias and give a more reliable multiplicity fraction, we proceeded by building a volume-limited sample with a maximum distance of 14 pc and a completeness of 86 %. This completeness was estimated by assuming that all M0–M5 dwarfs are known within 7 pc and that their density in the solar vicinity is constant. This third sample is composed of 425 dwarfs with spectral types between M0.0 V and M5.0 V, of which 83 have companions (either from FastCam and other works) in the range from 0.2 to 5.0 arcsec. This translates into a close multiplicity fraction of $19.5 \pm 2.3\%$, which is consis-

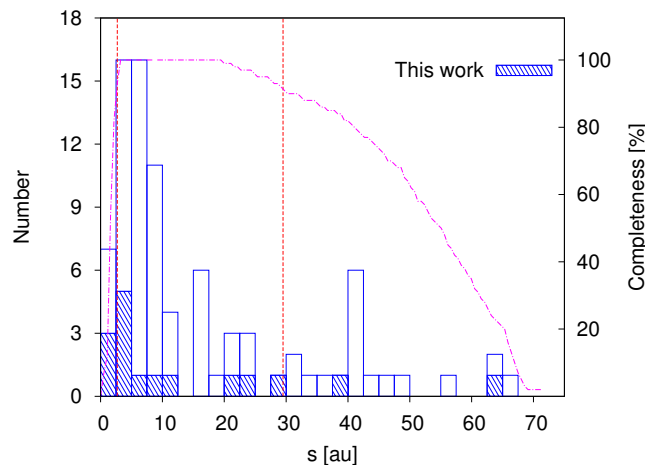


Fig. 6. Projected physical separation distribution of the binaries in the volume-limited sample. Dashed bars represent our binaries. Vertical dashed lines mark the 90 % completeness limits, and the dash-dotted curve represents the completeness as a function of the projected physical separation.

tent within error bars with the 13.6 %–27 % fractions obtained for M dwarfs in most surveys (Table 1), although some authors provided higher multiplicity fractions (Fischer & Marcy 1992; Bergfors et al. 2010). In Sects. 4.8 and 4.9 we estimate the contribution to the multiplicity fraction of pairs separated by less than 0.2 arcsec and more than 5 arcsec.

4.3. Dependence of multiplicity on spectral type

To estimate the spectral types of the individual components of the binaries, we used the $I - J$ colours and M_I absolute magnitudes as a function of spectral type for M dwarfs from Table 3 in Kirkpatrick et al. (1994), together with the 2MASS photometry and spectral type of the pair.

For pairs resolved by 2MASS, we used these relations and values to obtain the I magnitude of the primary, and obtained the I magnitude of the secondary from our measured ΔI . We derived the absolute M_I magnitudes through the distance modulus and inferred the spectral types of the secondaries with the M_I -spectral type relation of Kirkpatrick et al. (1994).

For pairs not resolved by 2MASS, the J -band magnitude involves the contribution of all the components in the system. In these cases, we obtained the I magnitude of the system from the $I - J$ colours and the global spectral types of the pairs from the literature. Using the I magnitude and our measured ΔI , we computed the individual I magnitudes. We calculated the individual M_I absolute magnitudes by applying the distance modulus, and estimated individual spectral types from the M_I -spectral type relation.

The distances in our sample come mostly from literature parallax determinations (see references in Table A.1). For stars without parallactic distance, we calculated spectro-photometric distances from our own M_J -spectral type relation. This relation was obtained from a polynomial fit using single stars with well-determined spectral types between M0 V and M6 V, parallactic distances, and 2MASS J -band photometry from the Carmencita sample, and has the form:

$$M_J = a \text{ SpT}^2 + b \text{ SpT} + c, \quad (2)$$

where $a = 0.078 \pm 0.007$ mag, $b = 0.265 \pm 0.038$ mag and $c = 5.895 \pm 0.044$ mag, and SpT indicates the numerical spectral subtype within the M range.

For very close binaries, spectro-photometric distances are not reliable since the 2MASS photometry and the spectral type determination do not provide the contribution of the two components separately. In these cases, in an iterative way, we estimated new individual spectro-photometric distances for the two components in the system from spectral type estimations based on the global spectral type, the M_I -spectral type relation, the individual I magnitudes, and the distance modulus. These updated distances are given in Table A.1. Given the low number of close binaries not resolved in our survey (~ 10 %, see Sect. 4.8), we do not expect many additional unresolved components.

The individual spectral types are listed in Table A.5. SpT column indicates the combined spectral type of the system from which individual spectral types were derived. In the SpT₁ and SpT₂ columns, the spectral types indicated with capital “M” come from the literature, and with lower case “m” refer to our estimated spectral types.

In Fig. 5 we show the dependence of the multiplicity fraction of M dwarfs on the spectral type in our volume-limited sample. The multiplicity fractions for different spectral subtypes are consistent within the error bars among them, except for M1 stars, for which it is lower. We compared this distribution with the global multiplicity fraction obtained in the previous section and performed a χ^2 test. Without the M1 contribution, the distribution is consistent with a flat distribution with a confident level of 96 %.

In addition, our determined multiplicity fraction has intermediate values between Sun-like (44 %–65 %) and very low mass stars and brown dwarfs (9 %–15 %). This agrees with the generally accepted decreasing trend of the multiplicity fraction with decreasing mass of the primaries (Table 1).

4.4. Projected physical separation distribution

To study the distribution of the binaries in the volume-limited sample, we converted angular separations (ρ) into projected physical separations (s) by using the small-angle approximation $\tan \rho \approx \rho$. Hence, $s \approx \rho d$. The distances d come from parallax or photometry as in Sect. 4.3.

In Fig. 6 we show the projected physical separation distribution of the binaries in the volume-limited sample. We also represent the completeness of the volume-limited sample as a function of projected physical separation, and draw the completeness limits with a confidence level of 90 %, which correspond to the s interval between 2.6 and 29.5 au. We estimated these values as those separations at which we are able to detect companions in 90 % of the sample.

The projected physical separations of the observed pairs in the volume-limited sample range from 1.4 to 65.6 au and their distribution peaks at 2.5–7.5 au. This is consistent with the values of 5–10 au found by Jódar et al. (2013) for M0–M4 dwarfs, and of ~6 au found by Janson et al. (2014) for M3–M8 dwarfs and Ward-Duong et al. (2015) for M0–M6 dwarfs. However, these values are lower than those found for Sun-like stars (Duquennoy & Mayor 1991; Raghavan et al. 2010) and more similar to those found for ultracool dwarfs (4–6 au for M8.0–L0.5, Close et al. 2003; 2–4 au for M7.0–L8.0, Bouy et al. 2003; ~3 au for L dwarfs, Reid et al. 2008).

Within the physical separation completeness range from 2.6 to 29.5 au, there are 61 M dwarfs with low-mass companions in our volume-limited sample. This translates into a multiplicity fraction of $14.4 \pm 2.0\%$, which is lower than the fraction derived

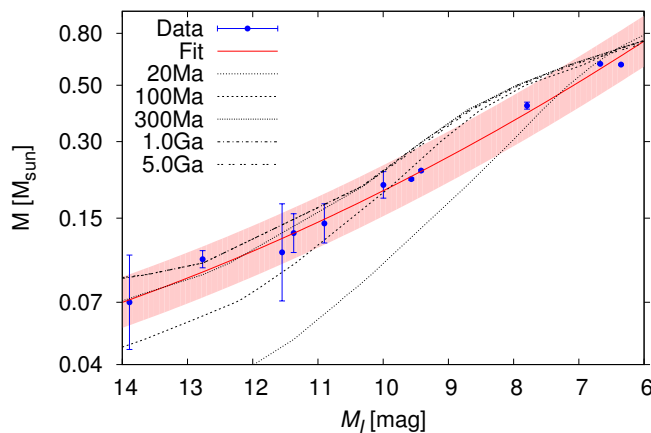


Fig. 7. Mass M vs. Absolute magnitude M_I . Blue points represent the dynamical masses and absolute magnitudes taken from the literature. The red solid line and shadowed area represent the best-fit $\pm 3\sigma$. Different dashed lines display the BT-Settl evolutionary models at 20 Ma, 100 Ma, 300 Ma, 1 Ga, and 5 Ga.

in Sect. 4.2 as a result of the missing systems at larger separations (see Fig. 6).

4.5. Masses

We derived masses from our own mass-luminosity relation in the Johnson-Cousins I band. To our knowledge, there is no published mass-luminosity relation employing this band. We collected dynamical masses and I -band magnitudes of eleven low-mass stars from different works (Delfosse et al. 2000; Henry 2004; Reid et al. 2004; Tokovinin 2008) and obtained an M_I - M relation using a parabolic fit of the form:

$$\log M = a M_I^2 + b M_I + c, \quad (3)$$

where M is the mass, M_I is the absolute I -band magnitude, $a = 0.005 \pm 0.002 \text{ mag}^{-2}$, $b = -0.222 \pm 0.037 \text{ mag}^{-1}$, and $c = 1.035 \pm 0.180$. This relation is valid for main-sequence stars in the M_I interval between 6 and 14 mag, which corresponds to $\sim M0\text{--}M8$ spectral types. Figure 7 shows the data taken from the literature, the corresponding best fit, and the comparison with BT-Settl evolutionary models from the Lyon group (Baraffe et al. 2015).

In some of our detected pairs, one or both components are also spectroscopic binaries (see Table 6). For these we estimated individual masses assuming equally bright components.

For main-sequence stars, the luminosity and effective temperatures are unambiguously related to the mass, and thus, the relation in Eq. 3 is only valid for stars older than ~ 300 Ma, as inferred from Fig. 7. For stars younger than 300 Ma, the mass-luminosity relation strongly depends on the age. We searched for young stars in our sample by collecting radial velocities from the literature (Caballero et al. in prep.) and computing UVW Galactocentric space velocities as in Montes et al. (2001) for 452 of the 490 observed stars (there are 38 stars without radial velocities). Of these, 155 have U and V velocity components inside or near the boundaries that delineate the young-disc population (Montes et al. 2016). In total, 42 stars of our 82 multiple systems are candidate members in young stellar kinematic groups. We checked the literature and found that 26 of the 42 are relatively old interloper stars that do not show any youth feature or

have been poorly investigated. The remaining 16 stars are confirmed members of stellar kinematic groups or the young-disc population. Their associations and ages are listed in Table 3.

Since $I - J$ colours of young stars and field stars do not show significant differences (see Bihain et al. 2010; Peña-Ramírez et al. 2016), we applied the colour-spectral-type relation from Kirkpatrick et al. (1994) to derive the individual I magnitudes of these stars as explained in Sect. 4.3. We considered Castor, Ursa Majoris, and young-disc members old enough to be main-sequence stars, and thus, to apply our mass- M_I relation with confidence. For these calculations, we assumed the ages given in Table 3. These stars appear in italics in Table A.5. The candidate pair to IC 2391 does not have a parallactic distance. Hence, we estimated its mass from the $I - J$ colours and the BT-Settl evolutionary models from the Lyon group (Baraffe et al. 2015). We also applied these models to derive masses from the individual I magnitudes and parallactic distances for β Pic, Columba/Carina and Local Association members.

Table A.5 lists the inferred I magnitudes (Sect. 4.3) and mass values of the components of 76 of our systems. All of the detected companions have absolute magnitudes brighter than 14 mag, the lowest limit of our empirical mass-magnitude relation, which corresponds to masses close to the hydrogen-burning limit ($\sim 0.07 M_\odot$). The only exception is the unconfirmed companion of J04352–161, which has an absolute magnitude fainter than 14 mag, and we were unable to determine its mass with the method explained before.

4.6. Mass ratios

The upper panel in Fig. 8 shows the mass ratio (M_2/M_1) histogram of our binaries in Table A.5. This global distribution slightly increases towards higher mass ratios and has its maximum above 0.8. The slightly lower number of equal-mass pairs with mass ratios near unity is not significant and could be related to the effect of the reduction process using the brightest pixel, which artificially sharpens the PSF of the primary with respect to the PSF of the secondary, and may produce a lower flux ratio than expected. This distribution is also affected by our sensitivity limit. While in spectral types earlier than M3.5 (i.e. more massive stars) our search of companions is complete for mass ratios greater than 0.3, in later spectral types (i.e. less massive stars) the search is complete for mass ratios greater than 0.35–0.60.

Empty and dashed bars represent the mass ratio distributions of M0.0–M3.5 and M4.0–M5.5 primaries, respectively. The distribution of the former shows the same trend as the global distribution, with a peak around 0.8–0.9. For the latter, the distribution increases towards higher ratios. As explained before, this might be due to our observational bias.

The high occurrence of binaries with mass ratios above 0.8 can also be seen in the lower panel in Fig. 8, which represents the spectral type of the primary versus the mass ratio. For later spectral types, our detected binaries also tend to have similar masses. This may be due to the lack of sensitivity to lower mass ratios at later spectral types. The distribution differs with the more homogeneous mass ratio distributions observed by Janson et al. (2012, 2014). The number of binaries with mass ratios closer to unity (i.e. similar masses) for M0.0–M3.5 contrasts with the relatively low numbers presented in Bergfors et al. (2010) in this range, but is more similar to their distribution for later M4.0–M5.5 spectral types.

Figure 9 displays the occurrence of mass ratios with physical separations. Pairs with separations shorter than 50 au tend

Table 3. Target members of stellar kinematic groups.

Karmn	Name	Moving group	Ref. ^a	Assumed age [Ma]	Ref. ^b
J01221+221	G 034–023	Young disc	Abe14	≥ 300	This work
J04153–076	o ⁰² Eri C	β Pic	AF15	~ 20	Bell15
J05019+099	LP 476–207	β Pic	AF15	~ 20	Bell15
J05068–215E	BD–21 1074 A	β Pic	AF15	~ 20	Bell15
J05068–215W	BD–21 1074 BC	β Pic	AF15	~ 20	Bell15
J05103+488	G 096–021 AB	IC 2391?	This work	~ 50	Barr04
J10028+484	G 195–055	Local Association?	This work	~ 100	Bas96
J10196+198	BD+20 2465	Castor	Cab10	≥ 300	Barr98, Mam13
J12123+544S	BD+55 1519 A	UMa	Mon01	≥ 300	Gia79,SM93
J12123+544N	BD+55 1519 B	UMa	Mon01	≥ 300	Gia79, SM93
J13317+292	DG CVn AB	Columba/Carina	Ried14	~ 40	Bell15
J18548+109	V 1436 Aql B	Castor	Cab10	≥ 300	Barr98, Mam13
J23293+414S	G 190–027	Local Association	Klu14	~ 100	Bas96
J23293+414N	G 190–028	Local Association	Klu14	~ 100	Bas96
J23318+199 E	EQ Peg Aab	Castor	Cab10	≥ 300	Barr98, Mam13
J23318+199 W	EQ Peg Bab	Castor	Cab10	≥ 300	Barr98, Mam13

Notes. ^(a) Abe14: Aberasturi et al. 2014; AF15: Alonso-Floriano et al. 2015b; Cab10: Caballero 2010; Klu14: Klutsch et al. 2014; Mon01: Montes et al. 2001; Ried14: Riedel et al. 2014. ^(b) Barr04: Barrado y Navascués et al. 2004; Barr98: Barrado y Navascués 1998; Bas96: Basri et al. 1996; Bell15: Bell et al. 2015; Gia79: Giannuzzi 1979; Mam13: Mamajek et al. 2013; SM93: Soderblom & Mayor 1993.

to have mass ratios over 0.8, while pairs at larger separations present a more homogeneous distribution.

Similar studies also show this observed trend in the relation between separation of the components and mass ratio: near equal-mass pairs (mass ratios ≥ 0.8) are found at smaller separations. Moreover, the lower the mass of the primary, the higher the mass ratio and the closer the semi-major axis at which companions are found (Jódar et al. 2013; Janson et al. 2012, 2014). The closer distance to the Sun of our sample compared to the samples of Bergfors et al. (2010) and Janson et al. (2014), who investigated the mass ratio at larger separations, may explain the difference with our results in the mass ratio distribution. However, Monte Carlo simulations of Sun-like stars and M-dwarf surveys from Duquennoy & Mayor (1991) and Raghavan et al. (2010), and Fischer & Marcy (1992) and Janson et al. (2012), respectively, suggest that the mass ratio distributions could be independent of the separation and dynamical evolution (Reggiani & Meyer 2011, 2013).

4.7. Periods and orbital motion

We derived periods for 70 systems with Kepler's third law, the masses of the components, and the maximum projected physical separations (Sect. 4.4). Since these measures are a lower limit estimate to the semi-major axis, the periods given in Table A.5 should be also considered as a lower limit.

In total, 26 systems have periods shorter than 50 a, of which 13 are known bound systems, 10 are newly discovered binaries, and three are the unconfirmed pairs J01221+221, J07349+147, and J10028+484.

Of the 26 systems, we consider four triple systems here: J05078+179, J08082+211, and J16554–083S, which are formed by a spectroscopic binary plus a third resolved component, and J23293+414S, for which we resolved the three components of

the system. In addition, the “triples” J08082+211 and J16654–083S belong to a hierarchical quadruple and quintuple system, respectively, with the fourth and fifth components outside the field of view of FastCam (Sect. 4.9).

Several systems were observed repeatedly during the programme, which allowed us to perform a multi-epoch analysis. Some of them showed appreciable variation of angular separation and position angle in different epochs of our data. When these variations were larger than 3σ with respect to constant values of ρ and θ and were consistent with an orbital trajectory, we considered that the orbital motion of the pair was detected. Because of the large uncertainties, the variations of ρ and θ of the pairs J05333+448, J08066+558, and J20407+199 lie within 3σ and therefore they do not fulfil our criterion, but they show appreciable variations that are probably related to the orbital motion. However, the time baseline is not long enough to provide a precise estimate of the orbital parameters of the systems.

Table 4 lists these 16 systems, of which 13 are new. We tabulate the WDS discoverer code of the previously known pairs, the number of used epochs, the time interval between the first and last measured epoch, and the estimated periods. We show an example of one of these binaries (J12332+090) in Fig. 10.

4.8. Known close and spectroscopic binaries (not detected in our search)

In the observed sample there were also previously known pairs that we were unable to resolve because of the small separation of the components ($\rho \lesssim 0.2$ arcsec) and/or the faintness of the companion. These pairs are listed in Table 5. In addition, there were also previously known spectroscopic binaries, taken into account for the period estimation of our detected binaries in Table A.5. They are listed in Table 6.

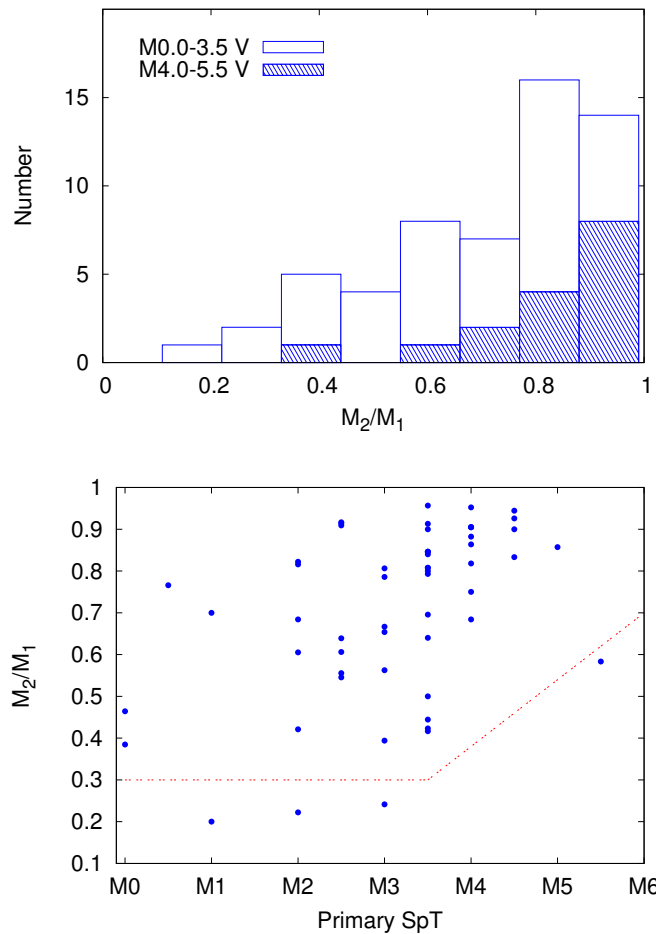


Fig. 8. Top panel: mass ratio distribution of our binaries. Empty and dashed bars separate the mass ratio distribution of M0.0–M3.5 and M4.0–M5.5 dwarfs. Bottom panel: mass ratio of the pairs vs. spectral type of the primary. The red dashed line represents the mass ratio completeness limits. The standard error of the mean mass ratio is 0.03 and the error bar is ± 0.5 in spectral type.

The close multiplicity fraction of $19.5 \pm 2.3\%$ given in Sect. 4.2 is a lower limit of the total multiplicity fraction of M dwarfs, since it only includes physical companions in the interval of angular separations between 0.2 and 5.0 arcsec. Although studies of spectroscopic binaries and very close binaries ($\rho < 0.2$ arcsec) are not complete, we know from the literature that we are missing 47 very close additional binaries in this range in our volume-limited sample (e.g. Delfosse et al. 2013; Schöfer et al. 2015; Tokovinin et al. 2015). This number is consistent with the fractional incidence of eclipsing binaries obtained from surveys like *Kepler* (Shan et al. 2015), and increases the given binary fraction by 11 %. Hence the multiplicity fraction at separations smaller than 5 arcsec would be at least $\sim 30\%$.

4.9. Known companions at separations larger than 5 arcsec

Many of our FastCam stars have stellar or substellar companions outside the field of view of the instrument or at angular separations larger than the 5.0 arcsec cut-off defined for statistical purposes. We compiled the multiplicity information of all of them using our observations and the WDS catalogue. Of the wide binaries present in the WDS catalogue, nearly 60 % come

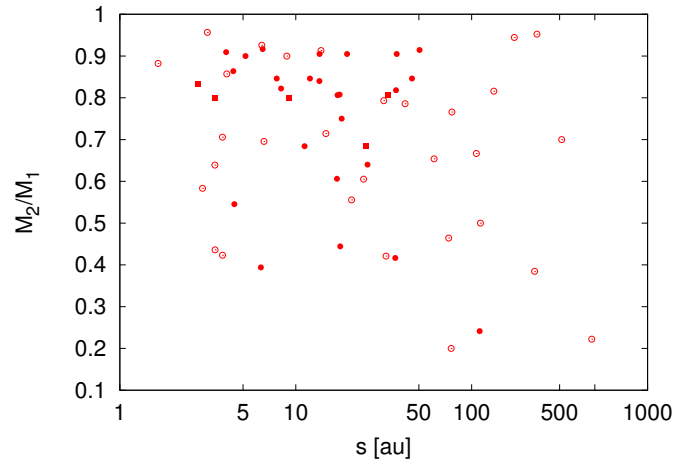


Fig. 9. Mass ratio vs. projected physical separation. Colour and symbol code is as in Fig. 3.

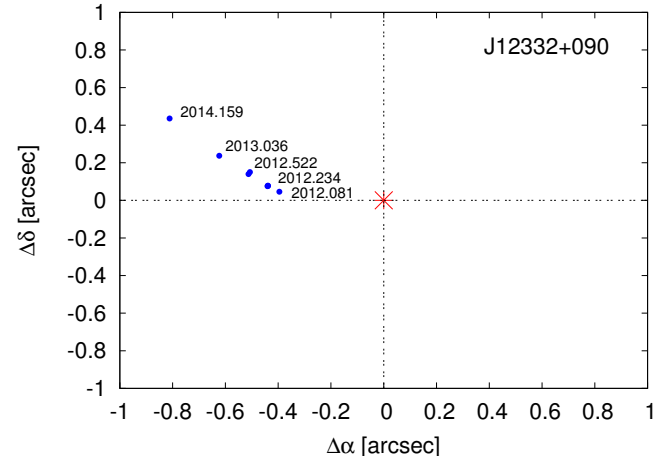


Fig. 10. Orbital variation of the pair J12332+090 from our FastCam data. The asterisk marks the position of the primary. Five of the eight epochs are labelled.

Table 4. Systems with measurable orbital motion.

Karmn	WDS	Epochs	Δt [a]	P [a]
J02518+294	...	3	4.2	130
J05068–215W	DON 93	3	1.2	62
J05078+179	...	2	1.1	50
J05333+448	BH 76	6	2.3	8.3
J06400+285	...	3	1.0	20
J08066+558	...	4	3.2	26
J08082+211	...	2	3.8	33
J08595+537	...	2	1.1	19
J11355+389	...	5	3.0	31
J11521+039	...	2	1.1	15
J12332+090	REU 1	8	2.1	16
J13180+022	...	4	3.1	73
J14210+275	...	2	3.0	97
J16487+106	...	3	1.1	10
J17530+169	...	5	3.0	110
J20407+199	RAO 23	2	2.8	8.4
J21518+136	...	3	3.0	66

Table 5. Astrometric properties of previously known imaging companions at $\rho < 5$ arcsec not resolved or detected in our data.

Karmn	WDS	Discoverer code	ρ [arcsec]	θ [deg]	Epoch [a]	Ref. ^a	Δmag (band) [mag]
J00088+208	00089+2050	BEU 1	0.133	271.9	2012.02	Jan14a	1.59 (i')
J05085-181	05086-1810	WSI 72	0.07	44.4	2011.04	WD15	0.1 (K_s)
J04311+589	0.07		1965.702	Str77	0.5 (V)
J06523-051	06523-0510	WSI 125	0.18	149.6	2010.068	Mas01	0.5 (o)
J07307+481	0.054	...	1960.60	Harr81	...
J09177+462	09177+4612	JNN 68	0.204	37.5	2011.073	Bow15	0.102 (K_s)
J10513+361	10513+3607	BWL 26	0.206	119.60	2012.357	Bow15	3.3 (H)
J12290+417	12290+4144	BWL 31	0.0503	255.5	2011.469	Bow15	0.647 (H)
J16241+483	16240+4822	HEN 1	0.1387	295.4	2006.62	Mar07	2.781 (H_{cont})
J16354+350 ^b	16355+3501	BWL 44	0.092	25.62	2011.469	Bow15	0.406 (H)
J17177+116 ^c	1977	Chr78	...
J18387-144	18387-1429	HDS 2641	0.107	358	1991	DN00	0.04 (H_p)
J19122+028	19121+0254	AST 1	0.16	319.7	2007.36	WD15	0.80 (H)
J20298+096 ^d	20298+0941	AST 2	0.160	89.1	2012.66	Jan14a	2.72 (z')
J20433+553	20433+5521	LLO 1	0.854	20.2	2007.66	Ire08	5.06 (H)
J21013+332	21013+3314	JNN 288	0.142	34.0	2012.01	Jan14a	1.07 (i')
J21160+298E	21161+2951	BWL 56	0.0543	354.6	2011.47	Bow15	0.37 (H)
J21313-097	21313-0947	BLA 9	0.16	128.2	2005.33	WD15	1.12 (H)
J23174+196	23175+1937	BEU 23	0.145	220.2	2012.65	Jan14b	1.17 (J)

Notes. ^(a) Bow15: Bowler et al. 2015; Chr78: Christy 1978; DN00: Dommanget & Nys 2000; Harr81: Harrington et al. 1981; Ire08: Ireland et al. 2008; Jan14a: Janson et al. 2014a; Jan14b: Janson et al. 2014b; Mar07: Martinache et al. 2007; Mas01: Mason et al. 2001; Str77: Strand 1977; Tok15: Tokovinin et al. 2015; WD15: Ward-Duong et al. 2015 ^(b) The BWL 44 companion at 2.2 arcsec is optical. ^(c) Astrometric perturbation with a 10 a period estimation in Chr78. ^(d) Spectroscopic binary identified by Benedict et al. 2000 and resolved by Janson et al. 2014a for the first time.

from the Luyten Double Star Catalogue (Luyten 1997) and the Lowell Proper Motion Survey (Giclas et al. 1971). In Table A.6, we list for each wide system the WDS discoverer code, names, spectral types, and angular separation.

As a summary, of the 490 observed stars, 50 are M-dwarf primaries with M-type wide companions, four with white dwarf companions, one with an L-dwarf, and three with a T-dwarf secondary. In addition, 11 M secondaries have F(2), G(3), K(4) or white dwarf (3) primaries. Five tertiary M dwarfs are in triple systems involving K+M(1), G+K(1), K+DA(1) or K+K(2) primaries.

In our volume-limited sample are 25 M dwarf primaries with wide M, L, or T dwarf secondaries at separations larger than 5 arcsec. Although our search at wide separations is not complete, since we carried out a compilation from different studies in the literature, we estimated an increment in the multiplicity fraction of 6 % (25 systems out of 425 M dwarfs in our volume-limited sample), which added to the percentage estimated for pairs at separations closer than 0.2 arcsec, and spectroscopic binaries would translate into a minimum multiplicity fraction at all separations of $\sim 36\%$.

5. Summary

We obtained high-resolution images in the I band of 490 M dwarfs of the CARMENES input catalogue (Carmencita) with the lucky imaging instrument FastCam at the 1.5 m Telescopio Carlos Sánchez.

Among the 490 observed M dwarfs, we identified 80 physically bound companions in 76 systems, of which 30 are presented here for the first time, plus six unconfirmed companions. For all of them, we measured angular separations, position angles, and I -band magnitude differences. From the ΔI differences, together with 2MASS photometry, spectral type, and colour-magnitude relations for field M dwarfs, we estimated individual

I -band magnitudes and spectral types of each component. We also derived individual masses M and estimated orbital periods for these pairs from our own M - M_I relation. For these calculations, we used parallactic distances. When not available, we derived spectro-photometric distances from our determined M_I -spectral type relation.

For our observed sample, we determined a multiplicity fraction of $16.7 \pm 2.0\%$. However, our sample has a strong selection bias because we discarded M stars with previously known companions at separations smaller than 5 arcsec. To obtain an unbiased multiplicity fraction, we built a volume-limited sample of Carmencita stars observed with FastCam and similar high-resolution imagers. It contains 425 M0–5 dwarfs and is complete up to 86 % within 14 pc. For this sample, we derived a multiplicity fraction of $19.5 \pm 2.3\%$ in the completeness range of angular separations between 0.2 and 5.0 arcsec, which agrees with previously reported values (Leinert et al. 1997; Janson et al. 2012, 2014; Jódar et al. 2013; Ward-Duong et al. 2015). The multiplicity fraction is consistent with a flat distribution from M0 V to M5 V within Poissonian error bars, and has intermediate values between solar-type stars and very low mass stars and brown dwarfs in accordance with the decreasing tendency observed towards lower masses.

The distribution of the number of pairs as a function of projected physical separation has a maximum between 2.5 and 7.5 au and decreases at wider separations. The pairs with projected physical separations smaller than 50 au tend to have mass ratios higher than 0.8, while for larger separations this distribution is more uniform.

We estimated that 26 of our systems have orbital periods shorter than 50 a, of which 10 are newly discovered systems. In 17 of them, we were able to detect orbital variations within our own multi-epoch measurements. These systems are especially interesting for future astrometric follow-up for determining their orbital solutions and measuring dynamical masses.

Table 6. Known spectroscopic binaries in the observed sample.

Karmn	Spectroscopic binarity	Ref. ^a
J03346-048	SB3	Llam14
J03526+170	SB2	Bon13
J04252+080S	SB2	Llam14
J04352-161	SB2	RB09
J04488+100	SB2	Jeff16
J05019+099	SB2	Del99
J05032+213	SB2	Jeff16
J05078+179	SB1	Jeff16
J05342+103S ^b	SB	Rein12
J05466+441	SB2	Jeff16
J07418+050	SB2	Llam14
J08082+211	SB2	Shk10
J09011+019	SB2	Jeff16
J09120+279	SB2	Jeff16
J09143+526	SB1	Jeff16
J11036+136	SB1	Jeff16
J12142+006	SB2	Bon13
J12191+318	SB2	Jeff16
J12290+417	SB2	Jeff16
J14171+088	SB2	Jeff16
J14368+583	SB2	Jeff16
J15191-127	SB	Bon13
J16255+260	SB2	Jeff16
J16487+106	SB2	Jeff16
J16554-083S	SB	Pett84
J18411+247S	SB2	GR96
J19354+377	SB1	Jeff16
J20433+553	SB2	Ire08
J20445+089N ^c	SB1	Jeff16
J23096-019	SB2	Jeff16
J23174+382	SB2	Jeff16
J23318+199E	SB1	Del99
J23318+199W	SB1	Del99
J23573-129W	SB2	Jeff16

Notes. ^(a) Bon13: Bonfils et al. 2013; Del99: Delfosse et al. 1999; GR96: Gizis & Reid 1996; Ire08: Ireland et al. 2008; Jeff16: Jeffers et al. in prep; Llam14: Llamas 2014; Pett84: Pettersen et al. 1984; RB09: Reiners & Basri 2009; Rein12: Reiners et al. 2012; Shk10: Shkolnik et al. 2010 ^(b) From the spectral types and magnitude differences of the components, we infer that the spectroscopic binary is the B companion. ^(c) Equal-brightness close binary previously suggested by Cortés-Contreras et al. 2014.

For our volume-limited sample, we also collected from the literature the physically bound companions at separations closer than 0.2 arcsec and larger than 5 arcsec, and unresolved spectroscopic binaries. The addition of these systems may increase the multiplicity fraction derived in this work to at least 36 %, a value consistent with the $42 \pm 9\%$ obtained by Fischer & Marcy (1992). Nevertheless, the sample is not complete at separations beyond the completeness limit of our survey (0.2–5.0 arcsec) and, hence, this value must only be considered as a rough estimation.

Finally, we provided a complete sample of multiple M dwarfs useful for studying the effect of low-mass stellar multiplicity on planet formation with the help of CARMENES and other near-infrared high-resolution spectrographs.

Acknowledgements. We thank A. Pérez-Garrido for the provision and support of the FastCam reduction software and X. Bonfils for the supply of radial velocity measurements from the ESO HARPS GTO Program ID 072.C-0488. MCC thanks L. Peralta de Arriba, V. Pereira and H. M. Tabernero for their assis-

tance and valuable conversations. This article is based on observations made with the Telescopio Carlos Sánchez operated on the island of Tenerife jointly by the Instituto de Astrofísica de Canarias and the Universidad de La Laguna in the Spanish Observatorio del Teide. This research made use of SIMBAD, operated at Centre de Données astronomiques de Strasbourg (France), the NASA's Astrophysics Data System, the Washington Double Star catalogue (WDS) maintained at the U.S. Naval Observatory, and the Image Reduction and Analysis Facility (IRAF), distributed by the National Optical Astronomy Observatory and operated by the Association of Universities for Research in Astronomy (AURA) under a cooperative agreement with the National Science Foundation. CARMENES is funded by the German Max-Planck-Gesellschaft (MPG), the Spanish Consejo Superior de Investigaciones Científicas (CSIC), the European Union through FEDER/ERF funds, and the members of the CARMENES Consortium (Max-Planck Institut für Astronomie, Instituto de Astrofísica de Andalucía, Landessternwarte Königstuhl, Institut de Ciències de l'Espai, Institut für Astrophysik Göttingen, Universidad Complutense de Madrid, Thüringer Landessternwarte Tautenburg, Instituto de Astrofísica de Canarias, Hamburger Sternwarte, Centro de Astrobiología, and the Centro Astronómico Hispano-Alemán), with additional contributions by the Spanish Ministry of Economy, the state of Niedersachsen, the German Science Foundation (DFG), and by the Junta de Andalucía. Financial support was also provided by the Junta de Andalucía, and the Spanish Ministries of Science and Innovation and of Economy and Competitiveness, under grants 2011-FQM-7363, AP2009-0187, AYA2014-54348-C3-01/02/03-R, AYA2015-69350-C3-2-P, ESP2013-48391-C4-1-R, and ESP2014-57495-C2-2-R.

References

- Aberasturi, M., Caballero J. A., Montesinos B. et al. 2014, AJ, 148, 36
 Aitken, R. G. & Doolittle, E. 1932, *New general catalogue of double stars within 120° of the north pole*, Carnegie Institution of Washington, USA
 Alonso-Floriano, F. J., Morales, J. C., Caballero, J. A. et al. 2015, A&A, 577, A128
 Alonso-Floriano, F. J., Caballero, J. A., Cortés-Contreras, M., Solano, E. & Montes, D. 2015, A&A, 583, A85
 Amado, P. J., Quirrenbach, A., Caballero, J. A. et al. 2013, Highlights of Spanish Astrophysics VII, 842
 Ans dell, M., Gaidos, E., Mann, An. W. et al. 2015, ApJ, 798, 41
 Artigau, E., Kouach, D., Donati, J.-F. et al. 2014, Proc. SPIE, 9147, E15
 Baraffe, I., Homeier, D., Allard, F. & Chabrier, G. 2015 A&A, 577, A42
 Barrado y Navascués, D. 1998, A&A, 339, 831
 Barrado y Navascués, D., Stauffer, J. R. & Jayawardhana, R. 2004, ApJ, 614, 38
 Basri, G., Marcy, G. W. & Graham, J. R. 1996, ApJ, 458, 600
 Basri, G. & Reiners, A. 2006, AJ, 132, 663
 Bate, M. R. 2012, MNRAS, 419, 3115
 Behall, A.L. & Harrington, R.S. 1976, PASP 88, 204
 Béjar, V. J. S., Gauza, B., Caballero, J. A. et al. 2012, 17th Cambridge Workshop on Cool Stars, Stellar Systems, and the Sun, published on-line
 Bell, C. P., Mamajek, E. E. & Naylor, T. 2015, MNRAS, 454, 593
 Benavides, R. 2014, *El Observador de Estrellas Dobles*, 12, 21
 Benedict, G. F., McArthur, B. E., Franz, O. G. et al. 2000, AJ, 120, 1106
 Bergfors, C., Brandner, W., Janson, M. et al. 2010, A&A, 520, A54
 Beuzit, J.-L., Ségransan, D., Forveille, T. et al. 2004, A&A, 425, 997
 Bihain, G., Rebolo, R., Zapatero Osorio, M. R. et al. 2010, A&A, 519, A93
 Bonfils, X., Delfosse, X., Udry, S. et al. 2013, A&A, 549, A109
 Bonnarel, F., Fernique, P., Bienaymé, O. et al. 2000, A&AS, 143, 33
 Bouy, H., Brandner, W., Martín, E. L. et al. 2003, AJ, 126, 1526
 Bowler, B. P., Liu, M. C., Shkolnik, E. L. & Tamura, M. 2015, ApJS, 216, 7
 Burgasser, A. J., Kirkpatrick, J. D., Reid, I. N. et al. 2003, ApJ, 586, 512
 Burgasser, A. J., Reid, I. N., Siegler, N. et al. 2007, Protostars and Planets V, 427
 Caballero, J. A. 2007, ApJ, 667, 520
 Caballero, J. A. 2010, A&A, 514, A98
 Caballero, J. A., Cortés-Contreras, M., López-Santiago, J. et al. 2013, Highlights of Spanish Astrophysics VII, 645
 Charbonneau, D., Berta, Z. K., Irwin, J. et al. 2009, Nature, 462, 891
 Christy, J. M. 1978, AJ, 83, 10
 Cortés-Contreras, M., Caballero, J. A., Alonso-Floriano, F. J. et al. 2013, Highlights of Spanish Astrophysics VII, 646
 Cortés-Contreras, M., Caballero, J. A. & Montes, D. 2014, The Observatory, 134, 348
 Cortés-Contreras, M., Béjar, V. J. S., Caballero, J. A. et al. 2015, Highlights of Spanish Astrophysics VIII, 597
 Cortés-Contreras, M., Caballero, J. A., Béjar, V. J. S. et al. 2015, 18th Cambridge Workshop on Cool Stars, Stellar Systems, and the Sun, 805
 Close, L. M., Siegler, N., Freed, M. & Biller, B. 2003, ApJ, 587, 407
 Cruz, K. L., Reid, I. N., Liebert, J. et al. 2003, AJ, 126, 2421
 Dawson, P. C. & De Robertis, M. M. 2005, PASP 117, 1

- Deacon, N. R., Liu, M. C., Magnier, E. A. et al. 2012, ApJ, 757, 100
 Delfosse, X., Forveille, T., Beuzit, J.-L. et al. 1999, A&A, 344, 897
 Desidera, S., Carolo, E., Gratton, R. et al. 2011 A&A, 533, A90
 Dieterich, S. B., Henry, T. J., Goliowski, D. A. et al. 2012, AJ, 144, 64
 Dittmann, J. A., Irwin, J. M., Charbonneau, D. & Berta-Thompson, Z. K. 2014, ApJ 784, 156
 Dommanget, J. & Nys, O. 2000, A&A, 363, 991
 Duchêne, G. & Kraus, A. 2013, ARA&A, 51, 269
 Duquennoy, A. & Mayor, M. 1991, A&A, 248, 485
 Fischer, D. A. & Marcy, G. W. 1992, ApJ, 396, 178
 Freedman, D & Diaconis, P. 1981, *Probability Theory and Related Field*, 57, 4, 453
 García-Piquer, A., Morales, J. C., Ribas, I. et al. 2016, A&A, submitted
 Gatewood, G. & Coban, L. 2009, AJ, 137, 402
 Giannuzzi, M. A. 1979, A&A, 77, 214
 Giclas H. L., Burnham Jr. R. & Thomas N.G. 1971, *Lowell proper motion survey Northern Hemisphere*, Lowell Observatory, Flagstaff, Arizona
 Gigoyan, K. S., Sinamyan, P. K., Engels, D. & Mickaelian, A. M. 2010, Astrophysics, 53, 123
 Ginski, C., Mugrauer, M., Seeliger, M. et al. 2015, MNRAS, 457, 2173
 Gizis J. E. & Reid I. N. 1996 AJ, 111, 365
 Gizis, J. E., Reid, I. N. & Hawley, S. L. et al. 2002, AJ, 123, 3356
 Goldman, B., Bouy, H., Zapatero Osorio, M. R. et al. 2008, A&A, 490, 763
 Goodwin, S. P., Kroupa, P., Goodman, A. & Burkert, A. 2007, Protostars and Planets V, 133
 Gray, R. O., Corbally, C. J., Garrison, R. F. et al. 2003, AJ, 126, 2048
 Gray, R. O., Corbally, C. J., Garrison, R. F. et al. 2006, AJ, 132, 161
 Guenther, E. W. & Wuchterl, G. 2003, A&A, 401, 677
 Guenther, E. W. & Tal-Or, L. 2010, A&A, 521, A83
 Hartkopf, W. I. & Mason, B.D. 2011, AJ, 142, 56
 Harrington, R. S. & Dahn C. C. 1980, AJ, 85, 454
 Harrington, R. S., Christy, J. W. & Strand, K. A. 1981, AJ, 86, 909
 Hawley, S. L., Gizis, J. E. & Reid, I. N. 1996, AJ, 112, 2799
 Henry, T. J. 2004, ASPC, 318, 159
 Henry, T. J., Jao, W.-C., Subasavage, J. P. et al. 2006, AJ, 132, 2360
 Hershey, J. L. & Taff, L. G. 1998, AJ, 116, 1440
 Ireland, M. J., Kraus, A., Martinache, F. et al. 2008 ApJ, 678, 463
 Jeffries, R. D. & Maxted, P. F. L. 2005, AN, 326, 944
 Janson, M., Hormuth, F., Bergfors, C. et al. 2012, ApJ, 754, 44
 Janson, M., Lafrenière, D., Jayawardhana, R. et al. 2013, ApJ, 773, 170
 Janson, M., Bergfors, C., Brandner, W. et al. 2014, ApJ, 789, 102
 Janson, M., Bergfors, C., Brandner, W. et al. 2014, ApJS, 214, 17
 Jenkins, L. F. 1952, *General catalogue of trigonometric stellar parallaxes*, Yale University Observatory, USA
 Jenkins, L. F. 1963, *General catalogue of trigonometric stellar parallaxes*, Yale University Observatory, USA
 Jenkins, J. S., Ramsey, L. W., Jones, H. R. A. et al. 2009 ApJ, 704, 975
 Joergens, V. 2008, A&A, 492, 545
 Jódar, E., Pérez-Garrido, A., Díaz-Sánchez, A. et al. 2013, MNRAS, 429, 859
 Kirkpatrick, J. D. & McCarthy, D. W. Jr 1994, AJ, 107, 333
 Klutsch, A., Freire Ferrero, R., Guillout, P. et al. 2014, A&A, 567, A52
 Koen, C., Kilkenny, D., van Wyk, F. & Marang, F. 2010, MNRAS, 403, 1949
 Labadie, L., Rebolo, R., Femenía, B. et al. 2010, Proc. SPIE, 7735, E0X
 Lafrenière, D., Doyon, R., Marois, C. et al. 2007, ApJ, 670, 1367
 Law, N. M. 2006, PhD thesis, Institute of Astronomy & Selwyn College, Cambridge University, UK
 Law, N. M., Hodgkin, S. T. & Mackay, C. D. 2008, MNRAS, 384, 150
 Leinert, C., Henry, T., Glindemann, A. & McCarthy, D. W. Jr. 1997, A&A, 325, 159
 Lépine, S., Hilton, E. J., Mann, A. W. et al. 2013 AJ, 145, 102
 Llamas, M. 2014, MSc thesis, Universidad Complutense de Madrid, Spain
 Losse, F. 2010, Observations & Travaux, 75, 17
 Luhman, K. L. 2012, ARA&A, 50, 65
 Luyten, W. J. 1997, VizieR Online Data Catalog I/130, *LDS Catalogue: Doubles with Common Proper Motion (Luyten 1940-87)*, Originally published in: Publ. Astr. Obs. Univ. Minnesota III, part 3, 35, and Proper motion survey with the 48-inch Schmidt Telescope XXI, XXV, XIX, XL, L, LXIV, LV, LXXI, Univ. Minnes. (1940-1987)
 Mahadevan, S., Ramsey, L. W., Terrien, R. et al. 2014, Proc. SPIE, 9147, E1G
 Mamajek, E. E., Bartlett, J. L., Seifahrt, A. et al. 2013, AJ, 146, 154
 Martinache, F., Lloyd, J. P., Ireland, M. J. et al. 2007, ApJ, 661, 496
 Mason, B. D., Wycoff, G. L., Hartkopf, W. I., Douglass G. G. & Worley C.E. 2001, AJ, 122, 3466
 Mason, B. D., Hartkopf, W. I. & Friedman, E. A. 2012, AJ, 143, 124
 Mason, B. D., Hartkopf, W. I. & Hurowitz, H. M. 2013, AJ, 146, 56
 Montagnier, G., Ségransan, D., Beuzit, J.-L., et al. 2006 A&A, 460, L19
 Montes, D., López-Santiago, J., Gálvez, M. C. et al. 2001, MNRAS, 328, 45
 Montes, D., Caballero, J. A., Jeffers, S. et al. 2015, Highlights of Spanish Astrophysics VIII, 605
 Montes, D., Caballero, J. A., Gallardo, I. et al. 2016, IAUS, 314, 71
 Morrison, J. E., Röser, S., McLean, B. et al. 2001, AJ, 121, 1752
 Newton, E. R., Charbonneau, D., Irwin, J., et al. 2014, AJ, 147, 20
 Oscoz, A., Rebolo, R., López, R. et al. 2008, Proc. SPIE, 7014, E47
 Peña-Ramírez, K., Béjar, V. J. S. & Zapatero Osorio, M. R. 2016, A&A, 586, A157
 Pettersen, B.R., Evans, D.S. & Coleman, L.A. 1984, ApJ, 282, 214
 Quirrenbach, A., Amado, P. J., Caballero, J. A., et al. 2014, Proc. SPIE, 9147, E1F
 Quirrenbach, A., Caballero, J. A., Amado, P. J. et al. 2015, 18th Cambridge Workshop on Cool Stars, Stellar Systems, and the Sun, 18, 897
 Raghavan, D., McAlister, H. A., Henry, T. J. et al. 2010, ApJS, 190, 1
 Reggiani, M. & Meyer, M. R. 2011, ApJ, 738, 60
 Reggiani, M. & Meyer, M. R. 2013, A&A, 553, A124
 Reiners, A. & Basri, G. 2009, ApJ, 705, 1416
 Reiners, A., Joshi, N. & Goldman, B. 2012, AJ, 143, 93
 Reid, I. N., Hawley, S. L. & Gizis, J. E. 1995, AJ, 110, 1838
 Reid, I. N. & Gizis, J. E. 1997, AJ, 113, 2246
 Reid, I. N. & Cruz, K. L. 2002, AJ, 123, 2806
 Reid, I. N., Cruz, K. L., Burgasser, A. J. et al. 2004, AJ, 128, 463
 Reid I. N., Cruz, K. L., Burgasser, A. J. & Liu, M. C. 2008, AJ, 135, 580
 Riedel, A. R., Subasavage, J. P., Finch, C. T. et al. 2010, AJ, 140, 897
 Riedel, A. R., Finch, C. T., Henry, T. J. et al. 2014, AJ, 147, 85
 Riaz, B., Gizis, J. E. & Harvin, J. 2006, AJ, 132, 866
 Röser, S., Demleitner, M. & Schilbach, E. 2010, AJ, 139, 2440
 Rivera, E. J., Lissauer, J. J., Butler, R. P. et al. 2005, ApJ, 634, 625
 Sarajedini, A., Bedin, L. R., Chaboyer, B. et al. 2007, AJ, 133, 1658
 Scardia, M., Ghiringhelli, D. & Debehogne, H. 1995, AN, 316, 125
 Scardia, M., Prieur, J. L., Pansecchi, L., Argyle, R.W. & Sala, M. 2011, AN, 332, 508
 Scardia, M., Prieur, J. L., Pansecchi, L. et al. 2013, MNRAS, 434, 2803
 Scholz, R.-D., Meusinger, H. & Jahreiß, H. 2005, A&A, 442, 211
 Shan, Y., Johnson, J. A. & Morton, T. D. 2015, ApJ, 813, 75
 Shkolnik, E. L., Hebb, L., Liu, M. C. et al. 2010, ApJ, 716, 1522
 Siegler, N., Close, L. M., Cruz, K. L. et al. 2005, ApJ, 621, 1023
 Silvestri, N. M., Hawley, S. L., Oswalt, T. D. 2005, AJ, 129, 2428
 Simon-Díaz, S., Caballero, J. A., Lorenzo, J. et al. 2015, ApJ, 799, 169
 Soderblom, D. R. & Mayor, M. 1993, AJ, 105, 226
 Strand K. Aa. 1977, AJ, 82, 9
 Subasavage, J. P., Jao, W.-C., Henry, T. J. et al. 2009, AJ, 137, 4547
 Tamura, M., Suto, H., Nishikawa, J. et al. 2012, Proc. SPIE, 8446, E1T
 Thorel, J. C., Thorel, Y. & Verhas, P. 2011, Observations & Travaux 78, 20
 Tody, D. 1986, Proc. SPIE, 627, 733
 Tokovinin, A. 2008, MNRAS, 389, 925
 Tokovinin, A. 2011, AJ, 141, 52
 Tokovinin, A., Mason, B. D., Hartkopf, W. I. et al. 2015, AJ, 150, 50
 van Altena, W. F., Lee, J. T. & Hoffleit, D. 1995, *General catalogue of trigonometric stellar parallaxes*, Yale University Observatory, USA
 van Leeuwen, F. 2007, A&A, 474, 653
 Wang, J., Xie, J.-W., Barclay, T. & Fischer, D. A. 2014a, ApJ, 783, 4
 Wang, J., Fischer, D. A., Xie, J.-W. & Ciardi, D. R. 2014b ApJ 791, 111
 Wang, J., Fischer, D. A., Horch, E. P. & Xie, J.-W 2015a, ApJ, 806, 248
 Wang, J., Fischer, D. A., Xie, J.-W & Ciardi, D. R. 2015b, ApJ, 813, 130
 Weinberger, A. J., Boss, A. P., Keiser, S. A. et al. 2016, AJ, 152, 24
 Ward-Duong, K., Patience, J., De Rosa, R. J. et al. 2015, MNRAS, 449, 2618
 Zuckerman B. & Song I. 2014, ARA&A, 42, 685

Appendix A: Long tables

Table A.1. Log of observed stars.

No.	Karmn	Name	α (J2000)	δ (J2000)	J [mag]	SpT	Ref. ^a	d [pc]	Ref. ^b	Observation date	N × t_{exp} [s]
1	J00067-075	GJ 1002	00:06:43.26	-07:32:14.7	8.323	M5.5 V	PMSU	4.82	Wein16	23 Oct 2011	10 × 50
2	J00088+208	LP 404-033	00:08:53.92	+20:50:25.2	8.870	M4.5 V	PMSU	14.8	Dit14	24 Oct 2011	10 × 50
3	J00154-161	GJ 1005 AB	00:15:27.99	-16:08:00.9	7.215	M4.0 V	PMSU	6.0	HT98	10 Jul 2012	10 × 50
4	J00158+135	GJ 12	00:15:49.20	+13:33:21.9	8.619	M3.0 V	PMSU	10.0	Dit14	16 Sep 2012	10 × 50
5	J00169+051	GJ 1007	00:16:56.29	+05:07:26.1	9.398	M4.5 V	PMSU	17.57	vAl95	25 Oct 2011	10 × 50
6	J00169+200	G 131-047	00:16:56.78	+20:03:55.1	9.681	M3.5 V	PMSU	24.5	This work	14 Jan 2013	10 × 50
										17 Nov 2015	10 × 50
7	J00182+102	GJ 16	00:18:16.59	+10:12:10.1	7.564	M1.5 V	PMSU	16.34	HIP2	17 Nov 2015	10 × 50
8	J00183+440	GX And	00:18:22.57	+44:01:22.2	5.252	M1.0 V	AF15	3.59	HIP2	23 Oct 2011	10 × 35
9	J00184+440	GQ And	00:18:25.50	+44:01:37.6	6.789	M3.5 V	PMSU	3.6	Dit14	23 Oct 2011	10 × 35
										17 Sep 2012	10 × 50
										13 Jan 2013	10 × 50
10	J00188+278	LP 292-066	00:18:53.53	+27:48:50.0	9.535	M4.0 V	PMSU	14.5	Dit14	25 Oct 2011	10 × 50
11	J00234+243	GJ 1011	00:23:28.03	+24:18:24.4	9.753	M4.0 V	PMSU	16.39	vAl95	25 Oct 2011	10 × 50
12	J00245+300	G 130-068	00:24:34.78	+30:02:29.5	9.776	M4.5 V	PMSU	18.94	vAl95	24 Oct 2011	10 × 50
13	J00253+228	LP 349-018	00:25:20.64	+22:53:12.1	9.716	M4.0 V	PMSU	14.2	Dit14	24 Oct 2011	10 × 50
14	J00271+496	G 217-051	00:27:06.74	+49:41:53.1	9.733	M4.5 V	PMSU	20.9	Dit14	25 Oct 2011	10 × 50
15	J00286-066	GJ 1012	00:28:39.48	-06:39:48.1	8.038	M4.0 V	PMSU	13.26	Rei02	25 Oct 2011	10 × 50
16	J00315-058	GJ 1013	00:31:35.39	-05:52:11.6	8.762	M3.5 V	PMSU	16.1	vAl95	16 Sep 2012	10 × 50
17	J00385+514	G 172-015	00:38:33.88	+51:27:58.0	8.892	M2.5 V	PMSU	15.6	vAl95	14 Jan 2013	10 × 50
18	J00389+306	Wolf 1056	00:38:58.79	+30:36:58.4	7.453	M2.5 V	AF15	12.5	vAl95	16 Sep 2012	10 × 50
19	J00409+313	G 069-011	00:40:56.23	+31:22:56.5	9.491	M4.0 V	PMSU	17.7	Dit14	24 Oct 2011	10 × 50
20	J00413+558	GJ 1015 A	00:41:20.78	+55:50:04.5	9.839	M4.0 V	PMSU	23.04	vAl95	25 Oct 2011	10 × 50
21	J00443+126	G 032-044	00:44:19.34	+12:37:02.7	8.868	M3.5 V	PMSU	16.5	This work	16 Sep 2012	10 × 50
22	J00443+091	NLTT 2413	00:44:20.70	+09:07:34.6	9.501	M4.5 V	PMSU	14.6	This work	25 Oct 2011	10 × 50
23	J00566+174	GJ 1024	00:56:38.42	+17:27:34.7	9.285	M4.0 V	PMSU	17.73	vAl95	25 Oct 2011	10 × 50
24	J00570+450	G 172-030	00:57:02.61	+45:05:09.9	8.101	M3.0 V	Lep13	13.8	This work	17 Nov 2015	10 × 50
25	J01009-044	GJ 1025	01:00:56.44	-04:26:56.1	9.042	M4.0 V	AF15	14.7	This work	16 Sep 2012	10 × 50
26	J01026+623	BD+61 195	01:02:38.96	+62:20:42.2	6.230	M1.5 V	AF15	9.96	HIP2	17 Sep 2012	10 × 50
										13 Jan 2013	10 × 50
27	J01033+623	V388 Cas	01:03:19.72	+62:21:55.7	8.611	M5.0 V	AF15	9.96	aHIP2	23 Oct 2011	10 × 50
28	J01056+284	GJ 1029	01:05:37.32	+28:29:34.0	9.486	M5.0 V	PMSU	11.3	Dit14	25 Oct 2011	10 × 50
29	J01066+152	GJ 1030	01:06:41.52	+15:16:22.9	8.005	M2.0 V	PMSU	22.1	HIP2	17 Sep 2012	10 × 50
30	J01119+049N	G 070-043	01:11:55.63	+04:55:04.9	8.804	M3.0 V	PMSU	15.9	vAl95	24 Oct 2011	10 × 50
31	J01119+049S	G 070-044	01:11:57.99	+04:54:12.0	9.641	M3.5 V	PMSU	15.9	avAl95	24 Oct 2011	10 × 50
32	J01182-128	GJ 56.1	01:18:15.99	-12:53:58.1	8.356	M2.0 V	PMSU	22.1	HIP2	17 Sep 2012	10 × 50
33	J01221+221	G 034-023	01:22:10.28	+22:09:03.2	8.412	M4.5 V	Lep13	10.2	This work	17 Nov 2015	10 × 50
34	J01384+006	G 071-024	01:38:29.98	+00:39:05.9	8.189	M2.0 V	PMSU	20.2	HIP2	17 Sep 2012	10 × 50
35	J01402+317	G 072-023	01:40:16.49	+31:47:30.7	9.437	M4.0 V	PMSU	18.7	Dit14	25 Oct 2011	10 × 50
36	J01433+043	GJ 70	01:43:20.15	+04:19:17.2	7.370	M2.0 V	PMSU	11.4	HIP2	17 Sep 2012	10 × 50
37	J01449+163	Wolf 1530	01:44:58.52	+16:20:39.7	9.584	M4.0 V	PMSU	16.39	vAl95	24 Oct 2011	10 × 50

Table A.1. Log of observed stars (continued).

No.	Karmn	Name	α (J2000)	δ (J2000)	J [mag]	SpT	Ref. ^a	d [pc]	Ref. ^b	Observation date	N × t_{exp} [s]
38	J01453+465	G 173-018	01:45:18.20	+46:32:07.8	8.058	M2.0 V	Lep13	25.63	HIP2	17 Nov 2015	10 × 50
39	J01510-061	NLTT 6192	01:51:04.05	-06:07:04.8	9.413	M4.5 V	PMSU	9.92	Hen06	25 Oct 2011	10 × 50
40	J01518-108	Ross 555	01:51:48.65	-10:48:12.0	8.375	M2.0 V	PMSU	16.6	HIP2	17 Sep 2012	10 × 50
41	J01518+644	G 244-037	01:51:51.08	+64:26:06.1	7.838	M2.5 V	PMSU	14.7	This work	17 Sep 2012	10 × 50
42	J01593+585	V596 Cas	01:59:23.50	+58:31:16.2	7.790	M4.0 V	PMSU	12.25	HIP2	23 Oct 2011	10 × 50
										17 Sep 2012	10 × 50
										13 Jan 2013	10 × 50
43	J02022+103	LP 469-067	02:02:16.21	+10:20:13.7	9.842	M5.5 V	AF15	9.19	Wein16	25 Oct 2011	10 × 50
44	J02044-018	G 159-034	02:04:27.55	-01:52:56.1	9.585	M4.0 V	PMSU	18.8	This work	25 Oct 2011	10 × 50
45	J02070+496	G 173-037	02:07:03.83	+49:38:44.1	8.366	M3.5 V	Lep13	17.4	Dit14	17 Nov 2015	10 × 50
46	J02088+494	G 173-039	02:08:53.60	+49:26:56.6	8.423	M3.5 V	PMSU	13.4	This work	17 Sep 2012	10 × 50
47	J02096-143	LP 709-040	02:09:36.09	-14:21:32.1	8.122	M2.5 V	PMSU	19.7	HIP2	14 Jan 2013	10 × 50
48	J02129+000	G 159-046	02:12:54.58	+00:00:16.8	9.055	M4.0 V	PMSU	10.0	Dit14	23 Oct 2011	10 × 50
49	J02149+174	GJ 1045	02:14:59.79	+17:25:09.0	9.966	M4.0 V	PMSU	20.41	vAl95	24 Oct 2011	10 × 50
50	J02155+339	G 074-011	02:15:34.38	+33:57:41.8	9.320	M3.5 V	PMSU	20.3	This work	14 Jan 2013	10 × 50
51	J02158-126	LP 709-062	02:15:48.83	-12:40:27.7	9.051	M3.5 V	PMSU	17.9	This work	17 Sep 2012	10 × 50
52	J02164+135	LP 469-206	02:16:29.78	+13:35:13.7	9.871	M5.5 V	PMSU	8.496	vAl95	24 Oct 2011	10 × 50
53	J02171+354	LP 245-010	02:17:09.93	+35:26:33.0	9.983	M5.0 V	PMSU	10.37	vAl95	25 Oct 2011	10 × 50
54	J02190+238	LT T 10787	02:19:02.29	+23:52:55.1	9.777	M4.0 V	PMSU	20.6	Dit14	25 Oct 2011	10 × 50
55	J02190+353	Ross 19	02:19:03.06	+35:21:18.2	8.662	M3.5 V	PMSU	17.7	vAl95	17 Sep 2012	10 × 50
56	J02256+375	G 074-025	02:25:38.42	+37:32:34.0	9.712	M4.0 V	PMSU	21.6	Dit14	25 Oct 2011	10 × 50
57	J02358+202	BD+19 381	02:35:53.28	+20:13:11.9	7.208	M2.0 V	PMSU	13.6	HIP2	17 Sep 2012	10 × 50
58	J02362+068	BX Cet	02:36:15.36	+06:52:19.1	7.333	M4.0 V	AF15	7.18	aHIP2	23 Oct 2011	10 × 50
59	J02392+074	G 076-019	02:39:17.35	+07:28:17.0	9.881	M4.0 V	PMSU	20.3	Dit14	25 Oct 2011	10 × 50
60	J02442+255	VX Ari	02:44:15.38	+25:31:25.0	6.752	M3.0 V	PMSU	7.51	HIP2	24 Oct 2011	10 × 50
61	J02518+294	LP 298-042	02:51:49.73	+29:29:13.2	9.518	M4.0 V	PMSU	22.7	Dit14	24 Oct 2011	10 × 50
										17 Nov 2015	20 × 50
										07 Jan 2016	20 × 50
62	J02519+224	RBS 365	02:51:54.09	+22:27:30.0	8.919	M4.0 V	Ria06	13.9	This work	17 Nov 2015	10 × 50
63	J02530+168	Teegarden's Star	02:53:00.85	+16:52:53.3	8.394	M7.0 V	AF15	3.84	Wein16	23 Oct 2011	10 × 50
64	J02555+268	HD 18143 C	02:55:35.73	+26:52:20.9	9.561	M4.0 V	AF15	23.49	aHIP2	25 Oct 2011	10 × 50
65	J02565+554W	Ross 364	02:56:34.35	+55:26:14.5	7.425	M1.0 V	PMSU	19.5	vAl95	17 Sep 2012	10 × 50
66	J02565+554E	Ross 365	02:56:35.07	+55:26:30.2	8.006	M3.0 V	PMSU	19.5	avAl95	17 Sep 2012	10 × 50
										13 Jan 2013	10 × 50
67	J02575+107	Ross 791	02:57:31.04	+10:47:24.6	9.162	M3.0 V	PMSU	20.0	vAl95	14 Jan 2013	10 × 50
68	J02591+366	Ross 331	02:59:10.60	+36:36:40.3	9.064	M3.5 V	PMSU	18.87	Daw05	14 Jan 2013	10 × 50
69	J03047+617	G 246-022	03:04:43.35	+61:44:09.7	8.877	M3.0 V	AF15	24.2	aHIP2	17 Sep 2012	10 × 50
70	J03102+059	EK Cet	03:10:15.47	+05:54:31.1	8.363	M2.0 V	PMSU	16.9	HIP2	17 Sep 2012	10 × 50
71	J03133+047	CD Cet	03:13:23.00	+04:46:29.4	8.775	M5.0 V	PMSU	8.62	Wein16	23 Oct 2011	10 × 50
72	J03181+382	HD 275122	03:18:07.42	+38:15:08.2	7.023	M1.5 V	PMSU	15.53	HIP2	09 Dec 2014	10 × 50
73	J03233+116	G 005-032	03:23:22.41	+11:41:13.4	8.386	M2.5 V	PMSU	18.3	vAl95	17 Sep 2012	10 × 50
74	J03242+237	GJ 140C	03:24:12.81	+23:46:19.3	8.276	M2.0 V	PMSU	19.49	aHIP2	13 Jan 2013	10 × 50

Table A.1. Log of observed stars (continued).

No.	Karmn	Name	α (J2000)	δ (J2000)	J [mag]	SpT	Ref. ^a	d [pc]	Ref. ^b	Observation date	N × t_{exp} [s]
75	J03288+264	LP 356–106	03:28:49.58	+26:29:12.2	9.288	M3.0 V	PMSU	15.0	Dit14	14 Jan 2013	10 × 50
76	J03317+143	GJ 143.3	03:31:47.12	+14:19:19.4	8.695	M2.0 V	PMSU	22.9	HIP2	14 Jan 2013	10 × 50
77	J03346-048	LP 653–008	03:34:39.59	-04:50:32.9	8.829	M3.5 V	PMSU	29.2	Ried10	13 Jan 2013	10 × 50
78	J03366+034	[R78b] 233	03:36:40.84	+03:29:19.5	9.295	M4.5 V	PMSU	13.3	This work	23 Oct 2011	10 × 50
79	J03394+249	KP Tau	03:39:29.72	+24:58:02.9	8.813	M3.0 V	PMSU	19.2	Dit14	24 Oct 2011	10 × 50
80	J03396+254E	Wolf 204	03:39:36.21	+25:28:20.3	8.747	M3.0 V	PMSU	21.3	bvAl95	24 Oct 2011	10 × 50
81	J03396+254W	Wolf 205	03:39:40.51	+25:28:47.7	9.079	M3.5 V	PMSU	21.3	vAl95	14 Jan 2013	10 × 50
82	J03437+166	BD+16 502B	03:43:45.22	+16:40:02.7	7.533	M1.0 V	PMSU	16.69	HIP2	09 Dec 2014	10 × 50
83	J03438+166	BD+16 502A	03:43:52.53	+16:40:19.9	7.406	M0.0 V	Lep13	17.71	HIP2	09 Dec 2014	10 × 50
84	J03463+262	HD 23453	03:46:20.12	+26:12:56.0	6.689	M0.0 V	PMSU	14.75	HIP2	09 Dec 2014	10 × 50
85	J03473+086	LT T 11262	03:47:20.91	+08:41:46.4	9.849	M4.5 V	PMSU	14.39	vAl95	23 Oct 2011	10 × 50
86	J03507-060	GJ 1065	03:50:44.32	-06:05:40.0	8.570	M3.5 V	PMSU	9.5	vAl95	13 Jan 2013	10 × 50
87	J03526+170	Wolf 227	03:52:41.69	+17:01:05.7	8.933	M4.5 V	PMSU	9.8	Dit14	24 Oct 2011	10 × 50
88	J03531+625	Ross 567	03:53:10.42	+62:34:08.2	7.782	M3.0 V	Lep13	11.9	This work	09 Dec 2014	10 × 50
89	J03574-011	BD-01 565B	03:57:28.92	-01:09:23.2	7.773	M2.5 V	AF15	15.5	aHIP2	13 Jan 2013	10 × 50
90	J03598+260	Ross 873	03:59:53.55	+26:05:24.1	8.714	M3.0 V	PMSU	22.8	vAl95	13 Jan 2013	10 × 50
91	J04122+647	G 247–015	04:12:16.93	+64:43:56.1	9.156	M4.0 V	PMSU	11.79	vAl95	13 Jan 2013	10 × 50
92	J04148+277	HG 8-1	04:14:53.49	+27:45:28.4	8.763	M3.5 V	Lep13	15.7	This work	17 Nov 2015	10 × 50
93	J04153-076	σ^2 Eri C	04:15:21.73	-07:39:17.4	6.747	M4.5 V	AF15	4.98	aHIP2	25 Oct 2011	10 × 50
94	J04173+088	LT T 11392	04:17:18.52	+08:49:22.1	9.030	M4.5 V	PMSU	14.8	Dit14	23 Oct 2011	10 × 50
95	J04218+213	G 008–029	04:21:50.06	+21:19:43.4	9.080	M3.5 V	PMSU	18.2	This work	13 Jan 2013	10 × 50
96	J04225+105	LSPM J0422+1031	04:22:31.99	+10:31:18.8	8.471	M3.5 V	Lep13	25.4	Dit14	02 Mar 2014	10 × 50
97	J04248+324	G 039–011	04:24:49.19	+32:26:58.4	8.818	M2.0 V	PMSU	26.0	This work	14 Jan 2013	10 × 50
98	J04252+080S	HG 7–206	04:25:15.07	+08:02:55.9	8.908	M2.5 V	PMSU	28.5	This work	14 Jan 2013	10 × 50
99	J04278+117	NLT T 13316	04:27:53.52	+11:46:54.8	9.699	M4.0 V	PMSU	25.1	Dit14	25 Oct 2011	10 × 50
100	J04290+219	BD+21 652	04:29:00.14	+21:55:21.5	5.674	M0.5 V	Gra06	11.39	HIP2	17 Nov 2015	10 × 50
101	J04293+142	LT T 11438	04:29:18.47	+14:13:59.5	9.350	M4.0 V	PMSU	16.9	This work	23 Oct 2011	10 × 50
102	J04304+398	V546 Per	04:30:25.27	+39:51:00.1	9.113	M4.5 V	PMSU	10.43	vAl95	24 Oct 2011	10 × 50
103	J04311+589	STN 2051 A	04:31:11.48	+58:58:37.6	6.622	M4.0 V	PMSU	5.62	HD80	25 Oct 2011	10 × 50
104	J04335+207	G 008–041	04:33:33.93	+20:44:46.2	9.769	M4.0 V	PMSU	13.6	Dit14	23 Oct 2011	10 × 50
105	J04352-161	LP 775–031	04:35:16.13	-16:06:57.5	10.406	M7.0 V	Cru03	10.46	Wein16	01 Mar 2014	10 × 50
106	J04376-110	BD-11 916	04:37:41.88	-11:02:19.8	6.943	M1.5 V	PMSU	11.1	HIP2	02 Mar 2014	10 × 50
107	J04376+528	BD+52 857	04:37:40.92	+52:53:37.2	5.866	M0.0 V	Gra03	10.11	HIP2	17 Nov 2015	10 × 50
108	J04429+189	HD 285968	04:42:55.81	+18:57:28.5	6.462	M2.0 V	PMSU	9.3	HIP2	31 Jan 2012	10 × 50
109	J04429+214	2M J04425586+2128230	04:42:55.86	+21:28:23.0	7.958	M3.5 V	Lep13	10.8	This work	02 Mar 2014	10 × 50
110	J04488+100	1RXS J044847.6+100302	04:48:47.39	+10:03:02.6	8.127	M3.0 V	Lep13	15.2	This work	02 Mar 2014	10 × 50
111	J04508+221	GJ 1072	04:50:50.83	+22:07:22.5	9.896	M5.0 V	PMSU	12.3	Dit14	23 Oct 2011	10 × 50
112	J04520+064	Wolf 1539	04:52:05.73	+06:28:35.6	7.814	M3.5 V	PMSU	12.29	HIP2	25 Oct 2011	10 × 50
113	J04525+407	GJ 1073	04:52:34.48	+40:42:25.5	9.071	M4.0 V	PMSU	12.7	Dit14	24 Oct 2011	10 × 50
114	J04538-177	GJ 180	04:53:49.95	-17:46:23.5	7.413	M2.0 V	PMSU	12.1	HIP2	14 Jan 2013	10 × 50
115	J04588+498	BD+49 1280	04:58:50.58	+49:50:57.3	6.925	M0.0 V	PMSU	16.31	HIP2	01 Mar 2014	10 × 50
116	J04595+017	V1005 Ori	04:59:34.83	+01:47:00.7	7.117	M0.0 V	PMSU	25.88	HIP2	28 Feb 2014	10 × 50

Table A.1. Log of observed stars (continued).

No.	Karmn	Name	α (J2000)	δ (J2000)	J [mag]	SpT	Ref. ^a	d [pc]	Ref. ^b	Observation date	N × t_{exp} [s]
117	J05019+099	LP 476–207 AB	05:01:58.81	+09:58:58.8	7.212	M4.0 V	PMSU	24.88	Ried14	01 Mar 2014	10 × 50
118	J05012+248	Ross 794	05:01:15.51	+24:52:24.5	8.084	M2.0 V	PMSU	29.1	vAl95	28 Feb 2014	10 × 50
119	J05032+213	HD 285190 A	05:03:16.08	+21:23:56.4	7.451	M1.5 V	AF15	27.4	vAl95	31 Jan 2012	10 × 50
										23 Oct 2011	10 × 50
120	J05033-173	LP 779–046	05:03:20.10	-17:22:24.5	7.819	M3.0 V	PMSU	9.2	HIP2	14 Jan 2013	10 × 50
121	J05034+531	BD+52 911	05:03:24.02	+53:07:41.2	7.001	M0.5 V	PMSU	13.62	HIP2	01 Mar 2014	10 × 50
										17 Nov 2015	20 × 50
122	J05042+110	G 097–015	05:04:14.76	+11:03:23.8	9.144	M4.0 V	PMSU	10.3	Dit14	23 Oct 2011	10 × 50
123	J05068-215E	BD–21 1074A	05:06:49.92	-21:35:09.2	7.046	M1.5 V	PMSU	19.79	Ried14	25 Oct 2011	10 × 50
										17 Sep 2012	10 × 50
										14 Jan 2013	10 × 50
124	J05068-215W	BD–21 1074BC	05:06:49.47	-21:35:03.8	7.003	M3.5 V	PMSU	18.3	Ried14	25 Oct 2011	10 × 50
										17 Sep 2012	10 × 50
										14 Jan 2013	10 × 50
125	J05078+179	G 085–041	05:07:49.24	+17:58:58.4	8.023	M3.0 V	PMSU	23.1	This work	13 Jan 2013	10 × 50
										02 Mar 2014	10 × 50
126	J05085-181	GJ 190 AB	05:08:35.01	-18:10:17.9	6.175	M3.5 V	PMSU	9.3	HIP2	14 Jan 2013	10 × 50
127	J05091+154	Ross 388	05:09:09.97	+15:27:32.5	8.770	M3.0 V	PMSU	29.7	vAl95	13 Jan 2013	10 × 50
128	J05103+488	G 096–021 AB	05:10:22.08	+48:50:32.7	7.827	M2.5 V	PMSU	13 Jan 2013	10 × 50
										15 Apr 2015	10 × 35
129	J05106+297	G 086–028	05:10:39.56	+29:46:47.9	8.600	M3.0 V	Lep13	17.4	This work	01 Mar 2014	10 × 50
130	J05127+196	GJ 192	05:12:42.23	+19:39:56.6	7.299	M2.0 V	PMSU	12.3	HIP2	31 Jan 2012	10 × 50
131	J05289+125	HD 35956 B	05:28:56.50	+12:31:53.9	9.649	M4.0 V	AF15	28.17	aHIP2	23 Oct 2011	10 × 50
132	J05298-034	Wolf 1450	05:29:52.05	-03:26:29.6	8.276	M2.5 V	PMSU	17.6	vAl95	31 Jan 2012	10 × 50
133	J05298+320	Ross 406	05:29:52.69	+32:04:52.5	8.649	M3.0 V	PMSU	20.6	Dit14	13 Jan 2013	10 × 50
134	J05314-036	HD 36395	05:31:27.35	-03:40:35.7	4.999	M1.5 V	AF15	5.66	HIP2	25 Oct 2011	10 × 50
135	J05339-023	RX J0534.0–0221	05:33:59.81	-02:21:32.5	8.564	M3.0 V	Ria06	17.1	This work	28 Feb 2014	10 × 50
136	J05333+448	GJ 1081	05:33:19.13	+44:48:58.8	8.197	M3.5 V	PMSU	15.34	vAl95	24 Oct 2011	20 × 50
										25 Mar 2012	10 × 50
										26 Mar 2012	10 × 50
										17 Sep 2012	10 × 50
										13 Jan 2013	10 × 50
										28 Feb 2014	10 × 50
137	J05342+103S	Ross 45 B	05:34:15.08	+10:19:09.2	9.186	M4.5 V	AF15	18.0	This work	13 Jan 2013	10 × 50
138	J05342+103N	Ross 45 A	05:34:15.14	+10:19:14.2	8.561	M3.0 V	AF15	17.1	This work	13 Jan 2013	10 × 50
139	J05348+138	Ross 46	05:34:52.12	+13:52:47.2	7.781	M3.5 V	PMSU	12.4	vAl95	13 Jan 2013	10 × 50
140	J05360-076	Wolf 1457	05:36:00.08	-07:38:58.1	8.464	M4.0 V	PMSU	11.2	This work	25 Oct 2011	10 × 50
141	J05365+113	V2689 Ori	05:36:30.99	+11:19:40.2	6.126	M0.0 V	Lep13	11.24	HIP2	02 Mar 2014	10 × 50
142	J05366+112	2M J05363846+1117487	05:36:38.47	+11:17:48.8	8.266	M4.0 V	Lep13	11.24	aHIP2	01 Mar 2014	10 × 50
143	J05421+124	V1352 Ori	05:42:08.98	+12:29:25.3	7.124	M4.0 V	AF15	5.83	Wein16	23 Oct 2011	3 × 50
										31 Jan 2012	10 × 50

Table A.1. Log of observed stars (continued).

No.	Karmn	Name	α (J2000)	δ (J2000)	J [mag]	SpT	Ref. ^a	d [pc]	Ref. ^b	Observation date	N × t_{exp} [s]
144	J05466+441	Wolf 237	05:46:38.45	+44:07:19.8	8.459	M4.0 V	PMSU	21.0	Dit14	24 Oct 2011 01 Mar 2014	10 × 50
145	J05484+077	LTT 17868	05:48:24.08	+07:45:38.8	9.784	M4.0 V	PMSU	20.6	This work	23 Oct 2011	10 × 50
146	J05530+251	LSPM J0553+2507	05:53:01.80	+25:07:44.0	8.552	M3.0 V	Lep13	17.0	This work	01 Mar 2014	10 × 50
147	J05532+242	Ross 59	05:53:14.04	+24:15:32.9	7.485	M1.5 V	PMSU	19.4	vAl95	01 Mar 2014	10 × 50
148	J05599+585	G 192–012	05:59:55.69	+58:34:15.6	9.028	M4.0 V	PMSU	13.53	aHIP2	25 Oct 2011	10 × 50
149	J06000+027	G 099–049	06:00:03.51	+02:42:23.6	6.905	M4.0 V	PMSU	5.22	Wein16	23 Oct 2011 26 Mar 2012 09 Dec 2014	10 × 50 10 × 50 10 × 50
150	J06024+498	G 192–015	06:02:29.18	+49:51:56.2	9.350	M5.0 V	AF15	9.3	Jen09	24 Oct 2011	10 × 50
151	J06054+608	LP 086–173	06:05:29.36	+60:49:23.2	9.096	M4.5 V	AF15	14.0	Dit14	15 Apr 2015	10 × 35
152	J06105–218	HD 42581 A	06:10:34.62	-21:51:52.2	5.104	M0.5 V	PMSU	5.75	HIP2	14 Jan 2013	10 × 50
153	J06140+516	G 192–022	06:14:02.40	+51:40:08.1	8.860	M3.5 V	PMSU	14.9	Dit14	13 Jan 2013	10 × 50
154	J06212+442	G 101–035	06:21:13.00	+44:14:30.7	8.724	M2.0 V	PMSU	24.7	This work	14 Jan 2013 17 Nov 2015	10 × 50 20 × 50
155	J06277+093	Ross 603	06:27:43.97	+09:23:54.1	8.269	M2.0 V	Lep13	22.6	This work	17 Nov 2015	10 × 50
156	J06318+414	LP 205–044	06:31:50.74	+41:29:45.9	9.680	M5.0 V	PMSU	11.1	Jen09	24 Oct 2011	10 × 50
157	J06345+315	G 103–041	06:34:33.44	+31:30:08.4	8.705	M3.5 V	Lep13	15.3	This work	17 Nov 2015	10 × 50
158	J06361+116	NLTT 16724	06:36:06.39	+11:37:03.2	9.794	M4.5 V	PMSU	18.28	Jen09	23 Oct 2011 26 Mar 2012 17 Sep 2012	10 × 50 10 × 50 10 × 50
159	J06400+285	LP 307–008	06:40:05.50	+28:35:14.3	8.270	M2.0 V	PMSU	24.1	This work	31 Jan 2012 17 Sep 2012 13 Jan 2013 28 Feb 2014 15 Apr 2015	10 × 50 10 × 50 10 × 50 10 × 50 10 × 50
160	J06414+157	Wolf 289	06:41:28.18	+15:45:48.2	9.570	M4.0 V	PMSU	18.7	This work	23 Oct 2011	10 × 50
161	J06421+035	G 108–021	06:42:11.18	+03:34:52.7	8.166	M3.5 V	PMSU	15.39	Wein16	23 Oct 2011	10 × 50
162	J06422+035	G 108–022	06:42:13.34	+03:35:31.1	9.112	M4.0 V	PMSU	15.04	Wein16	23 Oct 2011	10 × 50
163	J06490+371	GJ 1092	06:49:05.42	+37:06:53.4	9.561	M4.0 V	PMSU	13.3	vAl95	24 Oct 2011	10 × 50
164	J06523–051	BD–05 1844Bab	06:52:18.04	-05:11:24.1	6.579	M2.0 V	Klu13	8.71	aHIP2	31 Jan 2012	10 × 50
165	J06524+182	LP 421–007	06:52:24.30	+18:17:04.7	9.052	M4.0 V	PMSU	14.7	This work	31 Jan 2012	10 × 50
166	J06548+332	Wolf 294	06:54:49.03	+33:16:05.9	6.104	M3.0 V	AF15	5.59	HIP2	24 Oct 2011 26 Mar 2012	10 × 50 10 × 50
167	J06594+193	GJ 1093	06:59:28.69	+19:20:57.7	9.160	M5.0 V	PMSU	7.8	vAl95	23 Oct 2011	10 × 50
168	J07033+346	LP 255–011	07:03:23.17	+34:41:51.0	8.773	M4.0 V	PMSU	13.7	Dit14	24 Oct 2011	10 × 50
169	J07076+486	G 107–048	07:07:37.76	+48:41:13.8	9.106	M3.5 V	PMSU	10.8	Dit14	14 Jan 2013	10 × 50
170	J07163+331	GJ 1096	07:16:18.02	+33:09:10.4	9.763	M4.0 V	PMSU	14.9	vAl95	24 Oct 2011	10 × 50
171	J07195+328	BD+33 1505	07:19:31.27	+32:49:48.3	7.184	M0.0 V	AF15	12.39	HIP2	09 Dec 2014	10 × 50
172	J07227+306	G 087–036	07:22:42.03	+30:40:12.0	9.506	M3.5 V	PMSU	23.7	vAl95	27 Mar 2012	10 × 50
173	J07274+052	Luyten's Star	07:27:24.50	+05:13:32.9	5.714	M3.5 V	AF15	3.8	HIP2	24 Oct 2011	10 × 50
174	J07307+481	GJ 275.2 A	07:30:42.80	+48:12:00.0	9.141	M4.0 V	PMSU	11.1	vAl95	25 Oct 2011	10 × 50

Table A.1. Log of observed stars (continued).

No.	Karmn	Name	α (J2000)	δ (J2000)	J [mag]	SpT	Ref. ^a	d [pc]	Ref. ^b	Observation date	N × t_{exp} [s]
175	J07319+392	G 111–009	07:31:56.52	+39:13:38.5	9.164	M3.0 V	AF15	22.6	This work	15 Apr 2015	10 × 35
176	J07319+362N	BL Lyn	07:31:57.35	+36:13:47.8	7.571	M3.5 V	PMSU	11.87	aHIP2	14 Jan 2013	10 × 50
177	J07342+009	GJ 1099	07:34:17.58	+00:59:09.3	8.261	M2.5 V	PMSU	14.6	vAl95	23 Oct 2011	10 × 50
178	J07349+147	TYC 777–141–1	07:34:56.33	+14:45:54.5	7.287	M3.0 V	Lep13	9.1	This work	31 Jan 2012	10 × 50
179	J07361-031	BD–02 2198	07:36:07.08	−03:06:38.5	6.791	M1.0 V	AF15	14.2	aHIP2	02 Mar 2014	10 × 50
180	J07386-212	LP 763–001	07:38:40.89	−21:13:27.6	7.848	M3.0 V	PMSU	10.6	HIP2	27 Mar 2012	10 × 50
181	J07395+334	G 090–016	07:39:35.81	+33:27:45.8	8.420	M2.0 V	PMSU	35.66	HIP2	31 Jan 2012	10 × 50
182	J07403-174	LP 783–002	07:40:19.22	−17:24:45.0	10.155	M6.0 V	PMSU	9.1	aSub09	27 Mar 2012	10 × 50
183	J07418+050	G 050–001	07:41:52.82	+05:02:24.3	8.910	M2.5 V	PMSU	28.5	This work	14 Jan 2013	10 × 50
184	J07446+035	YZ CMi	07:44:40.18	+03:33:09.0	6.581	M4.5 V	PMSU	5.96	HIP2	23 Oct 2011	10 × 50
185	J07472+503	2M J07471385+5020386	07:47:13.85	+50:20:38.5	8.855	M4.0 V	Lep13	13.5	This work	09 Dec 2014	10 × 50
186	J07518+055	G 050–006	07:51:51.38	+05:32:57.3	9.966	M4.5 V	PMSU	15.9	vAl95	31 Jan 2012	10 × 50
187	J07581+072	G 050–012	07:58:09.10	+07:17:01.5	9.272	M4.0 V	PMSU	12.1	Dit14	27 Mar 2012	10 × 50
188	J07582+413	GJ 1105	07:58:12.70	+41:18:13.5	7.734	M3.5 V	PMSU	8.3	Dit14	01 Mar 2014	10 × 50
189	J07583+496	LP 163–047	07:58:22.73	+49:39:53.4	8.706	M3.5 V	Lep13	13.8	Dit14	28 Feb 2014	10 × 50
190	J08005+258	TYC 1930–667–1	08:00:34.71	+25:53:33.5	8.204	M2.0 V	Lep13	19.6	This work	15 Apr 2015	10 × 50
191	J08017+237	TYC 1926–794–1	08:01:43.57	+23:42:27.1	7.670	M1.5 V	Lep13	17.4	This work	31 Jan 2012	10 × 50
192	J08066+558	LP 123–075	08:06:36.46	+55:53:38.4	8.050	M2.0 V	PMSU	30.1	HIP2	13 Jan 2013	10 × 50
193	J08068+367	G 090–044	08:06:48.42	+36:45:39.0	8.976	M3.0 V	PMSU	20.7	This work	27 Mar 2012	10 × 50
194	J08082+211	BD+21 1764B	08:08:13.59	+21:06:09.4	7.336	M3.0 V	AF15	16.64	aHIP2	31 Jan 2012	20 × 50
195	J08083+585	LP 089–101	08:08:18.19	+58:31:09.6	8.804	M3.0 V	PMSU	19.1	This work	17 Nov 2015	10 × 50
196	J08105-138	18 Pup B	08:10:34.29	−13:48:51.4	8.276	M2.5 V	AF15	22.4	Dit14	27 Mar 2012	10 × 50
197	J08108+039	G 050–021	08:10:53.63	+03:58:33.6	9.238	M3.5 V	PMSU	20.8	HIP2	14 Jan 2013	10 × 50
198	J08119+087	Ross 619	08:11:57.58	+08:46:22.1	8.424	M4.5 V	PMSU	6.80	Wein16	31 Jan 2012	10 × 35
199	J08126-215	GJ 300 AB	08:12:40.88	−21:33:05.7	7.601	M4.0 V	PMSU	5.9	vAl95	27 Mar 2012	10 × 50
200	J08161+013	GJ 2066	08:16:07.98	+01:18:09.2	6.625	M2.0 V	AF15	9.1	Dit14	31 Jan 2012	10 × 50
201	J08293+039	2M J08292191+0355092	08:29:21.92	+03:55:09.3	7.932	M2.5 V	Lep13	15.0	This work	01 Mar 2014	10 × 50
202	J08371+151	NLTT 19893	08:37:07.99	+15:07:47.6	8.122	M2.5 V	PMSU	18.96	HIP2	28 Feb 2014	10 × 50
203	J08413+594	LP 090–018	08:41:20.13	+59:29:50.6	9.615	M5.5 V	PMSU	9.2	Dit14	31 Jan 2012	10 × 50
204	J08428+095	BD+10 1857C	08:42:52.23	+09:33:11.2	8.122	M2.5 V	PMSU	15.43	aHIP2	13 Jan 2013	10 × 50
205	J08595+537	G 194–047	08:59:35.93	+53:43:50.5	9.014	M3.5 V	AF15	17.2	Dit14	01 Mar 2014	30 × 50
										14 Apr 2015	10 × 50

Table A.1. Log of observed stars (continued).

No.	Karmn	Name	α (J2000)	δ (J2000)	J [mag]	SpT	Ref. ^a	d [pc]	Ref. ^b	Observation date	$N \times t_{\text{exp}}$ [s]
206	J09003+218	LP 368–128	09:00:23.59	+21:50:05.4	9.436	M6.5 V	AF15	5.0	This work	27 Mar 2012	10×50
207	J09005+465	GJ 1119	09:00:32.54	+46:35:11.8	8.604	M4.5 V	PMSU	9.9	Dit14	31 Jan 2012	10×50
208	J09008+052W	Ross 686	09:00:48.53	+05:14:41.3	8.605	M3.0 V	PMSU	20.96	HIP2	31 Jan 2012	10×50
209	J09011+019	Ross 625	09:01:10.49	+01:56:35.0	7.932	M3.0 V	PMSU	16.2	This work	25 Mar 2012	20×50
										13 Jan 2013	10×50
										14 Apr 2015	10×50
										17 Nov 2015	10×50
210	J09023+084	NLTT 20817	09:02:19.88	+08:28:06.4	8.145	M2.5 V	PMSU	19.5	HIP2	27 Mar 2012	10×50
										02 Mar 2014	10×50
211	J09120+279	G 047–028	09:12:02.72	+27:54:24.2	8.430	M3.0 V	PMSU	27.8	vAl95	25 Mar 2012	10×50
212	J09140+196	LP 427–016	09:14:03.21	+19:40:06.0	8.424	M3.0 V	Lep13	16.1	This work	01 Mar 2014	10×50
213	J09143+526	HD 79210	09:14:22.98	+52:41:12.5	4.889	M0.0 V	AF15	5.81	HIP2	26 Mar 2012	10×50
214	J09144+526	HD 79211	09:14:24.86	+52:41:11.8	4.779	M0.0 V	AF15	5.81	aHIP2	26 Mar 2012	10×50
										02 Mar 2014	10×50
215	J09161+018	RX J0916.1+0153	09:16:10.19	+01:53:08.8	8.770	M4.0 V	Lep13	13.0	This work	22 May 2014	12×50
216	J09163-186	LP 787–052	09:16:20.66	-18:37:32.9	7.351	M1.5 V	PMSU	15.0	This work	02 Mar 2014	10×50
217	J09177+462	RX J0917.7+4612	09:17:44.73	+46:12:24.7	8.126	M2.5 V	Lep13	19.8	This work	22 May 2014	10×50
218	J09187+267	G 047–033 A	09:18:46.24	+26:45:11.4	8.296	M1.5 V	PMSU	23.2	This work	14 Jan 2013	10×50
219	J09288-073	Ross 439	09:28:53.34	-07:22:14.8	8.446	M2.5 V	PMSU	16.24	HIP2	30 Jan 2012	10×50
220	J09300+396	LP 211–012	09:30:01.67	+39:37:24.0	8.467	M2.5 V	PMSU	19.2	This work	30 Jan 2012	10×50
221	J09307+003	GJ 1125	09:30:44.58	+00:19:21.4	7.697	M3.5 V	PMSU	9.7	HIP2	25 Mar 2012	10×50
222	J09319+363	BD+36 1970	09:31:56.33	+36:19:12.9	7.121	M0.0 V	PMSU	13.91	HIP2	01 Mar 2014	10×50
										14 Apr 2015	10×50
										09 Jun 2015	10×50
223	J09360-216	GJ 357	09:36:01.61	-21:39:37.1	7.337	M2.5 V	PMSU	9.02	HIP2	14 Jan 2013	10×50
224	J09425-192	LP 788–024	09:42:35.73	-19:14:04.6	8.298	M2.5 V	PMSU	15.7	HIP2	14 Jan 2013	10×50
225	J09430+237	LP 370–035	09:43:01.33	+23:49:22.2	8.994	M1.0 V	Lep13	35.5	This work	22 May 2014	10×50
226	J09447-182	GJ 1129	09:44:47.31	-18:12:48.9	8.122	M4.0 V	PMSU	10.97	Wein16	14 Jan 2013	10×50
227	J09449-123	G 161–071	09:44:54.22	-12:20:54.4	8.496	M5.0 V	AF15	13.26	Wein16	01 Mar 2014	10×50
228	J09475+129	LP 488–037	09:47:34.81	+12:56:39.1	9.267	M4.0 V	PMSU	20.3	Dit14	26 Mar 2012	10×50
229	J09506-138	LP 728–070	09:50:40.54	-13:48:38.6	8.579	M4.0 V	Sch05	11.9	This work	09 Dec 2014	10×50
										17 Nov 2015	15×50
230	J09511-123	BD-11 2741	09:51:09.64	-12:19:47.8	6.988	M0.5 V	PMSU	13.7	HIP2	09 Dec 2014	10×50
231	J09539+209	NLTT 22870	09:53:55.23	+20:56:46.0	9.208	M4.5 V	PMSU	9.2	Hen06	30 Jan 2012	10×50
										13 Jan 2013	10×50
232	J09557+353	G 116–065	09:55:43.61	+35:21:42.2	8.850	M3.0 V	PMSU	19.5	This work	25 Mar 2012	10×50
										13 Jan 2013	10×50
233	J09564+226	NLTT 22978	09:56:27.00	+22:39:01.5	9.621	M4.0 V	PMSU	19.2	This work	14 Jan 2013	10×50
234	J10028+484	G 195–055	10:02:49.36	+48:27:33.4	9.963	M5.5 V	AF15	16.6	Dit14	26 Mar 2012	15×50
										14 Apr 2015	10×50
235	J10035+059	NLTT 23292	10:03:33.37	+05:57:48.1	9.290	M3.5 V	PMSU	20.0	This work	27 Mar 2012	10×50
236	J10043+503	G 196–003 A	10:04:21.49	+50:23:13.6	8.081	M2.5 V	Lep13	16.1	This work	02 Mar 2014	10×50

Table A.1. Log of observed stars (continued).

No.	Karmn	Name	α (J2000)	δ (J2000)	J [mag]	SpT	Ref. ^a	d [pc]	Ref. ^b	Observation date	N × t_{exp} [s]
237	J10087+027	LP 549–023	10:08:44.61	+02:43:56.8	8.590	M3.0 V	Lep13	17.3	This work	01 Mar 2014	10 × 50
238	J10094+512	LP 127–132	10:09:29.97	+51:17:19.8	9.299	M4.0 V	PMSU	13.3	vAl95	26 Mar 2012	10 × 50
239	J10125+570	LP 092–048	10:12:34.81	+57:03:49.6	7.759	M3.5 V	Lep13	9.9	This work	02 Mar 2014	10 × 50
240	J10151+314	G 118–043	10:15:06.91	+31:25:11.0	9.326	M4.0 V	PMSU	20.4	This work	25 Mar 2012	10 × 50
										13 Jan 2013	10 × 50
										28 Feb 2014	10 × 50
										14 Apr 2015	10 × 50
241	J10158+174	LSPM J1015+1729	10:15:53.90	+17:29:27.2	8.696	M3.5 V	Lep13	15.2	This work	22 May 2014	10 × 50
242	J10167–119	GJ 386	10:16:46.00	-11:57:41.3	7.323	M3.0 V	PMSU	13.6	HIP2	26 Mar 2012	10 × 50
243	J10185–117	LP 729–054	10:18:35.17	-11:42:59.9	9.007	M4.0 V	Sch05	14.4	This work	22 May 2014	10 × 50
244	J10196+198	BD+20 2465	10:19:36.35	+19:52:12.2	5.449	M3.0 V	AF15	4.89	vAl95	30 Jan 2012	11 × 40
										17 Nov 2015	11 × 40
245	J10243+119	StKM 1–852	10:24:20.17	+11:57:20.7	8.847	M2.0 V	PMSU	26.4	This work	30 Jan 2012	10 × 50
246	J10255+263	G 054–026	10:25:30.35	+26:23:18.5	9.030	M3.5 V	PMSU	17.8	This work	27 Mar 2012	10 × 50
247	J10260+504W	LP 127–371	10:26:02.66	+50:27:09.1	9.268	M4.0 V	PMSU	16.3	This work	25 Mar 2012	10 × 50
										02 Mar 2014	10 × 50
248	J10260+504E	LP 127–372	10:26:03.32	+50:27:22.0	9.404	M4.0 V	PMSU	17.3	This work	25 Mar 2012	10 × 50
249	J10284+482	G 146–035	10:28:27.81	+48:14:20.0	9.055	M3.5 V	PMSU	20.96	vAl95	27 Mar 2012	10 × 50
250	J10345+463	LP 167–064	10:34:30.21	+46:18:09.0	9.195	M3.0 V	PMSU	20.4	Dit14	27 Mar 2012	10 × 50
251	J10350–094	LP 670–017	10:35:01.11	-09:24:38.5	8.276	M3.0 V	Sch05	15.0	This work	02 Mar 2014	10 × 50
252	J10379+127	LP 490–042	10:37:55.28	+12:46:36.9	8.730	M3.0 V	Lep13	20.4	This work	01 Mar 2014	10 × 50
										17 Nov 2015	10 × 50
253	J10384+485	LP 167–071	10:38:29.81	+48:31:44.9	9.495	M3.0 V	PMSU	26.3	This work	27 Mar 2012	10 × 50
										14 Apr 2015	10 × 50
254	J10396–069	GJ 399	10:39:40.61	-06:55:25.6	7.664	M2.5 V	PMSU	16.4	HIP2	26 Mar 2012	10 × 50
255	J10416+376	GJ 1134	10:41:38.10	+37:36:39.8	8.493	M4.5 V	PMSU	10.3	vAl95	25 Mar 2012	10 × 50
256	J10448+324	LP 316–604 A	10:44:52.70	+32:24:41.2	9.494	M3.0 V	PMSU	39.1	Dit14	14 Jan 2013	10 × 50
										15 Apr 2015	10 × 50
257	J10504+331	G 119–037	10:50:26.00	+33:06:05.2	8.899	M4.0 V	PMSU	22.9	vAl95	25 Mar 2012	10 × 50
258	J10513+361	LP 263–035	10:51:20.60	+36:07:25.6	9.422	M3.0 V	PMSU	32.3	Dit14	14 Jan 2013	10 × 50
259	J10522+059	NLTT 25568	10:52:14.23	+05:55:09.9	9.834	M5.0 V	PMSU	11.6	Dit14	26 Mar 2012	10 × 50
260	J10546–073	LP 671–008	10:54:41.98	-07:18:32.7	8.877	M4.0 V	AF15	16.8	This work	02 Mar 2014	10 × 50
										14 Apr 2015	10 × 50
261	J10584–107	LP 731–076	10:58:28.00	-10:46:30.5	9.512	M5.0 V	AF15	11.7	This work	22 May 2014	10 × 50
262	J11031+366	LP 263–064	11:03:10.00	+36:39:08.5	9.464	M3.5 V	PMSU	24.0	Dit14	14 Jan 2013	10 × 50
263	J11033+359	HD 95735	11:03:20.24	+35:58:11.8	4.203	M1.5 V	AF15	2.547	HIP2	30 Jan 2012	11 × 35
264	J11036+136	LP 491–051	11:03:21.25	+13:37:57.1	8.759	M4.0 V	Lep13	16.8	Dit14	01 Mar 2014	10 × 50
265	J11055+435	WX UMa	11:05:31.33	+43:31:17.1	8.742	M5.5 V	AF15	4.85	aHIP2	26 Mar 2012	10 × 50
266	J11152+194	G 056–026	11:15:12.40	+19:27:12.4	8.919	M3.5 V	PMSU	16.9	This work	26 Mar 2012	10 × 50
267	J11289+101	Wolf 398	11:28:56.24	+10:10:39.5	8.478	M3.5 V	PMSU	15.7	vAl95	25 Mar 2012	10 × 50
268	J11355+389	G 122–034	11:35:31.98	+38:55:37.3	9.034	M3.5 V	PMSU	23.0	This work	26 Mar 2012	10 × 50
										10 Jul 2012	11 × 50

Table A.1. Log of observed stars (continued).

No.	Karmn	Name	α (J2000)	δ (J2000)	J [mag]	SpT	Ref. ^a	d [pc]	Ref. ^b	Observation date	N × t_{exp} [s]
269	J11376+587	Ross 112	11:37:38.99	+58:42:42.8	8.978	M3.5 V	PMSU	24.3	This work	11 Jul 2012	10 × 50
270	J11420+147	Ross 115	11:42:01.77	+14:46:35.7	8.859	M3.0 V	PMSU	19.6	This work	13 Jan 2013	10 × 50
271	J11467-140	GJ 443	11:46:42.82	-14:00:50.5	7.965	M3.0 V	PMSU	19.99	HIP2	28 Feb 2014	10 × 50
272	J11476+002	LP 613-049 A	11:47:40.74	+00:15:20.2	8.991	M4.0 V	PMSU	19.9	Dit14	14 Apr 2015	10 × 50
273	J11483-112	LP 733-024	11:48:19.43	-11:17:14.4	9.028	M3.0 V	PMSU	21.2	This work	31 Jan 2012	10 × 50
274	J11509+483	GJ 1151	11:50:57.88	+48:22:39.6	8.488	M4.5 V	PMSU	8.2	vAl95	14 Jan 2013	10 × 50
275	J11521+039	StM 162	11:52:09.82	+03:57:23.3	8.382	M4.0 V	Lep13	13.1	This work	26 Mar 2012	10 × 50
276	J11532-073	GJ 452	11:53:16.09	-07:22:27.3	8.303	M2.5 V	PMSU	19.6	HIP2	01 Mar 2014	10 × 50
277	J11575+118	Ross 122	11:57:32.78	+11:49:39.8	8.429	M2.0 V	PMSU	24.2	HIP2	14 Apr 2015	10 × 50
278	J12006-138	LP 734-011 A	12:00:36.91	-13:49:36.4	8.852	M3.5 V	PMSU	16.4	This work	25 Mar 2012	10 × 50
279	J12016-122	LT T 4484	12:01:40.80	-12:13:53.7	8.685	M3.0 V	PMSU	18.1	This work	13 Jan 2013	10 × 50
280	J12100-150	LP 734-032	12:10:05.60	-15:04:15.7	7.768	M3.5 V	PMSU	12.8	Ried10	14 Apr 2015	10 × 50
281	J12112-199	LP 794-031	12:11:16.98	-19:58:21.4	8.596	M3.5 V	PMSU	12.6	aHIP2	01 Mar 2014	10 × 50
282	J12123+544S	HD 238090	12:12:20.85	+54:29:08.7	6.875	M0.0 V	PMSU	15.52	HIP2	14 Jan 2013	10 × 50
283	J12123+544N	BD+55 1519B	12:12:21.12	+54:29:23.2	9.171	M3.0 V	PMSU	15.52	HIP2	26 Mar 2012	10 × 50
284	J12142+006	GJ 1154 A	12:14:16.54	+00:37:26.3	8.456	M5.0 V	PMSU	7.16	Wein16	22 May 2014	10 × 50
285	J12156+526	StKM 2-809	12:15:39.37	+52:39:08.9	8.588	M4.0 V	Lep13	11.9	This work	14 Apr 2015	10 × 50
286	J12162+508	RX J1216.2+5053	12:16:15.06	+50:53:37.7	9.291	M4.0 V	AF15	19.9	This work	26 Mar 2012	10 × 50
287	J12189+111	GL Vir	12:18:59.40	+11:07:33.9	8.525	M5.0 V	PMSU	6.44	Wein16	01 Mar 2014	10 × 50
288	J12191+318	LP 320-626	12:19:06.00	+31:50:43.3	8.289	M4.0 V	Lep13	14.7	This work	27 Mar 2012	10 × 50
289	J12248-182	Ross 695	12:24:52.43	-18:14:30.3	7.734	M2.0 V	PMSU	8.8	HIP2	31 Jan 2012	10 × 50
290	J12277-032	LP 615-149	12:27:44.72	-03:15:00.6	8.763	M3.5 V	Sch05	17.1	This work	14 Jan 2013	10 × 50
291	J12290+417	G 123-035	12:29:02.90	+41:43:49.7	8.786	M3.5 V	PMSU	15.9	This work	25 Mar 2012	10 × 50
292	J12332+090	FL Vir AB	12:33:17.38	+09:01:15.8	6.995	M5.0 V	PMSU	4.4	Jen52	26 Mar 2012	10 × 50
										11 Jul 2012	10 × 50

Table A.1. Log of observed stars (continued).

No.	Karmn	Name	α (J2000)	δ (J2000)	J [mag]	SpT	Ref. ^a	d [pc]	Ref. ^b	Observation date	N × t_{exp} [s]
293	J12364+352	G 123–045	12:36:28.70	+35:12:00.8	9.113	M4.5 V	AF15	11.3	Dit14	14 Jan 2013	10 × 50
294	J12373-208	LP 795–038	12:37:21.57	-20:52:34.9	8.972	M4.0 V	Sch05	14.2	This work	28 Feb 2014	20 × 50
295	J12428+418	G 123–055	12:42:49.96	+41:53:46.9	8.118	M4.0 V	Lep13	10.6	vAl95	28 Feb 2014	10 × 50
296	J12470+466	Ross 991	12:47:01.02	+46:37:33.4	8.104	M2.5 V	AF15	20.9	HIP2	30 Jan 2012	10 × 50
297	J12471-035	LP 616–013	12:47:09.77	-03:34:17.7	8.767	M3.0 V	PMSU	18.8	This work	25 Mar 2012	10 × 50
298	J12485+495	RX J1248.5+4933	12:48:34.49	+49:33:54.1	8.684	M3.5 V	Lep13	15.1	This work	01 Mar 2014	16 × 50
										22 May 2014	10 × 50
299	J13000-056	Ross 972	13:00:03.98	-05:37:47.7	8.655	M3.0 V	PMSU	17.8	This work	27 Mar 2012	10 × 50
300	J13130+201	GJ 1168	13:13:04.79	+20:11:26.5	8.867	M3.5 V	PMSU	16.5	This work	26 Mar 2012	10 × 50
301	J13140+038	G 062-018	13:14:05.83	+03:53:58.7	9.490	M3.0 V	PMSU	19.6	Dit14	27 Mar 2012	10 × 50
302	J13165+278	GJ 1169	13:16:32.84	+27:52:29.8	9.267	M3.5 V	PMSU	15.6	Dit14	26 Mar 2012	10 × 50
303	J13168+170	HD 115404 B	13:16:51.56	+17:01:00.1	6.532	M0.5 V	AF15	11.1	aHIP2	28 Feb 2014	10 × 50
										15 Apr 2015	10 × 50
304	J13180+022	G 062–028	13:18:01.81	+02:14:01.1	8.787	M3.5 V	PMSU	21.1	Dit14	25 Mar 2012	10 × 50
										13 Jan 2013	10 × 50
										28 Feb 2014	10 × 50
										14 Apr 2015	10 × 50
305	J13300-087	Wolf 485 B	13:30:02.85	-08:42:25.2	9.599	M4.0 V	PMSU	17.4	aHIP2	27 Mar 2012	10 × 50
306	J13317+292	DG CVn AB	13:31:46.62	+29:16:36.7	7.561	M4.0 V	PMSU	18.02	Ried14	10 Jul 2012	11 × 50
										12 Jul 2012	10 × 50
										14 Apr 2015	10 × 50
307	J13318+233	G 150–007	13:31:50.57	+23:23:20.3	8.608	M2.0 V	PMSU	23.6	This work	26 Mar 2012	10 × 50
308	J13343+046	BD+05 2767	13:34:21.50	+04:40:02.6	7.213	M0.0 V	Lep13	21.32	HIP2	01 Mar 2014	10 × 50
309	J13369+229	Ross 1021	13:36:55.22	+22:58:01.1	8.979	M2.5 V	PMSU	24.3	This work	26 Mar 2012	10 × 50
310	J13386+258	Ross 1022	13:38:37.05	+25:49:49.6	8.751	M3.0 V	PMSU	18.7	This work	01 Mar 2014	10 × 50
311	J13388-022	Ross 488	13:38:53.45	-02:15:47.1	8.595	M2.0 V	PMSU	23.5	This work	27 Mar 2012	10 × 50
312	J13417+582	StM 187	13:41:46.31	+58:15:19.8	8.733	M3.5 V	Lep13	19.9	This work	02 Mar 2014	10 × 50
										14 Apr 2015	10 × 50
313	J13430+090	G 063–050	13:43:01.27	+09:04:23.6	9.093	M3.0 V	PMSU	21.8	This work	26 Mar 2012	10 × 50
314	J13450+176	BD+18 2776	13:45:05.03	+17:47:10.5	6.997	M1.0 V	Koe10	13.6	HIP2	28 Feb 2014	10 × 50
315	J13458-179	LP 798–034	13:45:50.75	-17:58:04.8	7.745	M3.5 V	PMSU	10.2	HIP2	27 Mar 2012	10 × 50
316	J13481-137	LP 739–014	13:48:07.22	-13:44:32.1	10.413	M4.5 V	Deal12	22.3	This work	27 Mar 2012	10 × 50
317	J13503-216	LP 798–041	13:50:23.77	-21:37:19.3	9.458	M3.5 V	AF15	21.6	This work	27 Mar 2012	10 × 50
318	J13507-216	LP 798–044	13:50:44.00	-21:41:26.4	8.871	M3.0 V	PMSU	19.7	This work	27 Mar 2012	10 × 50
319	J13508+367	Ross 1019	13:50:51.82	+36:44:16.9	9.299	M3.5 V	PMSU	15.8	Dit14	26 Mar 2012	10 × 50
320	J13526+144	G 150–046	13:52:36.20	+14:25:20.9	8.013	M2.0 V	PMSU	19.4	This work	30 Jan 2012	10 × 50
										13 Jan 2013	10 × 50
										15 Apr 2015	10 × 50
321	J13582+125	Ross 837	13:58:13.93	+12:34:43.8	8.269	M3.0 V	PMSU	11.32	vAl95	26 Mar 2012	10 × 50
322	J13591-198	LP 799–007	13:59:10.46	-19:50:03.5	8.334	M4.0 V	PMSU	10.77	Ried14	27 Mar 2012	10 × 50

Table A.1. Log of observed stars (continued).

No.	Karmn	Name	α (J2000)	δ (J2000)	J [mag]	SpT	Ref. ^a	d [pc]	Ref. ^b	Observation date	N × t_{exp} [s]
323	J14152+450	Ross 992	14:15:17.07	+45:00:53.6	8.014	M3.0 V	PMSU	16.3	vAl95	26 Mar 2012	10 × 50
324	J14155+046	GJ 1182	14:15:32.54	+04:39:31.2	9.433	M5.0 V	PMSU	13.9	vAl95	25 Mar 2012	10 × 50
325	J14157+594	LP 097–674	14:15:42.49	+59:27:30.3	8.850	M2.0 V	Lep13	26.4	This work	02 Mar 2014	10 × 50
										22 May 2014	10 × 50
										15 Apr 2015	10 × 50
326	J14171+088	2M J14170731+0851363	14:17:07.31	+08:51:36.3	9.109	M4.5 V	AF15	17.4	This work	01 Mar 2014	10 × 50
327	J14173+454	RX J1417.3+4525	14:17:22.10	+45:25:46.1	9.467	M5.0 V	Gig10	19.01	aHIP2	28 Feb 2014	10 × 50
328	J14200+390	StKM 1–1145	14:20:04.69	+39:03:01.5	8.572	M2.5 V	PMSU	20.2	This work	26 Mar 2012	10 × 50
329	J14210+275	G 166–021	14:21:03.49	+27:35:32.8	8.928	M2.5 V	PMSU	25.1	This work	26 Mar 2012	10 × 50
										14 Apr 2015	10 × 50
330	J14212-011	LP 620–003	14:21:15.13	-01:07:19.9	8.948	M3.5 V	PMSU	13.4	Ried10	25 Mar 2012	10 × 50
331	J14249+088	LP 500–019	14:24:55.99	+08:53:15.6	8.420	M2.5 V	PMSU	14.3	HIP2	30 Jan 2012	10 × 50
										31 Jan 2012	10 × 50
332	J14251+518	θ Boo B	14:25:11.60	+51:49:53.6	7.883	M2.5 V	AF15	14.53	aHIP2	31 Jan 2012	10 × 50
333	J14257+236W	BD+24 2733A	14:25:43.49	+23:37:01.1	6.769	M0.0 V	PMSU	16.36	HIP2	28 Feb 2014	10 × 50
334	J14257+236E	BD+24 2733B	14:25:46.67	+23:37:13.3	6.889	M0.5 V	PMSU	16.36	aHIP2	28 Feb 2014	10 × 50
335	J14279-003S	GJ 1183A	14:27:56.07	-00:22:31.1	9.305	M4.5 V	PMSU	13.4	This work	25 Mar 2012	10 × 50
336	J14279-003N	GJ 1183B	14:27:56.40	-00:22:19.1	9.345	M4.5 V	PMSU	13.6	This work	25 Mar 2012	10 × 50
337	J14283+053	LP 560–027	14:28:21.52	+05:19:01.4	8.721	M3.0 V	Lep13	18.4	This work	01 Mar 2014	10 × 50
338	J14294+155	Ross 130	14:29:29.72	+15:31:57.9	7.229	M2.0 V	PMSU	14.0	HIP2	30 Jan 2012	10 × 50
339	J14310-122	Wolf 1478	14:31:01.20	-12:17:45.2	7.803	M3.5 V	PMSU	10.8	HIP2	25 Mar 2012	10 × 50
340	J14321+081	LP 560–035	14:32:08.50	+08:11:31.3	10.108	M6.0 V	New14	9.1	This work	22 May 2014	10 × 50
341	J14322+496	LP 174–355	14:32:14.54	+49:39:05.8	9.277	M3.5 V	PMSU	17.2	Dit14	26 Mar 2012	10 × 50
342	J14331+610	G 224–013	14:33:06.38	+61:00:44.5	8.171	M2.5 V	Lep13	18.3	This work	01 Mar 2014	10 × 50
										14 Apr 2015	10 × 50
343	J14342-125	HN Lib	14:34:16.83	-12:31:10.7	6.838	M4.0 V	PMSU	6.06	HIP2	30 Jan 2012	6 × 50
344	J14368+583	LP 098–132	14:36:53.02	+58:20:55.0	8.079	M2.5 V	PMSU	19.4	This work	31 Jan 2012	10 × 50
345	J15011+071	Ross 1030a	15:01:10.74	+07:09:47.7	8.682	M3.5 V	PMSU	15.1	This work	25 Mar 2012	10 × 50
										14 Apr 2015	10 × 50
346	J15013+055	G 015–002	15:01:20.11	+05:32:55.4	8.326	M3.0 V	PMSU	15.3	This work	26 Mar 2012	10 × 50
347	J15043+603	Ross 1051	15:04:18.56	+60:23:04.4	7.701	M1.0 V	PMSU	17.85	HIP2	01 Mar 2014	10 × 50
348	J15018+550	LP 135–097	15:05:49.51	+55:04:43.1	9.239	M3.5 V	PMSU	19.6	This work	26 Mar 2012	10 × 50
349	J15073+249	BD+25 2874	15:07:23.62	+24:56:07.6	7.296	M0.0 V	Lep13	16.7	vAl95	02 Mar 2014	10 × 50
350	J15081+623	LSPM J1508+6221	15:08:11.93	+62:21:53.6	9.296	M4.0 V	AF15	19.9	This work	01 Mar 2014	10 × 50
										22 May 2014	10 × 50
										15 Apr 2015	10 × 50
351	J15095+031	Ross 1047	15:09:35.59	+03:10:00.8	7.720	M3.0 V	PMSU	14.4	HIP2	26 Mar 2012	10 × 50
352	J15100+193	G 136–072	15:10:04.81	+19:21:28.7	9.056	M4.0 V	PMSU	17.0	Dit14	25 Mar 2012	10 × 50
										15 Apr 2015	10 × 50
353	J15126+457	G 179–020	15:12:38.18	+45:43:46.4	8.977	M4.0 V	PMSU	18.5	Dit14	26 Mar 2012	10 × 50
										15 Apr 2015	10 × 50
354	J15191-127	LP 742–061	15:19:11.82	-12:45:06.2	8.507	M4.0 V	PMSU	21.12	Wein16	27 Mar 2012	10 × 50

Table A.1. Log of observed stars (continued).

No.	Karmn	Name	α (J2000)	δ (J2000)	J [mag]	SpT	Ref. ^a	d [pc]	Ref. ^b	Observation date	N × t_{exp} [s]
355	J15214+042	TYC 344–504–1	15:21:25.30	+04:14:49.3	8.553	M1.5 V	Lep13	26.1	This work	02 Mar 2014	10 × 50
356	J15305+094	NLTT 40406	15:30:30.33	+09:26:01.4	9.569	M5.5 V	AF15	8.1	Dit14	22 May 2014	10 × 50
357	J15357+221	LP 384–018	15:35:46.10	+22:09:03.7	8.681	M3.5 V	PMSU	18.6	vAl95	25 Mar 2012	10 × 50
358	J15369–141	Ross 802	15:36:58.68	–14:08:00.6	8.432	M4.0 V	PMSU	13.3	vAl95	28 Feb 2014	10 × 50
359	J15400+434N	vB 24 A	15:40:03.53	+43:29:39.7	8.312	M3.0 V	PMSU	13.5	vAl95	01 Mar 2014	10 × 50
										22 May 2014	10 × 50
360	J15474–108	LP 743–031	15:47:24.64	–10:53:47.1	7.582	M2.0 V	PMSU	15.1	HIP2	26 Mar 2012	10 × 50
										15 Apr 2015	10 × 50
361	J15496+348	LP 274–008	15:49:38.33	+34:48:55.5	8.728	M4.0 V	PMSU	16.98	vAl95	27 Mar 2012	10 × 50
										10 Jul 2012	10 × 50
										11 Jul 2012	10 × 50
										28 Feb 2014	10 × 50
362	J15531+347S	LP 274–021	15:53:06.64	+34:44:47.4	8.994	M3.5 V	PMSU	19.3	vAl95	25 Mar 2012	10 × 50
363	J15578+090	LSPM J1557+0901	15:57:48.27	+09:01:09.9	9.282	M4.0 V	AF15	16.4	This work	02 Mar 2014	10 × 50
364	J15598–082	BD-07 4156	15:59:53.37	–08:15:11.4	7.185	M1.0 V	PMSU	13.9	HIP2	01 Mar 2014	10 × 50
365	J16017+301	G 168–024	16:01:43.60	+30:10:50.2	8.666	M3.0 V	PMSU	18.4	Dit14	27 Mar 2012	20 × 50
366	J16092+093	G 137–084	16:09:16.25	+09:21:07.7	7.969	M3.0 V	Lep13	13.0	This work	22 May 2014	10 × 50
367	J16120+033	TYC 371–1053–1	16:12:04.65	+03:18:20.8	8.127	M2.0 V	Lep13	18.9	This work	01 Mar 2014	10 × 50
368	J16145+191	GJ 1200	16:14:32.85	+19:06:10.2	8.990	M3.5 V	PMSU	16.5	Dit14	27 Mar 2012	10 × 50
369	J16241+483	GJ 623 AB	16:24:09.32	+48:21:10.5	6.638	M2.5 V	PMSU	8.1	HIP2	10 Jul 2012	10 × 50
										12 Jul 2012	10 × 50
370	J16255+260	LT T 14889	16:25:32.35	+26:01:37.9	8.403	M3.0 V	PMSU	18.9	This work	25 Mar 2012	30 × 50
										15 Apr 2015	10 × 50
371	J16313+408	G 180–060	16:31:18.79	+40:51:51.6	9.461	M5.0 V	PMSU	12.0	Dit14	27 Mar 2012	10 × 50
372	J16315+175	GJ 1202	16:31:35.08	+17:33:49.5	8.926	M3.5 V	PMSU	15.5	Dit14	27 Mar 2012	10 × 50
373	J16327+126	GJ 1203	16:32:45.25	+12:36:46.0	8.429	M3.0 V	PMSU	16.8	HIP2	25 Mar 2012	10 × 50
										22 May 2014	10 × 50
										09 Jun 2015	10 × 50
374	J16328+098	G 138–040	16:32:52.85	+09:50:26.0	8.988	M3.5 V	PMSU	13.8	Dit14	27 Mar 2012	10 × 50
										10 Jul 2012	10 × 50
										11 Jul 2012	10 × 50
										17 Sep 2012	10 × 50
										28 Feb 2014	10 × 50
										15 Apr 2015	10 × 50
375	J16354+350	LP 275–068	16:35:27.41	+35:00:57.7	8.615	M4.0 V	PMSU	16.2	Dit14	11 Jul 2012	10 × 50
376	J16360+088	G 138–043	16:36:05.63	+08:48:49.2	9.419	M4.0 V	PMSU	15.34	vAl95	25 Mar 2012	10 × 50
377	J16401+007	LP 625–034	16:40:06.00	+00:42:18.8	9.116	M4.0 V	PMSU	11.20	Wein16	11 Jul 2012	10 × 50
378	J16462+164	LP 446–006	16:46:13.72	+16:28:40.7	7.951	M2.5 V	PMSU	16.1	HIP2	25 Mar 2012	10 × 50
										10 Jul 2012	10 × 50
										11 Jul 2012	10 × 50
										17 Sep 2012	10 × 50
										28 Feb 2014	10 × 50

Table A.1. Log of observed stars (continued).

No.	Karmn	Name	α (J2000)	δ (J2000)	J [mag]	SpT	Ref. ^a	d [pc]	Ref. ^b	Observation date	N × t_{exp} [s]
379	J16487+106	LSPM J1648+1038	16:48:46.58	+10:38:51.7	7.820	M2.5 V	Lep13	17.1	This work	15 Apr 2015 01 Mar 2014 22 May 2014 14 Apr 2015	10 × 50 10 × 50 10 × 50 10 × 50
380	J16509+224	G 169–029	16:50:57.95	+22:27:05.8	9.136	M4.5 V	PMSU	10.0	Dit14	11 Jul 2012	10 × 50
381	J16528+630	GSC 04194–01561	16:52:49.48	+63:04:39.0	9.592	M5.0 V	New14	12.1	This work	22 May 2014	10 × 50
382	J16554–083N	GJ 643	16:55:25.27	−08:19:20.8	7.555	M3.5 V	PMSU	6.2	aHIP2	26 Mar 2012	10 × 50
383	J16554–083S	GJ 644 ABab	16:55:28.81	−08:20:10.3	5.270	M3.0 V	PMSU	6.2	HIP2	26 Mar 2012	10 × 50
384	J16555–083	vB 8	16:55:35.29	−08:23:40.1	9.776	M7.0 V	AF15	6.48	Wein16	26 Mar 2012	10 × 50
385	J16578+473	BD+47 2415B	16:57:53.58	+47:22:01.6	6.874	M1.5 V	Lep13	18.3	aHIP2	22 May 2014	10 × 50
386	J17010+082	G 139–005	17:01:02.11	+08:12:26.4	9.437	M3.5 V	PMSU	17.7	Dit14	10 Jul 2012	10 × 50
387	J17033+514	G 203–042	17:03:23.85	+51:24:21.9	8.768	M4.5 V	PMSU	9.5	vAl95	11 Jul 2012	10 × 50
388	J17115+384	Wolf 654	17:11:34.72	+38:26:34.1	7.630	M3.5 V	PMSU	12.0	HIP2	25 Mar 2012	10 × 50
389	J17177+116	GJ 1215	17:17:44.08	+11:40:11.8	9.817	M5.0 V	PMSU	12.7	vAl95	11 Jul 2012	10 × 50
390	J17177–118	LT T 6883	17:17:45.32	−11:48:54.2	8.818	M3.0 V	PMSU	19.2	This work	26 Mar 2012	10 × 50
391	J17219+214	G 170–036	17:21:54.65	+21:25:46.8	9.344	M4.0 V	PMSU	13.4	Dit14	25 Mar 2012	10 × 50
392	J17321+504	LP 180–017	17:32:07.83	+50:24:51.0	9.008	M2.5 V	PMSU	28.1	vAl95	27 Mar 2012	10 × 50
393	J17338+169	1RXS J173353.5+165515	17:33:53.15	+16:55:12.9	8.895	M5.5 V	Lep13	11.7	Dit14	01 Mar 2014	10 × 50
394	J17340+446	2M J17340562+4447082	17:34:05.62	+44:47:08.2	8.742	M3.5 V	Lep13	20.2	This work	22 May 2014 14 Apr 2015	10 × 50 10 × 50
395	J17425–166	GJ 690.1	17:42:32.29	−16:38:23.6	9.441	M2.5 V	PMSU	19.4	vAl95	27 Mar 2012	10 × 50
396	J17460+246	LP 389–032	17:46:04.66	+24:39:05.0	8.814	M3.5 V	Klu13	14.5	vAl95	11 Jul 2012	10 × 50
397	J17530+169	G 183–010	17:53:00.63	+16:55:02.9	8.699	M3.0 V	PMSU	19.8	This work	26 Mar 2012 10 Jul 2012 12 Jul 2012 16 Sep 2012 15 Apr 2015	10 × 50 10 × 50 10 × 50 10 × 50 10 × 50
398	J17542+073	GJ 1222	17:54:17.10	+07:22:44.7	8.772	M4.0 V	PMSU	15.0	Dit14	25 Mar 2012	10 × 50
399	J17578+046	Barnard’s Star	17:57:48.49	+04:41:40.5	5.244	M3.5 V	AF15	1.824	HIP2	11 Jul 2012	10 × 50
400	J17578+465	G 204–039	17:57:50.96	+46:35:18.2	7.847	M2.5 V	AF15	14.1	HIP2	11 Jul 2012	10 × 50
401	J18010+508	Wolf 1403	18:01:05.58	+50:49:36.9	8.927	M1.5 V	Lep13	31.0	This work	22 May 2014	11 × 50
402	J18027+375	GJ 1223	18:02:46.25	+37:31:04.9	9.720	M5.0 V	PMSU	12.0	vAl95	12 Jul 2012	10 × 50
403	J18075–159	GJ 1224	18:07:32.93	−15:57:46.5	8.639	M4.5 V	PMSU	8.10	Wein16	10 Jul 2012	10 × 50
404	J18165+048	G 140–051	18:16:31.54	+04:52:45.6	9.798	M5.0 V	New14	13.3	This work	22 May 2014	10 × 50
405	J18180+387W	G 204–057	18:18:03.46	+38:46:36.0	9.197	M4.0 V	PMSU	10.4	Dit14	11 Jul 2012	10 × 50
406	J18180+387E	G 204–058	18:18:04.28	+38:46:34.2	8.040	M3.0 V	PMSU	10.7	Dit14	11 Jul 2012	10 × 50
407	J18224+620	GJ 1227	18:22:27.19	+62:03:02.5	8.640	M4.0 V	AF15	8.23	vAl95	12 Jul 2012	10 × 50
408	J18240+016	G 021–013	18:24:05.18	+01:41:16.1	8.297	M2.0 V	PMSU	20.5	This work	11 Jul 2012	10 × 50
409	J18264+113	G 141–010	18:26:24.59	+11:20:57.5	8.918	M3.5 V	PMSU	16.9	This work	10 Jul 2012	10 × 50
410	J18312+068	LP 570–092	18:31:16.06	+06:50:09.7	7.579	M1.0 V	Lep13	18.5	This work	22 May 2014	10 × 50
411	J18319+406	G 205–028	18:31:58.40	+40:41:10.4	8.065	M3.5 V	PMSU	11.4	This work	12 Jul 2012	10 × 50
412	J18354+457	GJ 720 B (vB 9)	18:35:27.23	+45:45:40.3	8.886	M2.5 V	AF15	13.1	Dit14	12 Jul 2012	10 × 50

Table A.1. Log of observed stars (continued).

No.	Karmn	Name	α (J2000)	δ (J2000)	J [mag]	SpT	Ref. ^a	d [pc]	Ref. ^b	Observation date	N × t_{exp} [s]
413	J18387-144	GJ 2138	18:38:44.75	-14:29:25.0	7.661	M2.5 V	PMSU	12.9	HIP2	10 Jul 2012	10 × 50
414	J18411+247S	GJ 1230 Aab	18:41:09.78	+24:47:14.4	7.528	M4.5 V	PMSU	10.2	This work	12 Jul 2012	10 × 50
415	J18411+247N	GJ 1230 B	18:41:09.82	+24:47:19.5	8.860	M5.0 V	PMSU	10.2	This work	12 Jul 2012	10 × 50
416	J18427+139	V816 Her	18:42:44.99	+13:54:16.8	8.361	M4.0 V	PMSU	10.91	Wein16	11 Jul 2012	10 × 50
										17 Sep 2012	10 × 50
417	J18427+596N	HD 173739	18:42:46.66	+59:37:49.9	5.189	M3.0 V	AF15	3.57	HIP2	12 Jul 2012	10 × 50
418	J18427+596S	HD 173740	18:42:46.88	+59:37:37.4	5.721	M3.5 V	AF15	3.57	aHIP2	12 Jul 2012	10 × 50
419	J18451+063	TYC 460-624-1	18:45:10.27	+06:20:15.8	7.656	M1.0 V	Lep13	19.2	This work	22 May 2014	10 × 50
420	J18453+188	G 184-024	18:45:22.94	+18:51:58.5	9.273	M4.0 V	AF15	16.3	This work	01 Mar 2014	10 × 50
421	J18480-145	G 155-042	18:48:01.29	-14:34:50.8	8.375	M2.5 V	PMSU	18.4	This work	10 Jul 2012	10 × 50
422	J18482+076	G 141-036	18:48:17.52	+07:41:21.0	8.853	M5.0 V	AF15	7.2	Dit14	22 May 2014	10 × 50
423	J18507+479	G 205-038	18:50:45.21	+47:58:19.5	8.686	M3.5 V	PMSU	15.2	This work	12 Jul 2012	10 × 50
424	J18516+244	G 184-036	18:51:40.84	+24:27:32.2	8.925	M3.0 V	PMSU	20.2	This work	12 Jul 2012	10 × 50
425	J18548+109	V1436 Aql B	18:54:53.81	+10:58:43.5	7.139	M3.5 V	PMSU	19.2	aJen63	22 May 2014	10 × 50
426	J18571+075	LP 571-080	18:57:10.54	+07:34:17.1	8.331	M2.0 V	PMSU	20.8	This work	11 Jul 2012	10 × 50
427	J19032+034	G 141-057	19:03:13.61	+03:24:02.8	8.665	M3.0 V	Lep13	17.9	This work	15 Apr 2015	10 × 50
428	J19084+322	G 207-019	19:08:29.96	+32:16:52.0	7.905	M3.0 V	PMSU	12.6	This work	11 Jul 2012	10 × 50
429	J19098+176	GJ 1232	19:09:50.98	+17:40:07.4	8.819	M4.5 V	PMSU	10.3	Dit14	10 Jul 2012	10 × 50
430	J19122+028	Wolf 1062 AB	19:12:14.55	+02:53:11.2	7.087	M3.5 V	PMSU	10.2	HIP2	10 Jul 2012	10 × 50
431	J19124+355	G 207-022	19:12:29.38	+35:33:52.6	8.399	M2.5 V	PMSU	17.2	vAl95	12 Jul 2012	10 × 50
432	J19220+070	GJ 1236	19:22:02.07	+07:02:31.0	8.524	M3.0 V	PMSU	10.54	Wein16	15 Apr 2015	10 × 50
433	J19354+377	RX J1935.4+3746	19:35:29.23	+37:46:08.2	7.562	M3.5 V	Lep13	9.2	This work	15 Apr 2015	10 × 50
434	J19463+320	BD+31 3767A	19:46:23.86	+32:01:02.1	6.883	M0.5 V	PMSU	13.61	HIP2	11 Jul 2012	10 × 50
										17 Sep 2012	10 × 50
										15 Apr 2015	10 × 50
435	J19464+320	BD+31 3767B	19:46:24.15	+32:00:58.6	7.323	M2.5 V	Kir91	13.61	aHIP2	11 Jul 2012	10 × 50
										17 Sep 2012	10 × 50
										15 Apr 2015	10 × 50
436	J19511+464	G 208-042	19:51:09.31	+46:28:59.9	8.586	M4.0 V	PMSU	11.9	vAl95	12 Jul 2012	10 × 50
437	J19539+444W	V1581 Cyg AB	19:53:54.43	+44:24:54.2	7.791	M5.5 V	AF15	4.6	HD80	12 Jul 2012	10 × 50
										17 Sep 2012	10 × 50
438	J19539+444E	GJ 1245 C	19:53:55.09	+44:24:55.0	8.275	M5.5 V	AF15	4.4	Dit14	12 Jul 2012	10 × 50
										17 Sep 2012	10 × 50
439	J19582+020	LP 634-002	19:58:15.72	+02:02:15.2	8.371	M2.5 V	PMSU	15.8	vAl95	12 Jul 2012	10 × 50
440	J20039-081	LP 694-016	20:03:58.92	-08:07:47.3	9.184	M4.0 V	PMSU	15.7	This work	12 Jul 2012	10 × 50
441	J20187+158	LTT 15944	20:18:44.54	+15:50:46.4	8.174	M2.5 V	PMSU	16.8	This work	11 Jul 2012	10 × 50
442	J20298+096	HU Del AB	20:29:48.34	+09:41:20.2	8.228	M4.5 V	PMSU	8.86	Ben00	10 Jul 2012	10 × 50
443	J20336+617	GJ 1254	20:33:40.31	+61:45:13.6	8.287	M4.0 V	PMSU	15.9	vAl95	12 Jul 2012	10 × 50
444	J20347+033	G 024-020	20:34:43.04	+03:20:50.9	8.446	M2.5 V	PMSU	26.9	HIP2	12 Jul 2012	10 × 50
445	J20367+388	G 209-038	20:36:46.01	+38:50:33.0	9.270	M3.5 V	PMSU	19.8	This work	11 Jul 2012	10 × 50
446	J20407+199	GJ 797 B	20:40:44.50	+19:54:02.3	8.160	M2.5 V	AF15	20.9	aHIP2	12 Jul 2012	10 × 50
										17 Sep 2012	10 × 50

Table A.1. Log of observed stars (continued).

No.	Karmn	Name	α (J2000)	δ (J2000)	J [mag]	SpT	Ref. ^a	d [pc]	Ref. ^b	Observation date	N × t_{exp} [s]
447	J20433+553	GJ 802 AabB	20:43:19.21	+55:20:52.1	9.563	M5.0 V	PMSU	15.7	Ire08	14 Apr 2015	10 × 50
448	J20445+089N	LP 576–039	20:44:30.45	+08:54:25.3	8.607	M3.5 V	PMSU	22.2	This work	10 Jul 2012	10 × 50
449	J20445+089S	LP 576–040	20:44:30.73	+08:54:10.7	8.136	M1.5 V	PMSU	22.2	This work	12 Jul 2012	10 × 50
450	J20488+197	G 144–039	20:48:52.46	+19:43:05.0	9.236	M4.0 V	PMSU	33.56	vAl95	17 Sep 2012	10 × 50
451	J20535+106	G 025–008	20:53:33.04	+10:37:02.0	9.348	M4.0 V	PMSU	13.9	vAl95	11 Jul 2012	10 × 50
452	J20556-140N	GJ 810 A	20:55:37.72	-14:02:07.8	8.117	M4.0 V	PMSU	12.66	Wein16	17 Sep 2012	10 × 50
453	J21012+332	LP 340–547	21:01:16.10	+33:14:32.8	8.439	M3.0 V	PMSU	18.2	This work	12 Jul 2012	10 × 50
										17 Sep 2012	10 × 50
										14 Apr 2015	10 × 50
										15 Apr 2015	10 × 50
454	J21013+332	LP 340–548	21:01:20.62	+33:14:28.0	8.936	M3.5 V	PMSU	18.2	This work	11 Jul 2012	10 × 50
455	J21152+257	LP 397–041	21:15:12.59	+25:47:45.4	8.403	M3.0 V	PMSU	15.9	This work	12 Jul 2012	10 × 50
456	J21160+298E	Ross 776	21:16:05.77	+29:51:51.1	8.448	M3.5 V	PMSU	20.1	This work	12 Jul 2012	10 × 50
457	J21313-097	BB Cap AB	21:31:18.61	-09:47:26.5	7.316	M4.5 V	PMSU	8.3	HIP2	10 Jul 2012	10 × 50
458	J21323+245	LP 397–034	21:32:21.98	+24:33:41.9	8.476	M3.5 V	PMSU	22.0	Dit14	11 Jul 2012	10 × 50
										17 Sep 2012	10 × 50
459	J21512+128	G 018–001	21:51:17.41	+12:50:30.3	9.349	M4.0 V	PMSU	26.2	vAl95	11 Jul 2012	10 × 50
460	J21518+136	LP 518–058	21:51:48.32	+13:36:15.5	9.311	M4.5 V	PMSU	16.0	Dit14	17 Sep 2012	10 × 50
										29 Jul 2015	10 × 50
461	J21593+418	G 215–030	21:59:21.92	+41:51:32.7	8.982	M3.0 V	PMSU	20.8	This work	16 Sep 2012	10 × 50
462	J22012+283	V374 Peg	22:01:13.11	+28:18:24.9	7.635	M4.0 V	PMSU	8.9	HIP2	11 Jul 2012	10 × 50
463	J22060+393	G 189–001	22:06:00.68	+39:18:02.7	8.912	M3.0 V	PMSU	20.1	This work	16 Sep 2012	10 × 50
464	J22097+410	G 214–012	22:09:43.01	+41:02:05.3	8.755	M3.5 V	PMSU	22.5	vAl95	11 Jul 2012	10 × 50
465	J22252+594	G 232–070	22:25:17.06	+59:24:49.6	8.745	M4.0 V	PMSU	12.8	This work	16 Sep 2012	10 × 50
466	J22279+576	HD 239960 + DO Cep	22:27:59.58	+57:41:45.3	5.575	M3.0 V	PMSU	4.0	vAl95	23 Oct 2011	3 × 35
467	J22298+414	G 215–050	22:29:48.86	+41:28:48.0	8.849	M4.0 V	PMSU	13.8	vAl95	11 Jul 2012	10 × 50
468	J22426+176	GJ 1271	22:42:38.72	+17:40:09.1	8.062	M2.5 V	PMSU	20.3	HIP2	16 Sep 2012	10 × 50
469	J22507+286	LP 344–047	22:50:45.49	+28:36:08.5	8.810	M3.0 V	PMSU	19.2	This work	16 Sep 2012	10 × 50
470	J23096-019	G 028–044	23:09:39.32	-01:58:23.0	8.671	M3.5 V	PMSU	20.2	This work	14 Jan 2013	10 × 50
										17 Sep 2012	10 × 50
471	J23174+382	G 190–017	23:17:24.41	+38:12:42.0	7.761	M2.5 V	PMSU	17.5	vAl95	11 Jul 2012	10 × 50
472	J23174+196	G 067–053 AB	23:17:28.07	+19:36:46.9	8.020	M3.5 V	PMSU	9.1	Dit14	10 Jul 2012	10 × 50
473	J23216+172	LP 462–027	23:21:37.52	+17:17:28.5	7.391	M4.0 V	PMSU	10.99	HIP2	16 Sep 2012	10 × 50
474	J23265+121	LP 522–049	23:26:32.39	+12:09:32.8	8.962	M3.0 V	PMSU	38.3	vAl95	16 Sep 2012	10 × 50
475	J23293+414S	G 190–027	23:29:22.58	+41:27:52.2	8.017	M4.0 V	PMSU	14.9	avAl95	29 Jul 2015	10 × 50
										11 Jul 2012	10 × 50
476	J23293+414N	G 190–028	23:29:23.46	+41:28:06.9	7.925	M3.5 V	PMSU	14.9	vAl95	29 Jul 2015	10 × 50

Table A.1. Log of observed stars (continued).

No.	Karmn	Name	α (J2000)	δ (J2000)	J [mag]	SpT	Ref. ^a	d [pc]	Ref. ^b	Observation date	$N \times t_{\text{exp}}$ [s]
477	J23318+199E	EQ Peg Aab	23:31:52.09	+19:56:14.2	6.162	M3.5 V	PMSU	6.2	HIP2	23 Oct 2011 25 Oct 2011	69 × 150 60 × 150
478	J23318+199W	EQ Peg Bab	23:31:52.48	+19:56:13.8	7.101	M4.5 V	PMSU	6.2	aHIP2	23 Oct 2011 25 Oct 2011	69 × 150 60 × 150
479	J23351-023	GJ 1286	23:35:10.50	-02:23:21.4	9.148	M5.5 V	PMSU	7.21	Wein16	16 Sep 2012	10 × 50
480	J23381-162	G 273-093	23:38:08.19	-16:14:10.0	7.813	M2.0 V	PMSU	16.4	This work	16 Sep 2012	10 × 50
481	J23428+308	GJ 1288	23:42:52.74	+30:49:21.9	9.637	M4.5 V	PMSU	12.6	Dit14	16 Sep 2012	10 × 50
482	J23431+365	GJ 1289	23:43:06.29	+36:32:13.2	8.110	M4.0 V	PMSU	8.1	vAl95	11 Jul 2012	10 × 50
483	J23455-161	LP 823-004 AB	23:45:31.28	-16:10:19.8	9.206	M5.0 V	PMSU	12.5	Ried10	10 Jul 2012	10 × 50
484	J23492+024	BR Psc	23:49:12.56	+02:24:03.8	5.827	M1.0 V	PMSU	5.98	HIP2	16 Sep 2012	10 × 50
485	J23492+100	G 029-069	23:49:15.02	+10:05:38.5	9.459	M4.0 V	PMSU	17.8	This work	16 Sep 2012	10 × 50
486	J23505-095	LP 763-012	23:50:31.59	-09:33:32.1	8.943	M4.0 V	PMSU	16.0	Ried10	16 Sep 2012	10 × 50
487	J23517+069	G 030-026	23:51:44.83	+06:58:15.9	8.841	M3.0 V	PMSU	21.0	This work	16 Sep 2012 14 Jan 2013 29 Jul 2015	10 × 50 10 × 50
488	J23573-129W	LP 704-014 Bab	23:57:19.35	-12:58:40.7	9.128	M4.0 V	PMSU	15.6	This work	14 Jan 2013	10 × 50
489	J23573-129E	LP 704-015 A	23:57:20.57	-12:58:48.7	8.636	M3.0 V	PMSU	17.7	This work	14 Jan 2013	10 × 50
490	J23577+233	GJ 1292	23:57:44.10	+23:18:17.0	7.800	M3.5 V	PMSU	13.7	vAl95	11 Jul 2012	10 × 50

Notes. ^(a) AF15: Alonso-Floriano et al. 2015a; Cru03: Cruz et al. 2003; Dea12: Deacon et al. 2012; Gig10: Gigoyan et al. 2010; Gra03: Gray et al. 2003; Gra06: Gray et al. 2006; Klutsch et al. priv. comm.; Koe10: Koen et al. 2010; Lep13: Lépine et al. 2013; Mon01: Montes et al. 2001; New14: Newton et al. 2014; PMSU: (Palomar/Michigan State University survey catalogue of nearby stars) Reid et al. 1995., Hawley et al. 1996, Gizis et al. 2002; Ria06: Riaz et al. 2006; Sch05: Scholz et al. 2005; Sim15: Simon-Díaz et al. 2015; ZS04: Zuckerman & Song 2014 ^(b) Ben00: Benedict et al. 2000; Cru03: Cruz et al. 2003; Daw05: Dawson et al. 2005; Dit14: Dittmann et al. 2014; GC09: Gatewood & Coban 2009; HD80: Harrington & Dahn 1980; Hen06: Henry et al. 2006; HT98: Hershey & Taff 1998; HIP2: van Leeuwen 2007; Ire08: Ireland et al. 2008; Jen52: Jenkins 1952; Jen63: Jenkins 1963; Jen09: Jenkins et al. 2009; Lep13: Lépine et al. 2013; New14: Newton et al. 2014; PMSU: (Palomar/Michigan State University survey catalogue of nearby stars) Reid et al. 1995., Hawley et al. 1996, Gizis et al. 2002; Rei02: Reid et al. 2002; Ried10: Ria06: Riaz et al. 2006; Reidel et al. 2010; Ried14: Riedel et al. 2014; Sub09: Subasavage et al. 2009; vAl95: van Altena et al. 1995; Wein16: Weinberger et al. 2016. An “a” or “b” preceding the reference indicates that no measure for this component was found but we used instead the measure of the A or B companion, respectively.

Table A.2. ADS standard stars.

ADS	Literature		Epoch	Ref. ^a	This work		Epoch
	ρ [arcsec]	θ [deg]			ρ [arcsec]	θ [deg]	
2999	3.55	222.2	J2011.662	Mas12	3.634 ± 0.016	222.56 ± 0.22	J2012.078
					3.621 ± 0.010	222.43 ± 0.16	J2012.081
					3.611 ± 0.010	222.19 ± 0.17	J2013.034
3297	2.93	276.8	J2011.064	Mas12	3.073 ± 0.012	276.98 ± 0.23	J2012.078
					3.070 ± 0.009	276.92 ± 0.18	J2012.081
					3.067 ± 0.013	277.05 ± 0.17	J2012.229
					3.069 ± 0.008	277.03 ± 0.16	J2012.231
					3.073 ± 0.010	276.74 ± 0.16	J2013.034
3853	3.041	74.2	J2008.867	Har11	3.072 ± 0.012	74.80 ± 0.30	J2012.078
					3.085 ± 0.013	74.85 ± 0.13	J2012.081
					3.070 ± 0.009	74.92 ± 0.15	J2012.231
					3.079 ± 0.023	74.66 ± 0.12	J2013.034
					0.243 ± 0.008	85.89 ± 2.46	J2012.234
4241 (A–B) ^b	0.2526 ± 0.0010	80.1 ± 0.4	J2013.710	Sim15	11.439 ± 0.071	238.25 ± 0.24	J2012.234
4241 (AB–C)	11.24	239.2	J2013.168	Schl13	3.768 ± 0.011	161.81 ± 0.13	J2012.234
7878	3.743 ± 0.021	161.7 ± 0.3	J2008.036	Pru09	3.769 ± 0.010	161.74 ± 0.18	J2014.936
8105	3.678 ± 0.035	96.8 ± 0.3	J2010.392	Pru12	3.665 ± 0.012	97.64 ± 0.13	J2012.234
8220	3.495	208.14	J2013.314	Ben14	3.673 ± 0.012	97.54 ± 0.15	J2014.936
9168	2.199 ± 0.013	254.9 ± 0.3	J2011.491	Sca13	3.506 ± 0.009	207.84 ± 0.14	J2012.234
					3.510 ± 0.010	207.91 ± 0.18	J2014.936
9312	3.029 ± 0.016	37.6 ± 0.3	J2011.496	Sca13	2.200 ± 0.006	255.52 ± 0.19	J2012.231
					2.203 ± 0.008	255.19 ± 0.16	J2012.527
					2.209 ± 0.011	255.31 ± 0.13	J2013.034
					2.197 ± 0.011	255.42 ± 0.25	J2013.036
					2.182 ± 0.008	255.62 ± 0.20	J2014.159
					2.188 ± 0.010	255.52 ± 0.23	J2014.162
					3.049 ± 0.010	37.95 ± 0.19	J2012.229
					3.046 ± 0.007	37.88 ± 0.19	J2012.231
9461	4.130 ± 0.015	276.95 ± 0.16	J2008.608	Des11	3.052 ± 0.011	37.81 ± 0.13	J2012.234
					3.048 ± 0.010	37.96 ± 0.19	J2012.527
					3.047 ± 0.009	37.83 ± 0.18	J2013.036
					3.042 ± 0.012	37.54 ± 0.18	J2014.159
					3.052 ± 0.016	37.55 ± 0.19	J2014.162
					3.035 ± 0.018	37.57 ± 0.14	J2014.164
					4.111 ± 0.012	277.05 ± 0.16	J2012.229
					4.118 ± 0.017	277.01 ± 0.16	J2012.231
14708	2.48	28.6	J2010.693	Thor11	4.104 ± 0.013	276.76 ± 0.16	J2012.527
					4.092 ± 0.014	276.76 ± 0.14	J2013.036
					4.084 ± 0.012	276.95 ± 0.16	J2014.159
					4.094 ± 0.012	277.10 ± 0.22	J2014.162
					4.094 ± 0.012	277.06 ± 0.13	J2014.164
14733	2.601 ± 0.021	123.9 ± 0.4	J2011.876	Sca13	2.453 ± 0.015	28.15 ± 0.16	J2011.812
					2.454 ± 0.014	28.45 ± 0.13	J2012.708
					2.460 ± 0.014	28.57 ± 0.16	J2012.710
					2.451 ± 0.011	28.06 ± 0.12	J2014.386
					2.662 ± 0.012	125.11 ± 0.13	J2011.812
14878	6.85	113.9	J2012.595	Mas13	2.631 ± 0.013	125.19 ± 0.16	J2012.708
					2.647 ± 0.015	125.54 ± 0.16	J2012.710
					2.638 ± 0.012	125.60 ± 0.14	J2014.386
					6.897 ± 0.012	113.60 ± 0.12	J2011.807
					6.842 ± 0.015	113.57 ± 0.14	J2012.708
15935	3.593	224.19	J1990.809	Ha4	6.864 ± 0.013	113.98 ± 0.13	J2012.710
					6.842 ± 0.012	113.96 ± 0.13	J2014.386

Table A.2. ADS standard stars (continued).

ADS	Literature		Epoch	Ref. ^a	This work		Epoch
	ρ [arcsec]	θ [deg]			ρ [arcsec]	θ [deg]	
16389	3.893 ± 0.019	13.9 ± 0.3	J2009.957	Sca11	3.906 ± 0.011	225.29 ± 0.14	J2012.710
					3.970 ± 0.012	13.85 ± 0.15	J2011.810
					3.999 ± 0.011	14.20 ± 0.17	J2012.522
					3.973 ± 0.011	14.55 ± 0.18	J2012.524
					3.983 ± 0.013	14.47 ± 0.16	J2012.527
16496	2.664 ± 0.027	164.9 ± 0.5	J2011.860	Sca13	3.982 ± 0.013	14.45 ± 0.14	J2012.708
					2.702 ± 0.010	165.07 ± 0.20	J2012.522
					2.681 ± 0.012	165.59 ± 0.13	J2012.708
16982	2.590 ± 0.028	210.8 ± 0.7	J2011.874	Sca13	2.626 ± 0.015	211.37 ± 0.14	J2011.810
					2.625 ± 0.014	211.81 ± 0.13	J2012.708
					2.637 ± 0.014	211.96 ± 0.13	J2012.710
17140	3.094 ± 0.030	325.4 ± 0.5	J2011.874	Sca13	3.197 ± 0.012	325.81 ± 0.18	J2012.522
					3.155 ± 0.007	326.24 ± 0.14	J2012.524
					3.149 ± 0.015	326.08 ± 0.12	J2012.708

Notes. ^(a) Ben14: Benavides 2014; Des11: Desidera et al. 2011; Har11: Hartkopf et al. 2011; Mas12: Mason et al. 2012; Mas13: Mason et al. 2013; Sca11: Scardia et al. 2011 ; Sca13: Scardia et al. 2013; Schl13: Schlimmer 2013; Sim15: Simon–Díaz et al. 2015; Thor11: Thorel et al. 2011.

^(b) $\Delta I = 0.35$ mag for A-B and $\Delta I = 5.39$ mag for AB-C (this work).

Table A.3. List of observed stars with confirmed visual (unbound) companions.

Karmn	No.	ρ [arcsec]	θ [deg]	Observation date
J00234+243	#1	2.4	257	J2011.812
J00413+558	#1	13.1	129	J2011.812
J01033+623	#1	10.6	13	J2011.807
J01593+585	#1	7.5	7	J2011.807
	#1	7.8	5	J2013.034
	#2	4.2	93	J2013.034
J02565+554W	#1	7.6	241	J2012.710
	#1	7.7	242	J2013.034
J03102+059	#1	10.6	174	J2012.710
J05106+297	#1	3.1	308	J2014.162
J06000+027	#1	7.8	313	J2011.807
	#1	7.9	315	J2012.231
	#1	8.5	311	J2014.936
J06361+116	#1	8.7	114	J2011.807
	#1	8.7	112	J2012.231
J06422+035	#1	8.2	34	J2011.807
J06490+371	#1	12.6	302	J2011.810
J07033+346	#1	9.3	357	J2011.810
J07227+306	#1	9.0	29	J2012.234
J07518+055	#1	9.7	340	J2012.081
J07581+072	#1	11.1	260	J2012.081
	#2	11.8	315	J2012.081
J08105-138	#1	9.6	55	J2012.234
	#1	9.74	55	J2013.036
J08126-215	#1	12.7	329	J2012.234
J08428+095	#1	6.2	145	J2012.081
	#1	5.62	144	J2013.034
J11289+101	#1	14.0	217	J2012.229
J11420+147	#1	6.4	93	J2012.234
J13165+278	#1	6.2	1	J2012.231
J16462+164	#1	12.8	35	J2012.229
	#1	13.0	36	J2012.524

Table A.3. List of observed stars with confirmed visual (unbound) companions (continued).

Karmn	No.	ρ [arcsec]	θ [deg]	Observation date
	#1	13.2	35	J2012.710
	#1	14.6	36	J2015.284
J16509+224	#1	9.1	318	J2012.524
J17177-118	#1	5.3	149	J2012.231
J17321+504	#1	12.5	23	J2012.234
J17425-166	#1	8.9	123	J2012.234
	#2	3.2	276	J2012.234
J17460+246	#1	6.4	357	J2012.524
J17530+169	#1	8.9	31	J2012.522
	#1	8.9	31	J2012.527
	#1	9.0	31	J2012.708
J18240+016	#1	7.0	216	J2012.524
J18264+113	#1	4.2	10	J2012.522
J18387-144	#1	4.8	261	J2012.522
	#2	9.6	300	J2012.522
	#3	7.3	61	J2012.522
J18427+139	#1	3.6	178	J2012.524
	#1	3.7	177	J2012.710
J18480-145	#1	7.6	234	J2012.522
J19098+176	#1	6.7	326	J2012.522
J19124+355	#1	12.4	125	J2012.527
J19220+070	#1	4.7	73	J2015.284
J19463+320	#1	11.8	186	J2012.524
	#1	11.7	186	J2012.710
	#1	11.0	194	J2015.284
	#2	8.5	25	J2012.524
	#2	8.7	27	J2012.710
	#3	8.8	117	J2012.524
	#3	9.0	117	J2012.710
J19539+444W	#1	14.9	116	J2012.527
	#1	14.9	112	J2012.710
J20298+096	#1	9.2	201	J2012.522
J20347+033	#1	10.5	300	J2012.527
J21013+332	#1	10.1	63	J2012.524
J21518+136	#1	11.4	124	J2012.524
J22252+594	#1	11.8	34	J2012.708
J23577+233	#1	4.6	76	J2012.524

Table A.4. Astrometric properties of the physically and likely bound binaries in the sample.

Karmn	WDS	ρ [arcsec]	θ [deg]	ΔI [mag]	Epoch	GSC 1.2 ^a
Physically bound systems						
J00154-161	00155-1608 HEI299	0.275 ± 0.013	204.96 ± 3.10	0.58 ± 0.08	J2012.522	F
J00413+558	00415+5550 GIC13	10.833 ± 0.047	68.25 ± 0.28	2.92 ± 0.13	J2011.812	F
J02518+294	New	0.626 ± 0.008	249.44 ± 1.29	0.53 ± 0.10	J2011.810	F
		0.798 ± 0.011	247.05 ± 0.11	0.50 ± 0.07	J2015.875	
		0.803 ± 0.015	246.30 ± 1.54	...	J2016.015	
J02565+554W	02565+5526 LDS5401	16.664 ± 0.051	21.15 ± 0.17	0.97 ± 0.04	J2012.710	F
J02591+366 ^b	New	1.949 ± 0.010	4.35 ± 0.28	3.10 ± 0.13	J2013.036	F
		1.900 ± 0.054	358.58 ± 0.83	...	J2016.094	
J03574-011	03575-0110 BU543	10.972 ± 0.027	14.61 ± 0.16	2.29 ± 0.01	J2013.034	F
J04153-076	04153-0739 STF518	8.598 ± 0.030	152.13 ± 0.14	1.62 ± 0.04	J2011.812	...

Table A.4. Astrometric properties of the physically and likely bound binaries in the sample (continued).

Karmn	WDS	ρ [arcsec]	θ [deg]	ΔI [mag]	Epoch	GSC 1.2
J04311+589	04312+5858 STI2051	9.885 ± 0.039	59.64 ± 0.23	3.64 ± 0.05	J2011.812	...
J05019+099	05020+0959 HDS654	1.354 ± 0.012	148.90 ± 0.34	0.67 ± 0.15	J2014.159	F
J05034+531	Ward-Duong et al. 2015	5.600 ± 0.021 5.614 ± 0.006	279.58 ± 0.19 279.27 ± 0.14	5.83 ± 0.07 5.53 ± 0.15	J2014.162 J2015.875	F
J05068-215E(A)	05069-2135 DON93	8.499 ± 0.053 8.459 ± 0.024 8.462 ± 0.019	307.94 ± 0.33 308.08 ± 0.17 308.04 ± 0.17	0.81 ± 0.04 0.82 ± 0.03 0.69 ± 0.02	J2011.812 J2012.710 J2013.036	T
J05068-215W(BC)	05069-2135 DON93	0.767 ± 0.004 0.803 ± 0.029 0.811 ± 0.010	128.97 ± 1.58 126.86 ± 1.52 125.54 ± 0.60	0.51 ± 0.07 0.61 ± 0.04 0.64 ± 0.02	J2011.812 J2012.710 J2013.036	T
J05078+179	New	0.540 ± 0.003 0.348 ± 0.010 Unresolved	286.30 ± 0.66 288.28 ± 1.34 ...	1.94 ± 0.02 1.99 ± 0.05 ...	J2013.034 J2014.164 J2015.284	T
J05103+488	05104+4850 HEI321	1.993 ± 0.051 1.989 ± 0.009	113.00 ± 0.87 112.78 ± 0.17	0.90 ± 0.02 0.50 ± 0.10	J2013.034 J2015.284	F
J05333+448 ^c	05333+449 BH76	0.205 ± 0.008 0.192 ± 0.011 0.183 ± 0.004 0.164 ± 0.066 0.144 ± 0.060 0.140 ± 0.070	38.55 ± 2.80 36.47 ± 0.19 35.75 ± 1.18 33.95 ± 5.65 35.24 ± 5.29 34.13 ± 5.10	0.24 ± 0.05 ...	J2011.810 J2012.229 J2012.231 J2012.710 J2013.034 J2014.159	T
J05342+103N	05342+1019 LDS6189	5.061 ± 0.012	188.72 ± 0.14	1.02 ± 0.03	J2013.034	F
J05466+441	New	3.729 ± 0.016 3.712 ± 0.022	222.80 ± 0.20 222.70 ± 0.41	5.71 ± 0.04 6.21 ± 0.08	J2011.810 J2014.162	F
J06212+442	Ansdell et al. 2015	1.222 ± 0.060 1.319 ± 0.019	204.6 ± 3.69 203.67 ± 0.22	...	J2013.036 J2015.875	F
J06400+285	New	0.258 ± 0.004 0.251 ± 0.001 0.269 ± 0.003 Unresolved Unresolved	80.35 ± 1.76 87.30 ± 0.18 91.35 ± 1.65 ...	0.30 ± 0.06 0.23 ± 0.05 ...	J2012.081 J2012.710 J2013.034 J2014.159 J2015.284	F
J07395+334	07397+3328 LDS3755	13.675 ± 0.066	48.97 ± 0.32	4.81 ± 0.08	J2012.081	F
J08066+558	New	0.274 ± 0.004 0.248 ± 0.004 0.202 ± 0.011 0.174 ± 0.060	257.27 ± 1.23 253.75 ± 0.88 245.61 ± 3.40 236.52 ± 8.48	0.53 ± 0.11 0.55 ± 0.08 0.54 ± 0.03 ...	J2012.081 J2013.034 J2014.159 J2015.284	T
J08082+211 ^d	08082+2106 COU91	10.617 ± 0.030 10.633 ± 0.095 New	144.74 ± 0.18 144.10 ± 1.52 0.329 ± 0.020 74.26 ± 0.74	1.03 ± 0.03 0.88 ± 0.01 ...	J2012.081 J2015.875 J2012.081	F
J08105-138	08107-1348 JOD4	0.927 ± 0.006 0.913 ± 0.009	283.74 ± 0.34 283.11 ± 0.87	1.80 ± 0.05 1.77 ± 0.05	J2012.234	T
J08595+537	New	0.229 ± 0.011 0.301 ± 0.012	219.10 ± 4.19 223.00 ± 1.49	0.29 ± 0.06 0.26 ± 0.05	J2014.162 J2015.281	F
J09011+019	New	2.954 ± 0.014 2.994 ± 0.016 3.096 ± 0.065	154.77 ± 0.17 155.08 ± 0.23 156.22 ± 0.40	4.68 ± 0.06 4.58 ± 0.07 4.40 ± 0.14	J2012.229 J2013.034 J2015.875	F
J10151+314	New	1.799 ± 0.005 1.806 ± 0.007 1.822 ± 0.012 1.815 ± 0.010	306.58 ± 0.20 306.43 ± 0.26 306.41 ± 0.58 306.40 ± 0.23	0.69 ± 0.05 0.69 ± 0.09 0.57 ± 0.10 0.66 ± 0.08	J2012.229 J2013.034 J2014.159 J2015.281	F
J10196+198	10200+1950 BAG32	0.195 ± 0.061	23.81 ± 3.68	2.00 ± 0.2	J2012.078	T
J10260+504W	10261+5029 LDS1241	14.413 ± 0.038 14.410 ± 0.045	25.83 ± 0.18 25.58 ± 0.25	0.24 ± 0.04 0.24 ± 0.09	J2012.229 J2014.164	T
J10379+127	New	0.848 ± 0.010 0.792 ± 0.013 0.806 ± 0.020	333.88 ± 1.08 336.27 ± 0.94 336.05 ± 0.83	0.47 ± 0.09 0.49 ± 0.10 0.58 ± 0.11	J2014.162 J2015.281 J2015.875	F
J10448+324	New	1.292 ± 0.025	157.62 ± 0.81	0.55 ± 0.11	J2013.036	T

Table A.4. Astrometric properties of the physically and likely bound binaries in the sample (continued).

Karmn	WDS	ρ [arcsec]	θ [deg]	ΔI [mag]	Epoch	GSC 1.2
J10546-073	New	1.267 ± 0.014 0.793 ± 0.028 0.813 ± 0.039	159.63 ± 0.57 60.71 ± 1.66 64.75 ± 2.66	0.47 ± 0.08 0.41 ± 0.08 0.45 ± 0.09	J2015.284 J2014.164 J2015.281	F
J11355+389	New	0.244 ± 0.020 0.219 ± 0.005 0.278 ± 0.004 0.281 ± 0.007 0.339 ± 0.017	50.84 ± 1.90 46.41 ± 2.14 55.49 ± 2.22 61.37 ± 1.43 65.67 ± 1.96	0.51 ± 0.10 0.63 ± 0.12 0.64 ± 0.12 0.44 ± 0.08 0.55 ± 0.10	J2012.231 J2012.524 J2013.034 J2014.159 J2015.281	F
J11521+039	New	0.224 ± 0.014 0.337 ± 0.008	29.25 ± 3.75 26.06 ± 2.08	0.51 ± 0.11 0.46 ± 0.10	J2014.162 J2015.281	F
J12006-138	12007-1348 LDS4166	6.839 ± 0.021 6.836 ± 0.023	234.14 ± 0.17 234.05 ± 0.16	2.44 ± 0.03 2.40 ± 0.03	J2012.081 J2013.034	F
J12016-122	New	6.123 ± 0.013 6.134 ± 0.012 6.109 ± 0.018	24.42 ± 0.13 24.41 ± 0.19 24.58 ± 0.16	5.05 ± 0.13 5.13 ± 0.19 5.14 ± 0.17	J2012.234 J2013.034 J2015.284	T
J12123+544S	12123+5429 VYS5	14.677 ± 0.044	9.91 ± 0.15	2.86 ± 0.04	J2012.231	F
J12162+508	New	1.884 ± 0.014 ... 1.828 ± 0.010	188.92 ± 0.84 ... 190.85 ± 0.33	0.48 ± 0.07 ... 0.42 ± 0.08	J2014.162 J2014.386 J2015.281	F
J12277-032	New	1.496 ± 0.018 1.459 ± 0.007	15.84 ± 0.45 15.73 ± 0.50	1.67 ± 0.04 1.75 ± 0.06	J2014.162 J2015.281	T
J12332+090	12335+0901 REU1	0.398 ± 0.005 0.447 ± 0.003 0.445 ± 0.003 0.446 ± 0.004 0.529 ± 0.003 0.531 ± 0.005 0.667 ± 0.007 0.921 ± 0.011	173.37 ± 0.76 170.25 ± 0.46 170.043 ± 0.49 169.92 ± 0.75 163.46 ± 0.35 164.74 ± 0.64 159.16 ± 0.31 151.76 ± 0.37	0.55 ± 0.11 0.46 ± 0.09 0.41 ± 0.07 0.40 ± 0.08 0.44 ± 0.04 0.52 ± 0.10 0.55 ± 0.06 0.46 ± 0.08	J2012.081 J2012.299 J2012.231 J2012.234 J2012.522 J2012.524 J2013.036 J2014.159	...
J13168+170	13169+1701 BU800	7.658 ± 0.024 7.659 ± 0.024	104.89 ± 0.18 104.50 ± 0.18	2.11 ± 0.02 2.04 ± 0.01	J2014.159 J2015.284	F
J13180+022	New	0.637 ± 0.007 0.646 ± 0.012 0.592 ± 0.004 0.530 ± 0.055	213.25 ± 0.51 217.48 ± 0.69 222.91 ± 0.37 225.78 ± 2.51	0.78 ± 0.15 0.45 ± 0.08 0.55 ± 0.10 0.53 ± 0.10	J2012.229 J2013.034 J2014.159 J2015.281	T
J13317+292	13318+2917 BEU17	0.193 ± 0.066 0.190 ± 0.095 Unresolved	79.42 ± 11.91 85.41 ± 3.58 ...	1.5 ± 0.2 ...	J2012.522 J2012.527 J2015.281	F
J13417+582	13418+5815 JNN94	0.675 ± 0.020 0.699 ± 0.022	251.26 ± 1.42 251.33 ± 0.56	0.38 ± 0.08 ...	J2014.164 J2015.281	F
J13526+144	13526+1425 JOD7	1.252 ± 0.008 1.231 ± 0.015 1.197 ± 0.016	356.75 ± 0.30 357.72 ± 0.34 359.55 ± 0.79	1.52 ± 0.03 1.64 ± 0.04 1.69 ± 0.04	J2012.078 J2013.034 J2015.284	T
J14157+594	14157+5928 LDS2707	5.014 ± 0.054 5.021 ± 0.075 5.064 ± 0.020	231.04 ± 0.59 230.87 ± 0.54 230.90 ± 0.19	0.46 ± 0.07 0.46 ± 0.09 0.76 ± 0.03	J2014.164 J2014.386 J2015.284	F
J14210+275	New	0.626 ± 0.008 0.683 ± 0.009	82.25 ± 0.93 84.96 ± 0.39	1.82 ± 0.04 1.73 ± 0.05	J2012.231 J2015.281	F
J14279-003S	14279-0032 GIC20	13.032 ± 0.007	21.96 ± 0.28	0.19 ± 0.03	J2012.229	F
J14331+610	New	0.899 ± 0.020 0.944 ± 0.005	255.34 ± 1.15 252.63 ± 0.27	0.65 ± 0.13 0.58 ± 0.11	J2014.162 J2015.281	F
J15081+623	New	0.983 ± 0.022 0.947 ± 0.032 0.884 ± 0.024	61.15 ± 1.62 68.06 ± 3.30 67.63 ± 0.37	0.50 ± 0.10 0.40 ± 0.08 0.42 ± 0.10	J2014.162 J2014.386 J2015.284	T
J15126+457	15126+4544 MCT8	0.527 ± 0.080 0.481 ± 0.021	216.82 ± 2.36 219.63 ± 1.32	0.37 ± 0.08 0.36 ± 0.08	J2012.231 J2015.284	F
J15191-127 ^e	New	0.305 ± 0.064	246.58 ± 2.22	3.4 ± 0.15	J2012.234	...
J15400+434N	15400+4330 VBS25	4.529 ± 0.028	154.66 ± 0.21	1.47 ± 0.01	J2014.162	...

Table A.4. Astrometric properties of the physically and likely bound binaries in the sample (continued).

Karmn	WDS	ρ [arcsec]	θ [deg]	ΔI [mag]	Epoch	GSC 1.2
J15496+348 ^f	15496+3449 BWL41	4.525 ± 0.016	154.78 ± 0.12	1.59 ± 0.07	J2014.386	
		0.211 ± 0.002	89.25 ± 0.42	3.00 ± 0.10	J2012.234	...
		Unresolved	J2012.522	
		0.226 ± 0.003	91.31 ± 1.54	...	J2012.524	
		0.208 ± 0.013	98.68 ± 1.40	...	J2012.708	
J16487+106	New	Unresolved	J2014.159	
		0.212 ± 0.010	20.25 ± 1.62	0.39 ± 0.08	J2014.162	F
		Unresolved	J2014.386	
J16554-083S	16555-0820 KUI75	0.235 ± 0.012	31.97 ± 2.08	0.30 ± 0.06	J2015.281	
		0.206 ± 0.004	216.03 ± 1.02	0.43 ± 0.09	J2012.231	...
		5.082 ± 0.020	62.27 ± 0.25	2.48 ± 0.02	J2014.386	F
J16578+473	16579+4722 A1874	New	143.11 ± 2.15	0.54 ± 0.11	J2014.386	T
		0.544 ± 0.018	144.97 ± 0.71	0.47 ± 0.09	J2015.281	
		0.596 ± 0.009	123.69 ± 0.49	0.60 ± 0.06	J2012.231	T
J17530+169	New	0.896 ± 0.006	122.86 ± 0.24	0.66 ± 0.09	J2012.522	
		0.887 ± 0.003	122.56 ± 0.21	0.61 ± 0.12	J2012.527	
		0.893 ± 0.004	122.20 ± 0.41	0.69 ± 0.11	J2012.708	
		0.871 ± 0.010	114.50 ± 1.37	0.68 ± 0.13	J2015.284	
		0.823 ± 0.016	134.79 ± 0.43	0.81 ± 0.01	J2012.524	
J18180+387E	18180+3846 GIC151	9.940 ± 0.031	277.79 ± 0.13	1.50 ± 0.03	J2012.524	...
		8.141 ± 0.030	196.27 ± 0.33	5.89 ± 0.09	J2012.522	F
		4.828 ± 0.015	5.67 ± 0.15	2.25 ± 0.02	J2012.527	F
		11.712 ± 0.034	178.19 ± 0.17	0.88 ± 0.03	J2012.527	...
		3.854 ± 0.017	44.30 ± 0.24	2.33 ± 0.08	J2014.386	F
J18264+113	18264+1121 NI38	5.603 ± 0.040	19464+3201 KAM3	0.81 ± 0.01	J2012.524	
		5.576 ± 0.016	134.66 ± 0.15	0.79 ± 0.02	J2012.710	
		5.675 ± 0.017	134.85 ± 0.19	0.74 ± 0.01	J2015.284	
		6.461 ± 0.024	70.41 ± 0.16	0.30 ± 0.05	J2012.527	F
		6.454 ± 0.027	70.28 ± 0.20	0.65 ± 0.07	J2012.710	
J19539+444E	19539+4425 GIC59	0.642 ± 0.016	352.19 ± 1.49	2.11 ± 0.02	J2012.527	
		0.615 ± 0.048	349.91 ± 1.67	2.58 ± 0.13	J2012.710	
		0.642 ± 0.016	134.71 ± 1.71	0.31 ± 0.06	J2012.710	
		0.246 ± 0.022	7.38 ± 1.70	1.61 ± 0.09	J2012.524	F
		0.232 ± 0.016	6.31 ± 2.67	1.75 ± 0.10	J2012.710	
J20407+199	20408+19656 RAO23	Unresolved	J2015.281	
		0.290 ± 0.080	227.02 ± 6.45	1.4 ± 0.2	J2012.527	F
		15.075 ± 0.064	245.37 ± 3.69	2.1 ± 0.3	J2015.281	
		15.173 ± 0.049	344.47 ± 0.14	1.06 ± 0.04	J2012.527	F
		0.191 ± 0.006	344.42 ± 0.14	0.97 ± 0.03	J2012.710	
J20488+197	20488+1943 JNN286	0.184 ± 0.011	132.95 ± 1.68	0.33 ± 0.09	J2012.524	F
		0.246 ± 0.022	134.71 ± 1.71	0.31 ± 0.06	J2012.710	
		0.232 ± 0.016	7.38 ± 1.70	1.61 ± 0.09	J2012.524	F
		Unresolved	J2015.281	
		Unresolved	J2015.284	
J21323+245	21324+2434 MCT12	1.426 ± 0.005	243.98 ± 0.14	0.75 ± 0.15	J2012.524	T
		1.438 ± 0.006	243.66 ± 0.27	0.72 ± 0.10	J2012.710	
J21518+136	New	0.701 ± 0.010	116.96 ± 1.25	1.50 ± 0.03	J2012.524	F
		0.686 ± 0.022	118.08 ± 1.40	1.40 ± 0.05	J2012.710	
		0.674 ± 0.011	130.80 ± 1.04	...	J2015.572	
J22279+576	22280+5742 KR60	1.649 ± 0.010	359.82 ± 0.16	1.21 ± 0.03	J2011.807	T
		1.715 ± 0.006	19.37 ± 0.23	1.80 ± 0.04	J2012.708	T
J23096-019 ^g	New	1.672 ± 0.019	19.82 ± 0.37	1.84 ± 0.09	J2013.036	
		0.257 ± 0.027	209.09 ± 2.31	0.73 ± 0.09	J2012.524	F
		Unresolved	J2015.572	
J23293+414S(Bab)	23294+4128 BWL59	17.670 ± 0.069	213.92 ± 0.18	0.38 ± 0.01	J2012.524	F
		17.676 ± 0.024	214.40 ± 0.15	0.38 ± 0.01	J2015.572	
J23318+199E	23317+1956 WIR1	5.412 ± 0.019	81.14 ± 0.14	1.67 ± 0.02	J2011.807	F
		5.411 ± 0.018	81.07 ± 0.14	1.66 ± 0.01	J2011.812	
J23455-161 ^h	23455-1610 MTG5	~0.50	~15	...	J2012.522	
		2.178 ± 0.015	102.48 ± 0.40	0.47 ± 0.09	J2012.708	F
		2.165 ± 0.013	102.51 ± 0.35	0.55 ± 0.11	J2013.036	
J23517+069	New	2.181 ± 0.013	103.23 ± 0.13	...	J2015.572	

Table A.4. Astrometric properties of the physically and likely bound binaries in the sample (continued).

Karmn	WDS	ρ [arcsec]	θ [deg]	ΔI [mag]	Epoch	GSC 1.2
Likely bound systems						
J00169+200	New	1.076 ± 0.023	288.33 ± 0.54	0.70 ± 0.12	J2013.036	F
J01221+221	New	0.271 ± 0.014	175.04 ± 2.00	0.86 ± 0.17	J2015.875	F
J04352-161	New	7.887 ± 0.043	131.61 ± 0.56	4.60 ± 0.38	J2014.162	
J06277+093	New	1.103 ± 0.090	221.11 ± 1.26	1.16 ± 0.04	J2015.875	F
J07349+147	New	1.008 ± 0.019	297.13 ± 0.64	0.77 ± 0.04	J2014.164	T
		0.988 ± 0.014	293.70 ± 0.32	0.74 ± 0.03	J2015.281	
		0.995 ± 0.010	292.83 ± 0.21	0.78 ± 0.08	J2015.281	
J10028+484 ⁱ	New	0.208 ± 0.014	336.81 ± 3.05	0.31 ± 0.06	J2012.231	F

Notes. ^(a) Guide Star Catalog multiplicity flag. “F” is False, “T” is true, and “...” indicates no data. ^(b) ρ and θ measures in the second epoch correspond to observations with the CARMENES acquisition and guiding camera, which were carried out only for confirming physical association. ^(c) Similar periods between Behall & Harrington 1976 and this work suggest that we are resolving the same pair. ^(d) The B component is a double lined spectroscopic binary with a period shorter than 215.0 d (Shkolnik et al. 2010) and is not the third component resolved here. ^(e) We considered that this resolved binary is the spectroscopic binary identified by Bonfils et al. 2013, according to the radial-velocity amplitude and period estimation of the pair. Nevertheless, we can not affirm whether the system is double or triple. ^(f) Close visual binary in Bowler et al. 2015 in one epoch. Our multi-epoch images confirm physical binding. ^(g) It is also a spectroscopic binary. ^(h) Faint pair for which we could not measure ρ and θ with precision. The companion, also detected by Tokovinin et al. 2015, seems to be physically related and consistent over time with the companion identified by Montagnier et al. 2006 at 0.068 arcsec. ⁽ⁱ⁾ Also observed and identified as single in Law et al. 2008, probably due to the crossing of the companion behind the primary at the observing epoch, in agreement with the 13 a period estimated in this work.

Table A.5. Derived parameters for confirmed physical pairs.

Karmn ^a	Component	ΔI [mag]	I_1 [mag]	I_2 [mag]	SpT	SpT ₁	SpT ₂	M_1 [M _⊕]	M_2 [M _⊕]	P^b [a]
J00154-161	A, B	0.58 ± 0.08	9.24	9.82	M4.0 V	m4.0	m5.0	0.17 ± 0.08	0.15 ± 0.07	3.7
J00413+558	A, B	2.92 ± 0.13	11.36	M4.0	DC	0.22 ± 0.10
J02518+294	A, B	0.52 ± 0.10	11.56	12.08	M4.0 V	m4.0	m5.0	0.20 ± 0.09	0.15 ± 0.08	130
J02565+554W	A, B	0.97 ± 0.04	8.56	9.53	...	M1.0	m2.5	0.50 ± 0.16	0.35 ± 0.13	6400
J02591+366	A, B	3.10 ± 0.13	10.50	13.60	M3.5 V	m3.5	m6.0	0.24 ± 0.13	0.10 ± 0.07	380
J03574-011	A, B	2.29 ± 0.01	...	9.10	...	K4	M2.5	...	0.34 ± 0.12	...
J04153-076	AB, C	1.62 ± 0.04	...	8.39	...	K0.5+DA	M4.5	...	0.33 ± 0.05	...
J04311+589	A, B	3.64 ± 0.05	8.14	M4.0	DC	0.23 ± 0.10
J05019+099	Aab, B	0.67 ± 0.15	9.20	9.87	M4.0 V	0.33 ± 0.05	200
J05019+099	Aa, Ab	...	9.95	9.95	0.31 ± 0.05	0.31 ± 0.05	
J05034+531	A, B	5.68 ± 0.07	8.04	13.72	M0.5 V	m1.0	m7.0	0.45 ± 0.16	0.09 ± 0.05	910
J05068-215E	A, BC	0.77 ± 0.08	8.19	8.96	...	M1.5	...	0.62 ± 0.05	...	1600
J05068-215W	B, C	0.59 ± 0.08	8.67	9.26	M3.5	0.49 ± 0.05	0.35 ± 0.05	62
J05078+179	Aab, B	1.96 ± 0.05	9.51	11.47	M3.0 V	m2.0	m4.0	...	0.23 ± 0.08	...
J05078+179	Aa, Ab	...	10.26	10.26	m2.0	m2.5	m2.5	0.33 ± 0.05	0.33 ± 0.05	50
J05103+488	A, B	0.70 ± 0.06	9.62	10.32	M2.5 V	0.45 ± 0.05	0.31 ± 0.05	...
J05333+448	A, B	0.23 ± 0.05	10.31	10.54	M3.5 V	m3.5	m3.5	0.23 ± 0.10	0.22 ± 0.09	8.3
J05342+103N	A, Bab	1.02 ± 0.03	9.88	10.90	...	M3.0	m4.0	...	0.30 ± 0.10	990
J05342+103N	Ba, Bb	...	11.65	11.65	M4.5	m4.5	m4.5	0.18 ± 0.08	0.18 ± 0.08	...
J05466+441	Aab, B	5.76 ± 0.09	9.98	15.74	...	M4.0	m8.0	...	0.07 ± 0.03	920
J05466+441	Aa, Ab	...	10.73	10.73	M4	m3.5	m3.5	0.25 ± 0.09	0.25 ± 0.09	...
J06212+442	A, B	2.85 ± 0.13	9.99	12.84	M2.0 V	m2.0	m5.0	0.38 ± 0.11	0.16 ± 0.06	250
J06400+285	A, B	0.24 ± 0.10	10.09	10.33	M2.0 V	m2.5	m2.5	0.36 ± 0.15	0.33 ± 0.14	20
J07395+334	A, B	4.81 ± 0.08	9.62	14.43	...	M2.0	m6.5	0.54 ± 0.19	0.12 ± 0.07	13000
J08066+558	A, B	0.54 ± 0.07	9.76	10.30	M2.0 V	m2.0	m2.5	0.45 ± 0.16	0.37 ± 0.14	26
J08082+211	Bab, C	2.76 ± 0.07	8.78	11.54	M3.0 V	m2.5	m5.0	...	0.17 ± 0.09	33
J08082+211	Ba, Bb	...	9.53	9.53	m2.5	m3.0	m3.0	0.32 ± 0.10	0.32 ± 0.10	...
J08105-138	B, C	1.78 ± 0.05	9.80	11.58	M2.5 V	m2.5	m4.5	0.36 ± 0.13	0.20 ± 0.09	130
J08595+537	A, B	0.28 ± 0.06	11.11	11.39	M3.5 V	m3.5	m3.5	0.20 ± 0.09	0.18 ± 0.08	19
J09011+019	Aab, B	4.55 ± 0.17	9.27	13.82	M3.0 V	m3.0	m6.5	...	0.09 ± 0.04	460
J09011+019	Aa, Ab	...	10.02	10.02	m3.0 V	m3.5	m3.5	0.26 ± 0.10	0.26 ± 0.10	...
J10151+314	A, B	0.65 ± 0.10	11.32	11.97	M4.0 V	m4.0	m4.5	0.22 ± 0.11	0.18 ± 0.10	360
J10196+198	A, B	2.00 ± 0.20	6.93	8.93	M3.0 V	m3.0	m5.0	0.32 ± 0.12	0.18 ± 0.11	1.5
J10260+504W	A, B	0.24 ± 0.06	10.79	11.03	...	M4.0	m4.5	0.21 ± 0.09	0.20 ± 0.08	5600
J10379+127	A, B	0.51 ± 0.12	10.73	11.24	M3.0 V	m3.5	m4.0	0.26 ± 0.10	0.22 ± 0.09	100
J10448+324	Aa, Ab	0.51 ± 0.11	11.07	11.58	M3.0 V	m2.5	m3.5	0.35 ± 0.13	0.32 ± 0.12	440
J10546-073	A, B	0.43 ± 0.09	11.08	11.51	M4.0 V	m4.0	m4.5	0.21 ± 0.09	0.19 ± 0.08	80
J11355+389	A, B	0.55 ± 0.13	11.02	11.57	M3.5 V	m3.5	m4.0	0.26 ± 0.10	0.22 ± 0.09	31
J11521+039	A, B	0.48 ± 0.11	10.44	10.92	M4.0 V	m4.0	m4.5	0.22 ± 0.09	0.19 ± 0.08	15
J12006-138	A, B	2.42 ± 0.04	10.32	12.74	...	M3.5	m5.5	0.24 ± 0.13	0.12 ± 0.08	2000
J12016-122	A, B	5.11 ± 0.10	10.00	15.11	...	M3.0	m8.0	0.29 ± 0.12	0.07 ± 0.05	2000

Table A.5. continued.

Karmn	Component	ΔI [mag]	I_1 [mag]	I_2 [mag]	SpT	SpT ₁	SpT ₂	M_1 [M_\odot]	M_2 [M_\odot]	P [a]
J12123+544S	A, B	2.86 ± 0.04	7.90	10.76	...	M0.0	m4.0	0.52 ± 0.17	0.20 ± 0.09	4100
J12162+508	A, B	0.45 ± 0.11	11.36	11.81	M4.0 V	m4.0	m5.0	0.21 ± 0.11	0.19 ± 0.09	360
J12277-032	A, B	1.71 ± 0.08	10.44	12.15	M3.5 V	m3.5	m5.0	0.25 ± 0.11	0.16 ± 0.08	200
J12332+090	A, B	0.47 ± 0.10	9.36	9.83	M5.0 V	m5.0	m5.5	0.14 ± 0.07	0.12 ± 0.07	16
J13168+170	A, B	2.08 ± 0.05	...	7.562	...	K2	M0.5	...	0.46 ± 0.16	...
J13180+022	A, B	0.58 ± 0.18	10.76	11.34	M3.5 V	m3.5	m4.5	0.25 ± 0.11	0.21 ± 0.09	73
J13317+292	A,B	1.5 ± 0.2	9.23	10.73	M4.0 V	0.39 ± 0.05	0.17 ± 0.05	8.6
J13417+582	A, B	0.38 ± 0.08	10.78	11.16	M3.5 V	m3.5	m4.0	0.23 ± 0.09	0.21 ± 0.08	78
J13526+144	A, B	1.62 ± 0.09	9.42	11.04	M2.0 V	m2.0	m4.0	0.38 ± 0.17	0.23 ± 0.11	150
J14157+594	A, B	0.56 ± 0.18	10.04	10.60	...	M2.0	m3.0	0.38 ± 0.17	0.31 ± 0.14	1900
J14210+275	A, B	1.77 ± 0.08	10.45	12.22	M2.5 V	m2.5	m4.5	0.33 ± 0.13	0.20 ± 0.09	97
J14279-003S	A, B	0.19 ± 0.03	10.82	11.01	...	M4.5	m5.0	0.18 ± 0.07	0.17 ± 0.07	3900
J14331+610	A, B	0.62 ± 0.13	9.99	10.61	M2.5 V	m3.0	m3.5	0.31 ± 0.12	0.25 ± 0.11	96
J15081+623	A, B	0.44 ± 0.11	11.37	11.81	M4.0 V	m4.0	m4.5	0.21 ± 0.10	0.19 ± 0.09	140
J15126+457	A, B	0.36 ± 0.08	11.20	11.56	M4.0 V	m4.5	m5.0	0.20 ± 0.09	0.18 ± 0.09	43
J15191-127	A, B	3.40 ± 0.15	10.03	13.43	M4.0 V	m3.0	m5.5	0.33 ± 0.06	0.13 ± 0.05	13
J15400+434N	A, B	1.53 ± 0.09	9.63	11.16	...	M3.0	m4.5	0.26 ± 0.10	0.17 ± 0.08	730
J15496+348	A,B	3.00 ± 0.10	10.30	13.30	M4.0 V	m3.5	m7.0	0.26 ± 0.11	0.11 ± 0.09	12
J16487+106	A, B	0.34 ± 0.09	9.60	9.94	M2.5 V	m2.5	m3.0	0.33 ± 0.14	0.30 ± 0.12	10
J16554-083S	A, Bab	0.43 ± 0.09	7.15	7.58	M3.0 V	m3.0	m3.0	0.34 ± 0.13	...	1.4
J16554-083S	Ba, Bb	...	8.33	8.33	m3.0 V	m3.5	m3.5	0.23 ± 0.13	0.23 ± 0.13	...
J16578+473	A, B	2.48 ± 0.02	...	8.01	...	K0.0 V	M1.5	...	0.57 ± 0.18	...
J17340+446	A, B	0.50 ± 0.11	10.74	11.24	M3.5 V	m3.5	m4.0	0.26 ± 0.12	0.22 ± 0.11	60
J17530+169	A, B	0.65 ± 0.11	10.64	11.29	M3.0 V	m3.5	m4.0	0.26 ± 0.14	0.21 ± 0.12	110
J18180+387E	A, B	1.50 ± 0.03	9.36	10.86	...	M3.0	m4.5	0.24 ± 0.10	0.16 ± 0.07	1700
J18264+113	A, B	5.89 ± 0.09	10.39	16.28	...	M3.5	WD	0.25 ± 0.08
J18411+247S	Aab, B	2.25 ± 0.02	9.18	11.43	...	M3.5	m5.5	...	0.14 ± 0.07	460
J18411+247S	Aa, Ab	...	9.92	9.92	M3.5	m4.0	m4.0	0.21 ± 0.08	0.21 ± 0.08	...
J18427+596N	A, B	0.88 ± 0.03	6.51	7.39	...	M3.0	m4.0	0.28 ± 0.10	0.22 ± 0.09	380
J18548+109	A, B	2.33 ± 0.08	8.29	10.62	...	M0.0	m3.0	0.56 ± 0.12	0.26 ± 0.11	700
J19463+320	A, B	0.78 ± 0.04	7.91	8.69	...	M0.5	m2.0	0.47 ± 0.15	0.36 ± 0.12	750
J19539+444W	A, B	2.34 ± 0.34	9.94	12.28	M5.5 V	m5.5	m8.0	0.12 ± 0.07	0.07 ± 0.05	11
J19539+444E	AB, C	0.48 ± 0.25	...	9.83	M5.5 V	...	M5.5	...	0.14 ± 0.06	260
J20407+199	B, C	1.4 ± 0.2	9.75	11.15	M2.5	m2.5	m4.0	0.36 ± 0.10	0.23 ± 0.09	8.4
J20445+089S	A, Bab	1.02 ± 0.07	9.28	10.30	...	M1.5	m3.0	0.44 ± 0.15	...	6400
J20445+089N	Ba, Bb	...	11.05	11.05	m3.0 V	m3.5	m3.5	0.25 ± 0.10	0.25 ± 0.10	...
J20488+197	A, B	0.32 ± 0.08	11.48	11.80	M4.0 V	m4.5	m5.0	0.27 ± 0.12	0.25 ± 0.11	22
J21012+332	Aa, Ab	1.68 ± 0.14	9.77	11.45	M3.0 V	m2.5	m4.5	0.33 ± 0.14	0.18 ± 0.10	13
J21323+245	A, B	0.74 ± 0.13	10.39	11.13	M3.5 V	m3.5	m4.5	0.29 ± 0.12	0.23 ± 0.11	250
J21518+136	A, B	1.45 ± 0.08	11.08	12.53	M4.5 V	m4.0	m5.5	0.19 ± 0.08	0.13 ± 0.07	66
J22279+576	A, B	1.21 ± 0.03	7.35	8.56	M3.0 V	m3.5	m5.0	0.23 ± 0.10	0.16 ± 0.09	27
J23096-019	Aab, B	1.82 ± 0.08	10.33	12.15	M3.5 V	m3.5	m5.0	...	0.17 ± 0.08	260

Table A.5. continued.

Karmn	Component	ΔI [mag]	I_1 [mag]	I_2 [mag]	SpT	SpT ₁	SpT ₂	M_1 [M _⊙]	M_2 [M _⊙]	P [a]
J23096-019	Aa, Ab	...	11.08	11.08	m3.0 V	m3.5	m3.5	0.23 ± 0.12	0.23 ± 0.12	...
<i>J23293+441N</i>	A, Bab	0.38 ± 0.02	9.39	9.77	M3.5 V	0.32 ± 0.05	...	4500
<i>J23293+414S</i>	Ba, Bb	0.73 ± 0.09	9.54	10.27	M4.0 V	0.34 ± 0.05	0.24 ± 0.05	10
J23318+199E	Aab, B	1.66 ± 0.02	7.63	9.29	...	M3.5	m5.0	230
J23318+199E	Aa, Ab	...	8.38	8.38	M3.5	m3.5	m3.5	0.23 ± 0.11	0.23 ± 0.11	...
J23318+199E	Ba, Bb	...	10.04	10.04	M4.5	m5.0	m5.0	0.14 ± 0.09	0.14 ± 0.09	...
J23517+069	A, B	0.51 ± 0.11	10.84	11.35	M3.0 V	m3.5	m4.0	0.26 ± 0.13	0.22 ± 0.12	450
J00169+200	A, B	0.70 ± 0.12	11.67	12.37	M3.5 V	m4.0	m4.5	0.23 ± 0.14	0.19 ± 0.09	210
<i>J01221+221</i>	A, B	0.86 ± 0.17	10.46	11.32	M4.5 V	0.18 ± 0.05	0.15 ± 0.05	8.0
J04352-161	Aab, B	4.60 ± 0.38	12.88	17.48	M7.0 V	10.07	1600 ^c
J04352-161	Aa, Ab	...	13.63	13.63	M7.0 V	m7.0	m7.0	0.08 ± 0.04	0.08 ± 0.04	
J06277+093	A, B	1.16 ± 0.04	9.78	10.94	M2.0 V	m2.0	m3.5	0.38 ± 0.12	0.26 ± 0.11	160
J07349+147	A, B	0.76 ± 0.04	9.19	9.95	M3.0 V	m3.5	m4.5	0.25 ± 0.11	0.20 ± 0.09	40
<i>J10028+484</i>	A, B	0.31 ± 0.06	12.61	12.92	M5.5 V	0.15 ± 0.08	0.12 ± 0.08	12

Notes. ^(a) Karmn stars in italics are associated to young stellar populations (see Table 3). ^(b) The periods given are a lower limit, as we equal our maximum separation measured to the semimajor axis. ^(c) The B component of the system is too faint to estimate its mass with our M_I -mass relation and the period was calculated using the stellar mass limit ($0.07 M_\odot$). Hence, the period of this system should be considered as a lower approximation.

Table A.6. Known binaries at $\rho > 5$ arcsec.

WDS		Primary		Secondary		ρ [arcsec]	Notes
	Name	SpT		Name	SpT		
GRB34	J00183+440	M1.0 V		J00184+440	M3.5 V	34.8	^a
GIC13	J00413+558	M4.0 V		EGGR 245	DC	10.8	
WNO51	J01026+623	M1.5 V		J01033+623	M5.0 V	293.1	
GIC20	J01119+049N	M3.0 V		J01119+049S	M3.5 V	63.6	
GIC27	J01518+644	M2.5 V		GJ3118 B	DAs	13.4	
PLW32	HD 16160 AB	K3 V + M7.0 V		J02362+068	M4.0 V	164.0	
LDS883	HD 18143 AB	G5 V + K7 V		J02555+268	M4.0 V	44.0	
LDS5401	J02565+554W	M1.0 V		J02565+554E	M3.0 V	16.7	
KUI11	HD 18757	G4 V		J03047+617	M3.0 V	263.2	
LDS884	GJ 140	M0.0 V+		J03242+237	M2.0 V	99.5	^b
LDS9158	J03396+254E	M3.0 V		J03396+254W	M3.5 V	64.4	
GIC44	J03438+166	M0.0 V		J03437+166	M1.0 V	106.50	^c
BU543	BD-01 564	K4 V		J03574-011	M2.5 V	11.0	^d
STF518	σ^2 Eri A	K0.5 V		J04153-076	M4.5 V	77.9	^e
STF518	σ^2 Eri B	DA		J04153-076	M4.5 V	8.6	^e
LDS3584	J04252+080S	M2.5 V+		HG 7-207	M4.0 V	73.4	^f
STI205	J04311+589	M4.0 V		EGGR 180	DC	10.0	^g
LDS6160	J05032+213	M1.5 V+		HD 285190 BC	M5.0 V + M5.5 V	167.0	^h
WDK1	J05034+531	M0.5 V		...	m7.0	5.6	ⁱ
DON93	J05068-215E	M1.5 V		J05068-215W	m3.0 V + m4.0 V	8.5	^j
LDS6186	HD 35956	G0 V+		J05289+125	M4.0 V	99.4	^k
LDS6189	J05342+103N	M3.0 V		J05342+103S	M4.5 V	5.1	
TOK255	J05365+113	M0.0 V		J05366+112	M 4.0 V	156.5	
GIC61	EG Cam	M0.5 V		J05599+585	M4.0 V	161.2	
NAJ1	J06105-218	M0.5 V		GJ229 B	T7	6.8	
GIC65	J06421+035	M2.0 V		J06422+035	M4.0 V	49.7	
WNO17	HD 50281	K3 V		J06523-051	M3.5 V+	58.3	^l
GIC75	J07307+481	M4.0+		EGGR 52	DC9+DC9	103.4	
LDS6206	VV Lyn AB	M2.5 V+		J07319+362N	M3.5 V	38.20	
Pov09	V869 Mon + GJ 282 B	K2 V + K5 V		J07361-031	M1.0 V	3892.0	
LDS3755	J07395+334	M2.0 V		LP 256-044	M6:	13.7	
LUY5693	EGGR 5 54 A	DAZ6		J07403-174	M6.0 V	21.0	^m
COU91	BD 21+1764A	K7 V		J08082+211	M3.0 + m3.0 + m5.0	10.7	ⁿ
LDS204	GJ 9255 A	F6.5 V		J08105-138	M2.0 V + M5.5 V	97.6	
LUY6218	BD+10 1857 AB	M0.0 V+		J08428+095	M2.5 V	114.4	
OSV2	J09008+052W	M3.0 V		Ross 687	M3.5 V	29.40	
STF1321	J09143+526	M0.0 V+		J09144+526	M0.0 V	17.20	^o
LDS6226	J09187+267	M1.5 V		LP 313-038	M5.0 V	76.3	
GIC87	J09288-073	M2.5 V		GJ 347 B	M4.5	35.9	
LDS3917	J09430+237	M1.0 V		LP 370-034	M7.0 V	131.20	
REB1	J10043+503	M2.5 V		G 196-003 B	L2	16.0	
LDS3977	J10185-117	M4.0 V		LP 729-055	M5.0 V	15.8	
LDS1241	J10260+504W	M4.0 V		J10260+504E	M4.0 V	14.4	
LDS3999	J10345+465	M3.0 V		NLTT 24709	M4.5 V	46.5	
LDS1258	J10448+324	M2.0 V + M4.0 V		LP 316-605 B	M4.5 V	35.1	
VBS18	BD+44 2051A	M1.0 V		J11055+435	M5.5 V	31.4	

Table A.6. continued.

WDS		Primary		Secondary	SpT	ρ [arcsec]	Notes
	Name	SpT	Name		SpT		
LDS5207	J11476+002	M4.0 V	LP 613–050 B		M5.5 V	24.8	
LDS4166	J12006–138	M3.5 V	LP 734–010 B		M4.5	6.8	
LDS390	LTT 4562	M3.0 V	J12112–199		M3.5 V	85.3	
VYS5	J12123+544S	M0.0 V	J12123+544N		M3.0 V	14.7	
(Haw96)	J12142+006	M5.0 V+	5.0	^p
BU800	HD 115404	K2 V	J13168+170		M0.5 V	7.5	
LDS448	BD–07 3632	DA5.0	J13300–087		M4.0 V	503.0	
DEA1	J13481–137	M4.5 V	LHS 2803B		T5.5	67.6	
LDS461	J13507–216	M3.0 V	J13503–216		M3.5 V	374.90	
VVO12	BD+46 1951	M0.0 V	J14173+454		M5.0 V	59.2	
STT580	θ Boo A	F7 V	J14251+518		M2.5 V	69.5	
BUI442	J14257+236W	M0.0 V	J14257+236E		M0.5 V	45.4	^q
GIC120	J14279–003S	M4.5 V	J14279–003N		M4.5 V	13.0	
LDS961	J14283+053	M3.0 V	LP 560–026		M3.5 V	60.2	
LDS6309	Ross 806	M2.5 V	J15531+347S		M3.5 V	26.50	
LDS573	J16554–083S	M3.0 V + M4.0V	J16554–083N		M3.5 V	72.2	^r
LDS573	J16554–083S	M3.0 V + M4.0V	J16555–083		M7.0 V	230.8	^r
A184	V1090 Her	K0 V	J16578+473		M1.5 V	5.08	^e
STFA32	V1089 Her	K0 V	J16578+473		M1.5 V	111.60	^e
LDS593	J17177–118	M3.0 V	2MASS J17174454–1148261		m4.0	30.1	^s
BDK9	J17578+465	M2.5 V	G 204–039 B		T6.5	197.0	
GIC151	J18180+387E	M3.0 V	J18180+387W		M4.0 V	9.9	
NI38	J18264+113	M3.5 V	2MASS J18262449+1120498		“WD”	8.1	
LDS6329	BD+45 2743	M0.5 V	J18354+457		M2.5 V	112.2	
STF2398	J18427+596N	M3.0 V	J18427+596B		M3.5V	11.7	
KAM3	J19463+320	M0.5 V	J19464+320		M2.5 V	5.7	^t
GIC159	J19539+444W	M4.5 V + M8.0 V	J19539+444E		M5.5 V	6.4	
LDS1045	GJ 797 A	G5 V	J20407+199		M2.5 V+	125.1	^u
LDS1046	J20445+089S	M1.5 V	J20445+089N		M3.5 V+	15.2	^v
LDS6418	J20556–140N	M4.0 V	GJ 810 B		M5.0 V	107.1	
LDS1049	J21012+332	m2.5 V + m4.5 V	J21013+332		M2.0 V + M5.0 V	56.9	
LDS1053	21160+298E	M3.5 V+	21160+298W		M3.5 V	26.1	^w
GIC193	J23293+414N	M3.5 V	J2393+414S		M4.0 V	17.7	^x
WIR1	J23318+199E	M3.5 V+	J23318+199W		M4.5 V+	5.3	^y
LDS830	J23573–129E	M3.0 V	J23573–129W		M4.0 V+	19.6	^z

Notes. ^(a) C is background (GRB34). ^(b) AB is separated by 2.5 arcsec (WOR4). ^(c) “B-G” are background (LMP3). ^(d) Simbad indicates that J03574–011 is a spectroscopic binary but we did not find any reference. ^(e) Triple system. ^(f) Primary is SB2 (Llamas 2014). ^(g) Primary is an astrometric binary separated by 0.07 arcseconds (Strand 1977). ^(h) The primary is a SB2 (Schöfer 2015). ⁽ⁱ⁾ It was also observed with the CAMELOT low resolution imager at the Observatorio del Teide (Tenerife) in September 2015 with the *BVI* filters in order to obtain more photometric information but we could not avoid the saturation of the primary. ^(j) BC is separated by 0.8 arcsec. ^(k) Primary is a SB (Simbad). ^(l) Background source at 9.62 arcsec (TNN6). ^(m) WDS VBS41 at 4 arcsec and 208 deg was not detected in this work nor in Davison et al. 2015. It could be an unrelated companion. The WDS “AC” designation refers to the pair in the table. ⁽ⁿ⁾ Hierarchical quadruple. ^(o) Primary is a SB1 (Schöfer 2015). Two other WDS entries under the same discoverer code (STF1321) are not physically bound components. ^(p) SB2 (Bonfils et al. 2013). Hawley et al. (1996) listed in Table 1.(b) a companion at 5.0 arcsec 1.2 mag fainter in *V*. 2MASS resolved a source 6.5 mag fainter in the *J*-band at 5.9 arcsec and 179 deg (quality flag: AUU). Neither Law et al. (2008) nor Dieterich et al. (2012 – with NICMOS onboard *Hubble*) detected it. We believe that Hawley et al. (1996) made reference to the background star 2MASS J12141817+0037297. ^(q) Other WDS entries under BU 1442 and STG 6 are unrelated sources. ^(r) Quintuple system. ^(s) Simbad mixes up the true primary GJ 3999 (“L 845-016”), the true secondary 2MASS J17174454–1148261, and the background star GJ 4000 B (“L 845-015”, see Table A.3). We preserve the current (wrong) nomenclature. ^(t) C is background (HEL3). ^(u) Other WDS entries under RAO 23 are unrelated sources. ^(v) Secondary is SB1 (Schöfer 2015). ^(w) AB is separated by 0.05 arcsec (BWL56). ^(x) Bab is separated by 0.26 arcsec (BWL59). AC is background (BWL59). ^(y) A and B are SB1 (Delfosse et al. 1999). Other WDS entries under LMP 24 are unrelated sources. ^(z) Secondary is SB2 (Schöfer 2015).